Theoretical aspects of superconductivity in very high magnetic fields

Mark Rasolt

Solid State Division, Oak Ridge National Laboratory, Oak Ridge, Tennessee 37831-6032

Zlatko Tešanović

Department of Physics and Astronomy, The Johns Hopkins University, 3400 North Charles Street, Baltimore, Maryland 21218
and Theoretical Division, MS B262, Los Alamos National Laboratory, Los Alamos, New Mexico 87545

This paper reviews the progress made in the last few years in theoretical understanding of the properties of superconductors in very high magnetic fields. The key ingredient in the new understanding is the recognition that the usual negative effect of orbital frustration in a superconducting state, reflected in diamagnetic pair breaking, is obviated when all electrons reside in only the few lowest Landau levels. A new relation between the superconducting order parameter and the magnetic field now exists which permits a strong enhancement of the critical temperature with increasing magnetic field. The issue of Pauli pair breaking and the effect of impurities in this new state are also discussed, along with the important observation that the attractive component of the effective electron-electron interaction in systems with low carrier density is enhanced with increasing magnetic field. While this paper emphasizes the theoretical aspects of this high-field limit, it does present a unified picture of superconductivity throughout the whole temperature and magnetic-field phase diagram. Numerical applications to simple models of low-carrier-density semiconductors and semimetals are also discussed, since these materials are the most likely candidates for this new phase.

CONTENTS

I. INTRODUCTION

Since the discovery of superconductivity in the early 1900s, it has become clear that the relationship between the external magnetic field and superconductivity is both fundamental in its physical origin and very important from a practical point of view. The existence of the Meissner effect, the expulsion of the external field from the interior of a superconductor, illustrates this fundamental relationship, which is based on the principle of gauge invariance. Yet, at the same time, this inherent property of superconductors can be used to provide shielding from external fields when an environment free of magnetic fields is needed in technological and industrial applications. Similarly, type-II superconductors, in which the external field can coexist with superconductivity in the form of a quantized flux lattice provide a basis for the construction of the most powerful magnets. These are just some of the reasons for the strong interest in the scientific community in understanding superconductivity in the presence of magnetic fields. This interest continues to grow, fueled further by the intense study of high-temperature and other exotic superconducting materials.

It has been an accepted "folklore" that an external magnetic field suppresses superconductivity. This is often, and sometimes superficially, attributed to the breaking of time-reversal symmetry caused by the presence of the external field. The fundamental reason is that the superconducting order parameter $\psi(\mathbf{r})$ becomes "frustrated" due to the gauge invariance, resulting in a supercurrent flow either at the surface (type-I behavior) or in the interior of a superconductor (type-II behavior). This orbital frustration, or diamagnetic pair breaking, is present in all superconductors and is based only on a completely general property of the superconducting ground state. Such a state has a broken global U(1) symmetry, the "magnitude" of this symmetry breaking being measured by $\psi(\mathbf{r})$. In type-I superconductors a small external field **H** induces diamagnetic surface currents by introducing a spatial variation in the phase of $\psi(\mathbf{r})$. [By small **H** we mean that the magnetic energy $H^2/8\pi$ is small compared to the absolute value of the free energy $F(T)$ of the condensate; $|F(T)| \approx |\psi|^4$.] Microscopically, the way **H** couples to electrons results in an overall momentum of the Cooper pairs transverse to **H** by shifting one of the momenta of the electrons in the pair, relative to the other (i.e., the effect of breaking time-reversal symmetry). The induced surface currents then exactly cancel **H** beyond a skin depth λ, hence the Meissner effect. As **H** increases, the Cooper pairs acquire greater and greater momentum perpendicular to **H**, and the gain from the reduction in the condensate free energy $F(T)$ decreases. The current j, which is proportional to the product of the increasing velocity v and the decreasing $|\psi|^2$, cannot then exceed an upper critical value j_c; i.e., above j_c (when $H \geq H_c$) **H** penetrates throughout the sample and superconductivity is destroyed. The order of magnitude of this H_c can be estimated from a consideration of the current j_c and the profile of the skin penetration of **H**. It, of course, can be also calculated exactly using thermodynamic considerations; this, however, does not provide any details on how the diamagnetic pair breaking is evolved.

Type-II superconductors have a slightly more complex relation between **H** and diamagnetic pair breaking, as illustrated by the phase diagram of Fig. 1. (The origin of the high-field portion of the phase diagram will be discussed in Sec. III). A type-II superconductor differs microscopically from a type-I in that, in the presence of **H**, the acquired transverse momentum of the Cooper pairs leads to a lower pair velocity than in type I. This has significant experimental consequences; type-II superconductors can accommodate **H** in their interior. Again, as in type I, up to a field H_{c1} the surface current screens **H** entirely out of the sample. H_{c1} can be estimated from the expense in the condensation energy required to generate a single quantized flux line in the interior of the sample. Above H_{c1}, however, the low velocity per Cooper pair momentum (or equivalently in the spin analog, a small stiffness coefficient and a corresponding relatively low frustration energy) leads to a smaller expense in $F(T)$ than in type I. The ground-state wave function can then modify itself to survive the presence of an internal magnetic field. The order parameter $\psi(\mathbf{r})$ must now become nonuniform in the bulk, even at the expense of the frustration caused by the presence of a bulk magnetic field $\mathbf{B}(\mathbf{r})=\mathbf{H}+\mathbf{b}(\mathbf{r})$. [$\mathbf{b}(\mathbf{r})$ opposes **H**, i.e., $\mathbf{B}(\mathbf{r}) \lesssim \mathbf{H}$.] Just above H_{c1} the order parameter is distorted to form a dilute array of vortices with a unit flux $\phi_0=\hbar c/2e$ and a range λ (see Fig. 2). Just below the H_{c2} line, on the other hand (see Fig. 1), $\psi(\mathbf{r})$ goes to zero while maintaining a nonuniform hexagonal lattice structure (the Abrikosov lattice) containing one flux quantum per unit cell area $2\pi l^{*2}$ [$l^*=(\hbar c/2eH)^{1/2}$]. Above H_{c2}, $\psi(\mathbf{r})=0$ and there is no superconductivity.

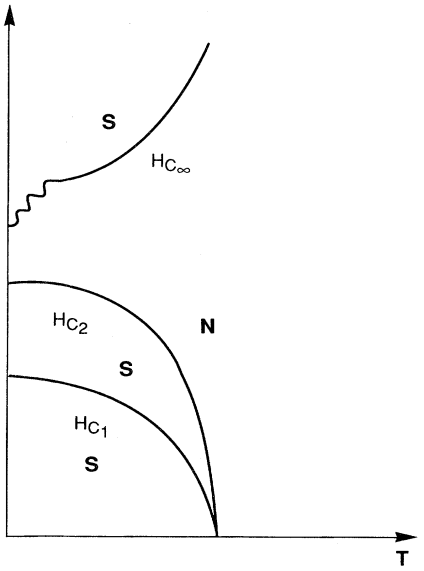

FIG. 1. A sketch of the phase diagram for the superconducting condensate in the T-H plane. Assuming the system is a type-II superconductor at zero field, as the field increases one crosses over from a Meissner state to the quantum-limit state at $H_{c\infty}$. The steplike crossover reflects the effect of the depopulation of higher Landau levels. Such oscillations will continue along H_{c2} with smaller amplitudes and periods. For a pure type-II superconductor the H_{c2} line comes close but *never* touches the vertical axis.

Of course, there are other ways in which **H** can affect superconductivity. The Zeeman splitting, which is also the consequence of the loss of time-reversal symmetry, will lead to Pauli pair breaking in a spin-singlet superconductor and suppression of superconductivity. **H**, via the Zeeman coupling, tends to align the spins of the electrons forming the Cooper pair. To find the field $H \equiv H_p$ for which such a spin alignment is profitable in type-I superconductors, we need to compare the energy of the paramagnetic state $-\frac{1}{2}\chi H_p^2$ (where χ is the Pauli susceptibility) with $-H_c^2/8\pi$. Since $\chi \ll 1/4\pi$, even for relatively low electron density, $H_p \gg H_c$ and plays almost no role. In a type-II superconductor Pauli pair breaking is more relevant than in type I. Since the field around H_{c2}

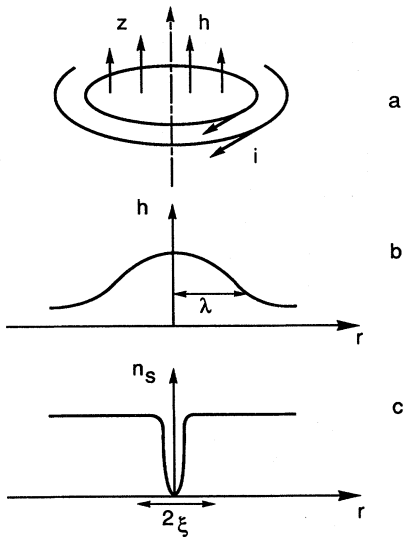

FIG. 2. Structure of one vortex line in a type-II superconductor. The magnetic field is maximum near the center of the line. Going outwards, h decreases because of the screening in an "electromagnetic region" or radius $\sim\lambda$ (the penetration depth). From de Gennes, 1966.

exists within the sample, **H** does couple to the spins and does modify the shape of the H_{c2} line. However, it is well known that the Pauli critical field H_p is now given by $\mu_B g H_p \approx k_B T_c$ and is found to lie above the H_{c2} line for the majority of type-II systems. The Pauli pair breaking will obviously become an important issue at very high magnetic fields, where $H \gg H_p > H_{c2}$ ($T=0$), i.e., along $H_{c\infty}$ of Fig. 1 (the origin of the high-field region of the phase diagram in Fig. 1 is discussed in detail in Sec. III). Furthermore, a strong magnetic field could modify the interactions leading to the superconducting instability in the first place. If localized magnetic atoms (or ions) are present in the system, **H** could affect their interaction with the superconducting electrons and thus change some superconducting properties. All of these effects, however, are not "fundamental" and are, in this important respect, different from diamagnetic pair breaking. For example, a spin-triplet superconductor could be largely insensitive to Pauli pair breaking, while, in some systems, the pairing interaction could actually be enhanced by **H**. In contrast, the orbital frustration and the diamagnetic pair breaking are always present and fundamentally tied to a superconducting state.

While orbital frustration is inherent to a superconducting state in an external field, it is an interesting question whether it always leads to a suppression of superconductivity, as in the standard Abrikosov-Gor'kov theory (Fig. 1). Until very recently, a resounding "yes" would be the response to this question by most physicists. In the last several years, however, it has become increasingly clear that the answer is "no" (Tešanović, Rasolt, and Xing, 1989; Rasolt, 1987) and that there is a regime in which the external magnetic field in fact enhances superconductivity. This unusual limit of superconductivity occurs only in very high magnetic fields, where electrons move in quantized Landau orbitals, and is most prominent in the extreme quantum limit, where all electrons are in the lowest Landau level. This limit arises through the transformed nature of the orbital frustration. When the electrons themselves occupy only several of the lowest Landau levels, the orbital frustration is resolved "naturally," in a sense that will become clear later, and superconductivity is enhanced in an increasing field, as T_c becomes a rapidly increasing function of H.[1]

This brings us to the main point of this review. The description of diamagnetic pair breaking presented above and leading to the usual H_{c2} line of Fig. 1 depends on the following assumption, which is generally well satisfied in most type-II superconductors considered so far: It is assumed that the bending of the semiclassical paths of electrons by the magnetic field **H** is negligible over the range of the single-particle Green's function G at zero magnetic field. This is the semiclassical phase-integral approximation, originally due to Gor'kov (1958). In the clean limit, this translates to $l^2 k_F \gg v_F/(2\pi k_B T)$ (or equivalently to $\hbar\omega_c \ll k_B T$), where $l=(\hbar c/eH)^{1/2}$ and $\omega_c = eH/m^* c$. For large impurity concentrations, it translates to $\omega_c/2\pi \ll \tau^{-1}$, where τ is the impurity scattering lifetime.

In both cases, either temperature or impurity scattering (or both) totally erase any signature of the Landau-level structure, a structure that must be there in a complete theory of type-II superconductors in the presence of a magnetic field. As already mentioned, this is a very good approximation in most cases, since the number of occupied Landau levels is huge and the separation between them is very small. In low-carrier-density semimetals and semiconductors with l of the order of the interparticle separation, a situation that can readily be achieved by application of fields in the 1–30 Tesla range, this assumption must be reexamined (Rasolt, 1987; Tešanović, Rasolt, and Xing, 1989). When this Landau-level structure is fully accounted for, one finds that, for a pure case or for a modest level of impurities, superconductivity does not terminate above the $H_{c2}(T)$ line. Rather, as H increases, the H_{c2} line crosses over (for the pure case) or reenters (for a modest level of impurities) a new superconducting state, above the $H_{c\infty}$ line (see Fig. 1), whose critical temperature is an increasing function of **H**. In fact, in the quantum limit $H > H_{\rm QL}$, where both spins occupy the lowest Landau level (if the Zeeman splitting is small), T_c is a rapidly increasing function of H (see Fig. 1 along the $H_{c\infty}$ line and beyond the last Landau-level oscillation).

[1]One final comment about diamagnetic pair breaking concerns the role of impurities. The addition of nonmagnetic impurities, not surprisingly, increases the "mass" of the Cooper pairs and makes a superconductor more type II. In fact (as we discuss in Sec. II), in the limit of high impurity density, the behavior of the $H_{c2}(T)$ line is correct all the way to $T=0$, and the crossover region to $H_{c\infty}$ (Fig. 1) disappears.

At this point, we should recall a more familiar instability of an electron gas, which is enhanced in strong magnetic fields: the spin-density wave (SDW). Celli and Mermin as early as 1965 observed that for $H > H_{QL}$ the quasi-one-dimensionality along **H** leads to a strong enhancement of SDW instabilities due to the nesting of opposite sides of the Fermi surface perpendicular to **H**. It is precisely this quasi-1D behavior that leads to the enhancement of superconductivity along the $H_{c\infty}$ line through the rapid increase in the density of states. However, unlike the SDW case, such a suggestion for superconductivity may encounter serious reservations. For example, the diamagnetic pair breaking and the orbital frustration that result in the Meissner effect, irrelevant in the SDW (or charge-density-wave) case, pose the physical question, How can a stable superconducting state exist in a magnetic field generally much higher than any characteristic H_{c2}? Another point is the effect of impurities. If we naively view the $H_{c\infty}$ line as an extension of the H_{c2} line to $\kappa \to \infty$ (where $\kappa \equiv \lambda/\xi$ with ξ the coherence length), we run into the following possible misconception: We argued that the larger the level of impurities, the more type II is the superconductor and the higher is H_{c2}, while at the same time the more appropriate is the approximation in which the Landau-level structure is ignored. So how do we ever reach the $H_{c\infty}$ line in real systems? We shall answer these questions in great detail in the following sections. In fact, in the early sixties corrections to the semiclassical phase-integral approximation due to the Landau-level structure were already being considered by Rajagopal and Vasudevan (1966a, 1966b) and by Gunther and Gruenberg (1966). The mathematical structure for studying the $H_{c\infty}$ line was largely in place. It was probably the kind of reservation mentioned above that left this most exciting region essentially unexplored. We have already briefly touched on how diamagnetic pair breaking is circumvented in the quantum limit. We shall see below that, while Pauli pair breaking and disorder impede superconductivity severely in the crossover region, they do not have any "catastrophic" effect in very high fields, and particularly not in the quantum limit, where Pauli pair breaking is largely circumvented by the nonuniform state along **H** (Tešanović, Rasolt, and Xing, 1989). It is nevertheless clear that the best candidates for high-field-limit superconductivity are materials that are relatively pure and that have a low effective g factor.

At present, the notion of superconductivity in high magnetic fields is a purely theoretical one. We are not aware of any experiments that have identified this state in a real material. Thus, in writing this review, we have set two major goals for ourselves: First, we want to present a thorough theoretical basis for this state (within the confines of the available literature) and to establish the relation of this subject to other more familiar ones: type-II superconductivity, many-body physics in the quantum limit of a magnetic field, quantum Hall effect, many-body physics in one dimension, etc. Second, by discussion of topics like the effect of Pauli pair breaking and impurity scattering on the superconducting state in a high field, the interplay of electron-phonon and electron-electron interaction in low-density systems, etc., we should like to give at least a rough outline of the conditions that must be met in real systems if one is ever to observe this limit of superconductivity. This message is clearly directed toward experimentalists, whose interest we would very much like to stimulate. If the experimental reader comes away from reading this review challenged and thinking of ingenious ways to prove the theory right or wrong, then we have attained our most important objective.

To elucidate the properties of this superconducting state along and above the $H_{c\infty}$ line we shall use a variety of methods: variational wave functions, field theory, and the Ginzburg-Landau expansion. Each approach will in turn lend additional insight into this novel superconducting state. We shall, as much as possible, try to relate the $H_{c\infty}$ line with the more familiar H_{c2} line, sometimes at the risk of being repetitive. Our goal is to leave no doubt that this superconducting state is as sound as the spin-density-wave, charge-density-wave (CDW), and valley-density-wave states, all believed to be enhanced in the high-field limit, where only a small number of Landau levels are occupied. Which broken symmetry will occur in which particular material will ultimately have to be answered by an experimental effort.

The review is organized as follows: In Sec. II we give a general discussion of the interaction of the electromagnetic vector potential and the superconducting state. We stress in particular the relevance of time reversal and the effect of impurities on the superconducting condensate along H_{c2}. In Sec. III we discuss the transition line from H_{c2} all the way along to $H_{c\infty}$ using a full Landau-level structure. Particular emphasis is given to the effect of Zeeman splitting and impurities. In Sec. IV, we discuss the nature of the order parameter along $H_{c2} \to H_{c\infty}$, with particular emphasis on the effect of diamagnetic pair breaking and the nature of the transport properties, such as current flow and dissipation. In Sec. V we go beyond the mean-field approximation and discuss fluctuations. In Sec. VI we discuss various aspects of this subject with an eye to experimental considerations. Finally, our conclusions are given in Sec. VII.

II. INTERACTION BETWEEN THE ELECTROMAGNETIC FIELD AND SUPERCONDUCTIVITY: GENERAL DISCUSSION

A. The Hamiltonian

The nonrelativistic Hamiltonian for a many-electron system in the presence of an external vector potential $\mathbf{A}(\mathbf{r})$ is given in second quantized form by

$$\hat{H} = \hat{H}_e + \hat{H}_{ph} + \hat{H}_{e\text{-}ph} + \hat{H}_{e\text{-}e} \ . \tag{2.1a}$$

Here $\hat{H}_e$ is the electron interaction with the fixed ions,

$$\hat{H}_e=\sum_{\substack{\sigma=1,2\\ \nu=1,2}}\int d^3r\,\psi^\dagger_\sigma(\mathbf{r})\left\{\frac{1}{2m}\left[\frac{\hbar}{i}\nabla-\left[\frac{e}{c}\mathbf{A}(\mathbf{r})+\mathbf{a}(\mathbf{r})\right]\right]^2\delta_{\sigma\nu}+U_{\sigma\nu}(\mathbf{r})-E_F\right\}\psi_\nu(\mathbf{r})\ , \tag{2.1b}$$

where $\mathbf{a}(\mathbf{r})$ accounts, in a mean-field way, for the e-e diamagnetic interaction (i.e., the Breit term), with $\mathbf{b}(\mathbf{r})=\nabla\times\mathbf{a}(\mathbf{r})$, and where the $\psi^\dagger_\sigma(\mathbf{r})$ are the creation field operators for the two spin components $\sigma=1,2$. In Eq. (2.1b), $U_{\sigma,\nu}(\mathbf{r})$ includes the fixed periodic background $\sum_{\mathbf{R}^0_j}U_0(\mathbf{r}-\mathbf{R}^0_j)$ and Zeeman splitting $-g\mu_B\hat{\sigma}\cdot\mathbf{H}(\mathbf{r})$ and a random impurity contribution $\sum_j U^i_{\sigma,\nu}(\mathbf{r}-\mathbf{R}^{\rm imp}_j)$ (the spin indices σ,ν allow for magnetic impurities). Assuming small displacements, to quadratic order, the ion-ion interaction is given by

$$\hat{H}_{\rm ph}=\sum_{\mathbf{q},s}\hbar\omega_{\mathbf{q}s}b^\dagger_{\mathbf{q}s}b_{\mathbf{q}s}\ , \tag{2.1c}$$

where $b^\dagger_{\mathbf{q}s}$ are the phonon creation operators of polarization s and $\hbar\omega_{\mathbf{q}s}$ are the corresponding phonon frequencies. The electron-phonon interaction is given by

$$\hat{H}_{\text{e-ph}}=i\int\sum_\sigma d^3r\left[\int\frac{d^3q}{(2\pi)^3}\left[\sum_s\alpha_{\mathbf{q},s}(b_{\mathbf{q},s}+b^\dagger_{-\mathbf{q},s})e^{i\mathbf{q}\cdot\mathbf{r}}\right]\psi^\dagger_\sigma(\mathbf{r})\psi_\sigma(\mathbf{r})\right]\ , \tag{2.1d}$$

where

$$\alpha_{\mathbf{q},s}=(N_i/M)^{1/2}\sum_\lambda[U_0(\mathbf{q})q_\lambda\epsilon_\lambda(q,s)/(2\omega_{q,s})^{1/2}]\ . \tag{2.1e}$$

In Eq. (2.1e) N_i is the number of ions, M the ion mass, and $U_0(\mathbf{q})$ the Fourier transform of the electron-ion potential. Finally, the electron-electron interaction $H_{\text{e-e}}$ is given by

$$H_{\text{e-e}}=\tfrac{1}{2}\sum_{\sigma_1,\sigma_2}^{2}\int d^3r_1\int d^3r_2\psi^\dagger_{\sigma_1}(\mathbf{r}_1)\psi^\dagger_{\sigma_2}(\mathbf{r}_2)v(\mathbf{r}_1-\mathbf{r}_2)\psi_{\sigma_2}(\mathbf{r}_2)\psi_{\sigma_1}(\mathbf{r}_1)\ , \tag{2.1f}$$

where $v(\mathbf{r}_1-\mathbf{r}_2)=e^2/|\mathbf{r}_1-\mathbf{r}_2|$.

If we set $\mathbf{A}(\mathbf{r})=0$ and consider only nonmagnetic impurities, then Eq. (2.1a) is invariant under the full SU(2) symmetry group and the time-reversal point-symmetry operation $\hat{K}$, which is the product of complex conjugation C and a unitary matrix U (i.e., $\hat{K}=\hat{U}C$). In this matrix $\hat{U}$ is given by

$$\hat{U}=e^{i(\pi/2)\hat{A}} \tag{2.2a}$$

and

$$\hat{A}=\sum_{\mathbf{k},i}(c^\dagger_{i-\mathbf{k}\sigma=1}c_{i\mathbf{k}\sigma=2}-c^\dagger_{i-\mathbf{k}\sigma=2}c_{i\mathbf{k}\sigma=1})+\sum_{\mathbf{q},s}b^\dagger_{-\mathbf{q}s}b_{\mathbf{q}s}\ , \tag{2.2b}$$

where the $c^\dagger_{i\mathbf{k}\sigma}$ are defined by

$$\psi^\dagger_\sigma(\mathbf{r})=\sum_{\mathbf{k},i}c^\dagger_{i\mathbf{k}\sigma}\phi^{i*}_{\mathbf{k}\sigma}(\mathbf{r}) \tag{2.2c}$$

such that

$$[\hat{H}'_e,c^\dagger_{i\mathbf{k}\sigma}]=\xi^i_{\mathbf{k}\sigma}c^\dagger_{i\mathbf{k}\sigma}\ . \tag{2.2d}$$

[In $\hat{H}'_e$ we have removed the impurities from $\hat{H}_e$ in Eq. (2.2b); $\hat{H}'_e$, therefore, represents the periodic part of the single-body Hamiltonian $\hat{H}_e$.] In Eq. (2.2), i is the band index, $\mathbf{k}$ the Bloch momentum, and $\xi^i_{\mathbf{k}\sigma}$ the band energy. [Incidentally, Eq. (2.1), with $\mathbf{A}(\mathbf{r})$ set to zero and without magnetic impurities, continues to be invariant under $\hat{K}$ even in the presence of spin-orbit interaction; we shall not, however, consider spin-orbit effects in this review article.] When $\mathbf{B}(\mathbf{r})\neq0$ [and therefore $\mathbf{A}(\mathbf{r})\neq0$], or when magnetic impurities are included, it is not difficult to see that Eq. (2.1) [and in particular Eq. (2.1b)] is no longer invariant under SU(2), but even more important to us, it is no longer invariant under time reversal, i.e., under $\hat{K}$ of Eq. (2.2) (we shall come back to the implications of this shortly).

In this review, the on-the-mass-shell processes we consider involve almost exclusively the electronic coordinates alone. It is then desirable to "integrate" out the phonon degrees of freedom into an effective e-e interaction. There are many ways to identify this interaction. Perhaps the easiest is to consider the field-theoretic expansion to lowest order in the e-e scattering cross section (see Fig. 3) at finite temperature. Using $\hat{H}$ of Eq. (2.1) (removing, for the moment the presence of the magnetic field), we find that this effective interaction $v_{\rm eff}$ is given by the wavy line of Fig. 3; its form is

$$v_{\rm eff}(\mathbf{r}_1-\mathbf{r}_2,\omega_2-\omega_1)=\sum_s\int\frac{d^3q}{(2\pi)^3}\frac{2\alpha^2_{\mathbf{q},s}\omega_{qs}e^{i\mathbf{q}\cdot(\mathbf{r}_1-\mathbf{r}_2)}}{(\omega_2-\omega_1)^2-\omega^2_{qs}}+\frac{e^2}{|\mathbf{r}_1-\mathbf{r}_2|}\ , \tag{2.3}$$

where $\omega=k_BT\pi(2l+1)$ are the electron Matsubara frequencies. [Incidentally, in $\alpha_{\mathbf{q},s}$ of Eq. (2.3) $U_0(\mathbf{q})$ of Eq. (2.1e) must now be replaced by the screened electron-ion potential]. For a weak-coupling superconductor, one uses a simple short-range attractive BCS (Bardeen, Coop-

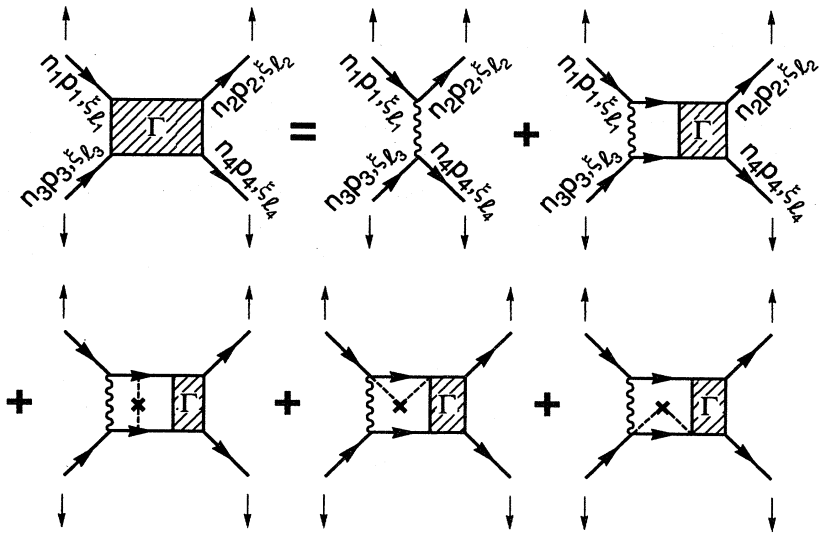

FIG. 3. The electron-electron scattering cross section Γ of two different spins in the ladder approximation. The wavy line is the effective e-e interaction, and the arrowed lines are the noninteracting electron propagators. The last three graphs include the effects of impurities to lowest order in impurity scattering.

er, and Schrieffer, 1957) point interaction $-V\delta(\mathbf{r}_1-\mathbf{r}_2)$, with some energy cutoff, to replace all of Eq. (2.3). This interaction, V, contains the effective electron-electron attraction arising through the exchange of phonons [the first term in Eq. (2.3)] and the effective Coulomb repulsion arising from the second term in Eq. (2.3). The second term will also be screened through a Thomas-Fermi (or similar) mechanism. Furthermore, this repulsive term has a different energy scale from the phonon term and is renormalized downward by retardation effects (for discussion of these points the reader should consult reviews on the theory of superconductivity found in Parks, 1969). The final Hamiltonian of interest here is then

$$\hat{H}=\hat{H}_e-\tfrac{1}{2}V\sum_\sigma\int d^3r\,\psi_\sigma^\dagger(\mathbf{r})\psi_{-\sigma}^\dagger(\mathbf{r})\psi_{-\sigma}(\mathbf{r})\psi_\sigma(\mathbf{r})\ . \tag{2.4}$$

We went to some length to write down Eq. (2.3) so that we could briefly consider the effect on $v_{\rm eff}(\mathbf{r}_1-\mathbf{r}_2)$ or $V\delta(\mathbf{r}_1-\mathbf{r}_2)$ of turning on the magnetic field. The magnetic field couples (to order m/M) only to the electrons. All the valence electrons participate in forming $\alpha_{q,s}$ or $\omega_{q,s}$ and, therefore, even in low-carrier-density systems the energy scale for modifying Eq. (2.3) is several electron volts. The **H** corresponding to the quantum limit (in low-carrier-density systems) has, therefore, little effect on the form of Eq. (2.3) (there are some subtle points here, like the coupling of the plasmon of low-density carriers to optical phonons. The reader should consult Sec. VI.B for further discussion). However, as we shall argue in Sec. VI, the actual scattering processes, which in the quantum limit include the matrix elements of Eq. (2.3), in the lowest Landau level are strongly modified due to the strong **H**. In fact, as we shall see, **H** reduces the repulsive part of $v_{\rm eff}$ relative to the attractive one and thus favors an attractive V (Rasolt, 1987); this is encouraging to the actual observation of superconductivity in very high fields.

The thermodynamics of the Hamiltonian (2.4) can be calculated from the partition function $Z\equiv T_r e^{-\beta H}$. It is sometimes more convenient to write Z in the Feynman path-integral form using the coherent-state representation, i.e.,

$$Z=\int D\psi_\sigma(\mathbf{r},\tau)D\psi_\sigma^*(\mathbf{r},\tau)D\mathbf{a}(\mathbf{r})\exp\left[-\int_0^\beta d\tau L(\tau)\right], \tag{2.5a}$$

where $\int D\psi_\sigma(\mathbf{r},\tau)D\psi_\sigma^*(\mathbf{r},\tau)$ denotes functional integration over Grassman variables $\psi_\sigma(\mathbf{r},\tau),\psi_\sigma^*(\mathbf{r},\tau),\mathbf{a}(\mathbf{r})$ is the fluctuating part of the vector potential, and

$$L(\tau)=\sum_\sigma\int d^3r\left[\psi_\sigma^*(\mathbf{r},\tau)\frac{\partial}{\partial\tau}\psi_\sigma(\mathbf{r},\tau)+\frac{1}{2m}D_r^*\psi_\sigma^*(\mathbf{r},\tau)D_r\psi_\sigma(\mathbf{r},\tau)+\sum_\nu\psi_\sigma^*(\mathbf{r},\tau)U_{\sigma\nu}(\mathbf{r})\psi_\nu(\mathbf{r},\tau)\right.$$
$$\left.-\frac{V}{2}\psi_\sigma^*(\mathbf{r},\tau)\psi_{-\sigma}^*(\mathbf{r},\tau)\psi_{-\sigma}(\mathbf{r},\tau)\psi_\sigma(\mathbf{r},\tau)+\frac{[\mathbf{H}+\mathbf{b}(\mathbf{r})]^2}{8\pi}\right]. \tag{2.5b}$$

Here

$$D_r\equiv\partial_r-\frac{ie}{c}[\mathbf{A}(\mathbf{r})+\mathbf{a}(\mathbf{r})]\ ,$$

and we have added the energy of the magnetic field.

B. Mean field

It is, of course, impossible to calculate Z of Eq. (2.5) exactly. A common approximation, which in many cases captures the essentials of the superconducting state

(*but not always*; see Sec. V), is the mean-field approximation. It corresponds to rewriting the quartic interaction of Eq. (2.5b) in terms of new auxiliary fields $\Delta(\mathbf{r},\tau), d_\alpha(\mathbf{r},\tau)$, the Hubbard Stratonovich fields, and *only* quadratic powers of the electron fields $\psi(\mathbf{r},\tau)$ and $\psi^*(\mathbf{r},\tau)$, and then setting these $\Delta(\mathbf{r},\tau), d_\alpha(\mathbf{r},\tau)$ to their saddle-point values. These saddle points correspond to what is traditionally taken as a mean-field solution of $\hat{H}$ in Eq. (2.4).

Here are three examples:

$$\Delta(\mathbf{r})=V\langle\psi(\mathbf{r}\uparrow)\psi(\mathbf{r}\downarrow)\rangle\ , \tag{2.6a}$$

$$d_1(\mathbf{r})=V[\langle\psi^\dagger(r\uparrow)\psi(\mathbf{r}\uparrow)\rangle+\langle\psi^\dagger(\mathbf{r}\downarrow)\psi(\mathbf{r}\downarrow)\rangle]\ , \tag{2.6b}$$

and

$$d_2(\mathbf{r})=V[\langle\psi^\dagger(r\uparrow)\psi(\mathbf{r}\downarrow)\rangle-\langle\psi^\dagger(\mathbf{r}\downarrow)\psi(\mathbf{r}\uparrow)\rangle]\ . \tag{2.6c}$$

The last two fields correspond to the usual charge and spin contributions and will be lumped into $\hat{H}_e$. Equation (2.6a) is related to the off-diagonal superconducting long-range order we are interested in. The mean-field approximation for $\hat{H}$ in Eq. (2.4) is then

$$\hat{H}_{\rm eff}=\hat{H}_e+\int d^3\mathbf{r}[\,\Delta(\mathbf{r})\psi^\dagger(\mathbf{r}\uparrow)\psi^\dagger(\mathbf{r}\downarrow)+\Delta^*(\mathbf{r})\psi(\mathbf{r}\downarrow)\psi(r\uparrow)]\ . \tag{2.7}$$

Incidentally, as is well known, the Hubbard-Stratonovich field of Eq. (2.6a) is only defined in a larger Hilbert space with varying number N of electrons. This change from a canonical to a grand canonical ensemble is very convenient, but certainly not necessary, and the mean-field approximation can be worked out equally well for fixed N (see below).

To solve for the eigenstates of $\hat{H}$ (and the corresponding Z), we follow the presentation of de Gennes (1966). Once we set this all up, it will help us identify (in the following sections) the similarities, differences, and crossover behavior along the whole $H_{c2}\to H_{c\infty}$ line.

1. Elementary excitations of $\hat{H}_{\rm eff}$

The elementary excitations of Eq. (2.7) are found by performing the Bogoliubov transformations,

$$\psi_\sigma(\mathbf{r})=\sum_n[u_n(\mathbf{r},\sigma)\gamma_n+v_n^*(\mathbf{r},\sigma)\gamma_n^\dagger]\ , \tag{2.8a}$$

where

$$[\hat{H}_{\rm eff},\gamma_n]=-E_n\gamma_n\ . \tag{2.8b}$$

From Eqs. (2.7) and (2.8) we see that the $u_n(\mathbf{r},\sigma)$ and $v_n(\mathbf{r},\sigma)$ satisfy the two coupled equations

$$E_nu_n(\mathbf{r},\sigma)=\left[\frac{(p-eA/c)^2}{2m}-E_F\right]u_n(\mathbf{r},\sigma)+\sum_\mu[\,U_{\sigma\mu}(\mathbf{r})u_n(\mathbf{r},\mu)+\Delta(r)\rho_{\sigma\mu}v_n(\mathbf{r},\mu)]\ , \tag{2.9a}$$

$$-E_nv_n(\mathbf{r},\sigma)=\left[\frac{(p+eA/c)^2}{2m}-E_F\right]v_n(\mathbf{r},\sigma)+\sum_\mu[\,U_{\sigma\mu}(\mathbf{r})v_n(\mathbf{r},\mu)+\Delta^*(r)\rho_{\sigma\mu}u_n(\mathbf{r},\mu)]\ , \tag{2.9b}$$

where

$$\rho_{\sigma\mu}\equiv\begin{bmatrix}0&1\\-1&0\end{bmatrix}$$

and E_n are the elementary excitations in the mean-field approximation.

2. Self-consistent equations for $\Delta(\mathbf{r})$

From Eqs. (2.6a) and (2.8a), $\Delta(\mathbf{r})$ is given by

$$\Delta(\mathbf{r})=\tfrac{1}{2}V\sum_{\sigma\mu}\sum_n\rho_{\sigma\mu}v_n^*(\mathbf{r},\sigma)u_n(\mathbf{r},\mu)[1-2f(E_n)]\ , \tag{2.10}$$

where $f(E_n)=1/(1+e^{\beta E_n})$. Since $\Delta(\mathbf{r})$ enters Eq. (2.9), Eqs. (2.9) and (2.10) constitute the self-consistent solution for $\hat{H}_{\rm eff}$ and the corresponding Z and $\Delta(\mathbf{r})$ (or, if we like, the saddle-point solution for the Hubbard-Stratonovich fields in the mean-field approximation). These two equations contain *all* possible effects for *any* size magnetic field in the presence or absence of impurities or Zeeman splitting within the mean-field approximation. Whatever we say, in later sections, about the behavior of superconductivity in high fields is included, within the mean-field approximation, in Eqs. (2.9) and (2.10). The full solution of these equations, for arbitrary magnetic field (e.g., an arbitrary uniform applied magnetic field) is very difficult. It will turn out, however, that in the quantum limit things actually become considerably simpler, and, in a certain sense, this is the "natural" limit in which to study the orbital effect of $\mathbf{H}$ on $\Delta(\mathbf{r})$.

3. The mean-field result for the $H_{c2}\to H_{c\infty}$ line

Assuming a continuous transition (in the mean-field approximation) on the $H_{c2}\to H_{c\infty}$ line, the order parameter $\Delta(\mathbf{r})$ goes to zero and Eqs. (2.9) and (2.10) can be treated as a perturbation to the electronic eigenfunctions ϕ_n in the normal metal, given by

$$\xi_n\phi_n(\mathbf{r},\sigma)=\left[\frac{1}{2m}\left[\mathbf{p}-\frac{e\,\mathbf{A}}{c}\right]^2-E_F\right]\phi_n(\mathbf{r},\sigma)+\sum_\mu U_{\sigma\mu}(\mathbf{r})\phi_n(\mathbf{r},\mu)\equiv\hat{H}_e\phi_n(\mathbf{r},\sigma)\ . \tag{2.11}$$

In Eq. (2.11) the zeroth-order u_n and v_n [i.e., with $\Delta(\mathbf{r})=0$] are

$$u_n^0=\begin{cases}\phi_n, & \xi_n>0\ ,\\ 0, & \xi_n<0\ ,\end{cases}\qquad v_n^0=\begin{cases}0, & \xi_n>0\ ,\\ \phi_n^*, & \xi_n<0\ .\end{cases} \tag{2.12}$$

To first order in $\Delta(\mathbf{r})$, u_n and v_n are given by

$$u_n = u_n^0 + \sum_{m \neq n} a_{nm}\phi_m \ , \quad v_n = v_n^0 + \sum_{m \neq n} b_{nm}\phi_m^* \ . \tag{2.13}$$

The coefficients a_{nm} and b_{nm} are obtained by the usual perturbation method:

$$a_{nm} = \begin{cases} 0 \ \ (\xi_n > 0) \ , \\ \dfrac{-1}{\xi_n + \xi_m} \displaystyle\sum_{\sigma\mu} \int d^3r_2 \phi_m^*(\mathbf{r}_2\sigma)\rho_{\sigma\mu}\phi_n^*(\mathbf{r}_2\mu)\Delta(\mathbf{r}_2) \ \ (\xi_n < 0) \ , \end{cases}$$

$$b_{nm} = \begin{cases} \dfrac{-1}{\xi_n + \xi_m} \displaystyle\sum_{\sigma\mu} \int d^3r_2 \phi_n(\mathbf{r}_2\sigma)\rho_{\sigma\mu}\phi_n(\mathbf{r}_2\mu)\Delta(\mathbf{r}_2) \ \ (\xi_n > 0) \ , \\ 0 \ \ (\xi_n < 0) \ . \end{cases} \tag{2.14}$$

If we now insert Eqs. (2.12), (2.13), and (2.14) into Eq. (2.10) (and replace E_n by ξ_n), we get, to lowest order in $\Delta(\mathbf{r})$, the following form for Eq. (2.10):

$$\Delta(\mathbf{r}_1) = V \int K_2^b(\mathbf{r}_1,\mathbf{r}_2)\Delta(\mathbf{r}_2) d^3r_2 \tag{2.15}$$

where

$$\begin{aligned} K_2^b(\mathbf{r}_1,\mathbf{r}_2) &= \frac{1}{\beta} \sum_{\omega} \sum_{n,m} \frac{\phi_n^*(\mathbf{r}_1)\phi_m^*(\mathbf{r}_1)\phi_n(\mathbf{r}_2)\phi_m(\mathbf{r}_2)}{(\xi_n - i\omega)(\xi_m + i\omega)} \\ &= \sum_{n,m} [1 - 2f(|\xi_n|)] \left[\frac{\phi_n^*(\mathbf{r}_2)\phi_n(\mathbf{r}_1)}{|\xi_n| + \xi_m} + \frac{\phi_n^*(\mathbf{r}_1)\phi_n(\mathbf{r}_2)}{|\xi_n| - \xi_m} \right] \\ &\quad \times \phi_m(\mathbf{r}_1)\phi_m^*(\mathbf{r}_2) \ . \end{aligned} \tag{2.16}$$

Equation (2.15) again describes the transition to superconductivity for *any* magnitude of the uniform magnetic field in the presence of any level of impurities (magnetic or nonmagnetic or both) and Zeeman splitting within the mean-field approximation. It then describes the transition along the whole $H_{c2} \to H_{c\infty}$ line.

4. The mean-field approximation in the vicinity of the $H_{c2} \to H_{c\infty}$ line

To get a first glimpse of the form of $\Delta(\mathbf{r})$ we can consider two regions. Just above the H_{c1} line a very small internal magnetic field $B(\mathbf{r})$ exists. $\Delta(\mathbf{r})$ resolves its frustration by screening this field in the form of a dilute vortex structure (see Fig. 2). This region will not be of interest here and will not be considered any further. Around the $H_{c2} \to H_{c\infty}$ line the form of $\Delta(\mathbf{r})$ first appears when Eqs. (2.9) and (2.10) are expanded to third order in $\Delta(\mathbf{r})$. Perhaps an easier (but equivalent) way is to write down the free energy F to quartic order in $\Delta(\mathbf{r})$ (appropriate to $\hat{H}_{\text{eff}}$) and then minimize with respect to $\Delta(\mathbf{r})$. The appropriate Feynman graphs for F are presented in Fig. 4; F is then given by

$$F = F_s + F_b \ , \tag{2.17a}$$

where

$$F_s = \int d^3r_1 d^3r_2 \Delta^*(\mathbf{r}_1)[K_2^b(\mathbf{r}_1,\mathbf{r}_2) - V^{-1}\delta(\mathbf{r}_1 - \mathbf{r}_2)]\Delta(\mathbf{r}_2) + \tfrac{1}{2}\int d^3r_1 d^3r_2 d^3r_3 d^3r_4 \Delta^*(\mathbf{r}_1)\Delta^*(\mathbf{r}_2)K_4(\mathbf{r}_1,\mathbf{r}_2,\mathbf{r}_3,\mathbf{r}_4)\Delta(\mathbf{r}_3)\Delta(\mathbf{r}_4) \ , \tag{2.17b}$$

$$F_b = \int d^3r \frac{(H+b)^2}{8\pi} \ . \tag{2.17c}$$

In Eq. (2.17c)

$$K_2^b(\mathbf{r}_1,\mathbf{r}_2) = \frac{1}{\beta} \sum_{w} G_{0\sigma}^b(w,\mathbf{r}_1,\mathbf{r}_2)G_{0-\sigma}^b(-w,\mathbf{r}_1,\mathbf{r}_2) \ , \tag{2.17d}$$

$$K_4(\mathbf{r}_1,\mathbf{r}_2,\mathbf{r}_3,\mathbf{r}_4) = \frac{1}{\beta} \sum_{w} G_{0\sigma}(w,\mathbf{r}_1,\mathbf{r}_2)G_{0-\sigma}(-w,\mathbf{r}_1,\mathbf{r}_3)G_{0-\sigma}(-w,\mathbf{r}_4,\mathbf{r}_2)G_{0\sigma}(w,\mathbf{r}_4,\mathbf{r}_3) \ , \tag{2.17e}$$

where $G_{0\sigma}^b(w,\mathbf{r}_1,\mathbf{r}_2)$ is the noninteracting Green's function that includes the contribution of $\mathbf{b}(\mathbf{r})$,

$$G_{0\sigma}^b(w,\mathbf{r}_1,\mathbf{r}_2) = \sum_n \frac{\phi_n^*(\mathbf{r}_1,\sigma)\phi_n(\mathbf{r}_2,\sigma)}{iw - \xi_n} \ , \tag{2.18a}$$

where

$$(iw-\hat{H}_e)G^b_{0\sigma}(w,\mathbf{r}_1,\mathbf{r}_2)=\delta(\mathbf{r}_1-\mathbf{r}_2)\ , \tag{2.18b}$$

while $G_{0\sigma}(w,\mathbf{r}_1,\mathbf{r}_2)$ is a solution of Eq. (2.18b) with $\mathbf{a}(\mathbf{r})$ set equal to zero in $\hat{H}_e$ of Eq. (2.1b). $G^b_{0\sigma}$ can be calculated to first order in $\mathbf{a}(\mathbf{r})$. (It turns out that this is all that is necessary for a consistent description of F to order $|\Delta|^4$.) It is given by

$$G^b_{0\sigma}(w,\mathbf{r}_1,\mathbf{r}_2)\approx G_{0\sigma}(w,\mathbf{r}_1,\mathbf{r}_2)-\int d^3r_3 G_{0\sigma}(w,\mathbf{r}_1,\mathbf{r}_3)\hat{h}(\mathbf{r}_3)G_{0\sigma}(w,\mathbf{r}_3,\mathbf{r}_2)\ , \tag{2.19a}$$

where

$$\hat{h}(\mathbf{r})=\left[(\mathbf{p}-\frac{e}{c}\mathbf{A}(\mathbf{r})\right]\cdot\mathbf{a}(\mathbf{r})+\mathbf{a}(\mathbf{r})\cdot\left[\mathbf{p}-\frac{e}{c}\mathbf{A}(\mathbf{r})\right]\ . \tag{2.19b}$$

Inserting Eq. (2.19) in Eq. (2.17d), we get for the first term on the right-hand side of Eq. (2.17a)

$$\int d^3r_1\int d^3r_2\Delta^*(\mathbf{r}_1)K^b_2(\mathbf{r}_1,\mathbf{r}_2)\Delta(\mathbf{r}_2)=\int d^3r_1\int d^3r_2\Delta^*(\mathbf{r}_1)K_2(\mathbf{r}_1,\mathbf{r}_2)\Delta(\mathbf{r}_2)+F_{s-b}\ , \tag{2.20a}$$

where

$$F_{s-b}=\int d^3r_1\int d^3r_2\Delta^*(\mathbf{r}_1)K_3(\mathbf{r}_1,\mathbf{r}_2)\Delta(\mathbf{r}_2)\ , \tag{2.20b}$$

with

$$K_3(\mathbf{r}_1,\mathbf{r}_2)=2\int d^3r_2\int d^3r_3\sum_w G_{0\sigma}(w,\mathbf{r}_1,\mathbf{r}_2)G_{0-\sigma}(-w,\mathbf{r}_1,\mathbf{r}_3)\hat{h}(\mathbf{r}_3)G_{0-\sigma}(-w,\mathbf{r}_3,\mathbf{r}_2)\ . \tag{2.20c}$$

Minimizing Eq. (2.17) with respect to $\Delta(\mathbf{r}_1)$ and $\mathbf{a}(\mathbf{r}_1)$, we get the following two self-consistent equations:

$$V^{-1}\Delta(\mathbf{r}_1)=\int d^3r_2[K_2(\mathbf{r}_1,\mathbf{r}_2)+K_3(\mathbf{r}_1,\mathbf{r}_2)]\Delta(\mathbf{r}_2)+\int d^3r_2\int d^3r_3\int d^3r_4\Delta(\mathbf{r}_2)K_4(\mathbf{r}_1,\mathbf{r}_2,\mathbf{r}_3,\mathbf{r}_4)\Delta^*(\mathbf{r}_3)\Delta(\mathbf{r}_4)=0 \tag{2.21a}$$

and

$$-\frac{1}{4\pi}\nabla\times\nabla\times\mathbf{a}(\mathbf{r})=\int d^3r_1\int d^3r_2\Delta^*(\mathbf{r}_1)\frac{\delta K_3(\mathbf{r}_1,\mathbf{r}_2)\Delta(\mathbf{r}_2)}{\delta\mathbf{a}(\mathbf{r})}\ . \tag{2.21b}$$

Again Eq. (2.21) describes, in the mean-field approximation, the order parameter around the $H_{c2}\rightarrow H_{c\infty}$ line no matter what the magnitude of the applied field.

Equation (2.21) takes an unfamiliar form. However, in the limit where the semiclassical phase-integral approximation is valid,

$$G^b_0(w,\mathbf{r}_1,\mathbf{r}_2)\approx\exp\{ie[\mathbf{A}(\mathbf{r})+\mathbf{a}(\mathbf{r})]\cdot(\mathbf{r}_1-\mathbf{r}_2)/\hbar c\}G_0(w,\mathbf{r}_1-\mathbf{r}_2)\ , \tag{2.22}$$

where now both $\mathbf{A}(\mathbf{r})+\mathbf{a}(\mathbf{r})$ are set equal to zero in G_0. In calculating $K^b_2(\mathbf{r}_1,\mathbf{r}_2)$ of Eq. (2.17b) in the presence of impurities (see Fig. 3), one multiplies $K_2(\mathbf{r}_1,\mathbf{r}_2)$ by $\exp\{ie[\mathbf{A}(\mathbf{r})+\mathbf{a}(\mathbf{r})]\cdot(\mathbf{r}_1-\mathbf{r}_2)\}$. Equations (2.21a) and (2.21b) reduce to the familiar Ginzburg-Landau forms,

$$\alpha(T)\psi(\mathbf{r})+\beta(T)|\psi(\mathbf{r})|^2\psi(\mathbf{r})+\frac{1}{2m}\left[-i\hbar\nabla-2e\frac{\mathbf{A}(\mathbf{r})+\mathbf{a}(\mathbf{r})}{c}\right]^2\psi(\mathbf{r})=0 \tag{2.23a}$$

and

$$\frac{1}{4\pi}\nabla\times\nabla\times[\mathbf{A}(\mathbf{r})+\mathbf{a}(\mathbf{r})]=\frac{-e\hbar}{imc}[\psi^*(\mathbf{r})\nabla\psi(\mathbf{r})-\psi(\mathbf{r})\nabla\psi^*(\mathbf{r})]-\frac{4e^2}{mc^2}\psi^*(\mathbf{r})\psi(\mathbf{r})\mathbf{A}(\mathbf{r})\ , \tag{2.23b}$$

where, for example, for a pure host (i.e., no impurities),

$$\alpha(T)=\left[\frac{-1}{CV}\right]+\left[\frac{\hbar^2}{C\beta 2m}\right]\sum_{n,w}\frac{1}{(iw-\xi_n)(iw+\xi_n)} \tag{2.24a}$$

and

$$\beta(T)=\frac{1}{C^2\beta}\left[\frac{\hbar^2}{2m}\right]^2\sum_{n,w}\frac{1}{(iw-\xi_n)^2}\frac{1}{(iw+\xi_n)^2}\ . \tag{2.24b}$$

Here

$$\psi(\mathbf{r})=\frac{(2mC)^{1/2}}{h}\Delta(\mathbf{r})\ ,$$

$$C=0.0165N(0)\left[\frac{\hbar v_F}{k_BT_c}\right]^2$$

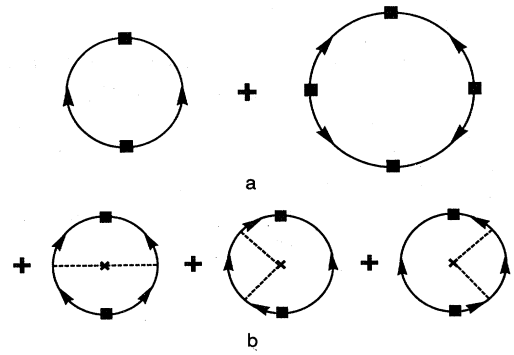

FIG. 4. Example of free-energy contributions. (a) Free-energy contribution of Eq. (2.17) to fourth order in the $\Delta(\mathbf{r})$. The filled squares are the $\Delta(\mathbf{r})$ and the arrowed lines the electron propagators. (b) Contribution to the free energy from impurities to lowest order in impurity scattering.

with $N(0)$ the density of states at the Fermi surface. The solution of Eq. (2.23) (along H_{c2}) is, of course, a saddle-point solution. Therefore a nonvanishing $\psi(\mathbf{r})$ does not necessarily correspond to an absolute minimum of $F(T)$. The first nonvanishing $\psi(\mathbf{r})$ can commence below the H_c line. In that case the superconductor is of type I; this occurs when $\kappa \approx \lambda/\xi < 1/\sqrt{2}$.

Finally, perhaps we should add that deriving Eq. (2.23b) directly from Eq. (2.20c) is very subtle, since Eq. (2.19a) assumes that $\hat{h}(\mathbf{r})$ is smaller than $|\mathbf{p}-(e/c)\mathbf{A}(\mathbf{r})|^2$ for all $\mathbf{r}$. This is certainly true along the transition line in the high-field limit. In the region along H_{c2}, where the semiclassical phase-integral approximation is valid, Eq. (2.22) is the appropriate starting point.

5. Ground-state wave function in the mean-field approximation

Most properties of any many-body system can be calculated without knowing the form for the many-body eigenstates (ground states or excited states). For example, Eqs. (2.21) or (2.23) describe the current distribution around the $H_{c2} \rightarrow H_{c\infty}$ line without ever calculating such eigenstates. In fact, even to calculate only the corresponding ground-state wave function, in the presence of a magnetic field, is very difficult. This is due to the breaking of time-reversal symmetry, leading to complicated mixing of the individual electron states in the pairing wave function, whose momenta are transverse to the field. This is what one usually refers to as "orbital frustration." As we shall show later, in the quantum limit this orbital frustration is resolved in a "natural" way. Time-reversal symmetry is, of course, still broken but, due to the constraints arising from the electrons being in the lowest Landau level, the ground-state wave function is easier to write down.

For future reference we write down the ground-state wave function $|\tilde{\phi}\rangle$ at zero field, which leads to the mean-field approximation discussed below. Directly from de Gennes (1966), this pairing wave function is given by

$$|\tilde{\phi}\rangle = \prod_n (u_n + v_n C_{n\uparrow}^{\dagger} C_{n\downarrow}^{*\dagger})|\text{vacuum}\rangle \ , \tag{2.25}$$

with $|u_n|^2+|v_n|^2=1$ where $C_{n\uparrow}^{\dagger}$ creates the state $\phi_n(\mathbf{r}\uparrow)$ and $C_{n\downarrow}^{*\dagger}$ creates the state $\phi^*(\mathbf{r}\downarrow)$ [see Eq. (2.11) with $\mathbf{A}=0$] and the product over n is over all the states. Note that $|\tilde{\phi}\rangle$ is invariant under time reversal and that $|\tilde{\phi}\rangle$ is not an eigenstate of the particle number operator. As already mentioned, this is very convenient but not essential. If we ignore the presence of impurities in $\hat{H}_e$, then the ϕ_n's become Bloch states and

$$|\tilde{\phi}\rangle = \prod_{\mathbf{k}} (u_{\mathbf{k}} + v_{\mathbf{k}} C_{\mathbf{k}\uparrow}^{\dagger} C_{\mathbf{k}\downarrow}^{\dagger})|\text{vacuum}\rangle \ . \tag{2.26}$$

C. Time reversal and impurities

In the absence of a magnetic field, nonmagnetic impurities have little effect on the critical temperature, unless the level of impurities is so high that they change the host to a new "alloy." An easy way to see this is to compare $K_2(\mathbf{r}_1,\mathbf{r}_2)$ [in Eq. (2.21a)] with and without the presence of a low level of impurities (see Fig. 3). In the presence of a magnetic field the interplay between the applied field and the impurities has important consequences. As already hinted in the Introduction, impurities can completely change the nature of the superconductor from type I to strongly type II (i.e., $\kappa \gg 1/\sqrt{2}$). Since our interest is primarily the quantum limit ($H_{c\infty}$), where the "penetration" of $\mathbf{H}$ is total (i.e., κ in some sense is infinite: however, one should always keep in mind that this is a clear oversimplification), it is important to cover in some detail the situation at low or modest fields (H_{c2}). We follow again the presentation of de Gennes (1966).

Equations (2.15) and (2.16) provide the mean-field approximation for any size magnetic field or level of impurities. As already mentioned in Sec. B.4, the effect of a low level of impurities can be calculated for K_2 [Eq. (2.16)] from the graphs of Fig. 3, in the absence of the magnetic field and then (in the semiclassical phase-integral approximation) multiplying K_2 by the exponential of the phase of the path of the vector potential. A more elegant way, which will also allow for a high level of impurities and provide further insight into the interplay between time-reversal symmetry and impurities, is to write $K_2(\mathbf{r}_1,\mathbf{r}_2)$ as

$$K_2(q) = N(0)k_B T \sum_{\omega} \int \frac{d\xi\, d\xi' g\left[\mathbf{q}, \frac{\xi-\xi'}{\hbar}\right]}{(\xi - i\hbar\omega)(\xi' + i\hbar\omega)} \ , \tag{2.27a}$$

where

$$g(\mathbf{q},\Omega) = \sum_{m,n} \overline{\langle n|e^{i\mathbf{q}\cdot\mathbf{r}_1}|m\rangle\langle m|e^{-i\mathbf{q}\cdot\mathbf{r}_2}|n\rangle}\,\delta(\xi_m - \xi_n - \hbar\Omega) \tag{2.27b}$$

and where

$$\langle n|e^{i\mathbf{q}\cdot\mathbf{r}}|m\rangle \equiv \int d^3r \phi_n(\mathbf{r}) e^{i\mathbf{q}\cdot\mathbf{r}} \phi_m(\mathbf{r}) \ ,$$

$$K_2(\mathbf{q}) \equiv \int d^3r_1 \int d^3r_2 e^{i\mathbf{q}\cdot\mathbf{r}_1} e^{-i\mathbf{q}\cdot\mathbf{r}_2} K_2(\mathbf{r}_1,\mathbf{r}_2) \ .$$

The bar in Eq. (2.27b) represents the impurity average of the ϕ_n's and ϕ_m's in Eq. (2.16). Equation (2.27) is equivalent to Eq. (2.16) for states $|n\rangle$ around the Fermi surface; i.e., the assumption of weak coupling; $g(\mathbf{q},\Omega)$ can also be written as

$$g(\mathbf{q},\Omega) = \frac{1}{2\pi\hbar} \int dt\, e^{i\Omega t} \overline{\langle n|e^{i\mathbf{q}\cdot\mathbf{r}_1(0)} e^{-i\mathbf{q}\cdot\mathbf{r}_2(t)}|n\rangle} \ , \tag{2.28}$$

where $\mathbf{r}(t)$ is the Heisenberg time dependence of $\mathbf{r}$. We were able to remove the intermediate states $|m\rangle$ because of time-reversal symmetry in the absence of $\mathbf{A}(\mathbf{r})+\mathbf{a}(\mathbf{r})$, specifically, because then both $|m\rangle$ and $\hat{K}|m\rangle$ [$\hat{K}$ given in Eq. (2.2)] are degenerate.

For an impure metal in which the mean free path l_d is small compared to the wavelength studied q^{-1}, $e^{i\mathbf{q}\cdot\mathbf{r}(t)}$ is

controlled by a diffusion (random-walk) process. If $D=v_F l_d/3$ is the diffusion coefficient, we have

$$\langle e^{-i\mathbf{q}\cdot\mathbf{r}(0)}e^{i\mathbf{q}\cdot\mathbf{r}(t)}\rangle_{E_F}=e^{-Dq^2|t|},\quad ql_d\ll 1\ , \tag{2.29a}$$

and therefore

$$g(\mathbf{q},\Omega)=\frac{1}{\pi\hbar}\frac{Dq^2}{\Omega^2+D^2q^4}\ . \tag{2.29b}$$

From Eq. (2.27) this leads to

$$K_2(\mathbf{q})=\frac{N(0)k_BT}{\hbar}\sum_{\omega}\frac{1}{Dq^2+2|\omega|},\quad q_d l\ll 1\ . \tag{2.30}$$

The fact that the effect of impurities enters only in the q^2 term of $K_2(\mathbf{q})$ [Eq. (2.30)] is an example of Anderson's theorem. Using Eq. (2.30) leads to a new value for C in Eq. (2.24),

$$C=\frac{\pi N(0)}{24}\frac{\hbar v_F l_d}{k_B T_c}\ .$$

For a dirty superconductor this C can be much smaller than in the clean limit. The "mass" of the Cooper pairs is now much heavier and the superconductor can become "more" type II.

In the above discussion we have introduced the effect of $\mathbf{A}(\mathbf{r})+\mathbf{a}(\mathbf{r})$ in the semiclassical phase-integral approximation. We can, however, write Eq. (2.16) in the form of Eqs. (2.27)–(2.29) for *any* size magnetic field. In the presence of $\mathbf{A}(\mathbf{r})+\mathbf{a}(\mathbf{r})$ removing the intermediate states $|m\rangle$, thus leading to Eq. (2.28), is no longer valid. We can do this, however, if we first insert the time-reversal operator [Eq. (2.2)] next to the $|m\rangle$'s. Equation (2.28) now takes the form

$$g(\mathbf{q},\Omega)=\frac{1}{2\pi\hbar}\int dt\, e^{i\Omega t}\langle n|e^{-i\mathbf{q}\cdot\mathbf{r}_1(t)}\hat{K}(t)\hat{K}^{\dagger}(0)e^{-i\mathbf{q}\cdot\mathbf{r}_2(t)}|n\rangle \tag{2.31a}$$

where

$$\hat{K}(t)=\exp\left[i\frac{\mathcal{H}_e t}{\hbar}\right]\hat{K}\exp\left[+i\frac{\mathcal{H}_e t}{\hbar}\right]\ . \tag{2.31b}$$

(Note the unusual sign in the last exponent, due to the fact that $\hat{K}i=-i\hat{K}$.) The rate of change of $\hat{K}$ is given by

$$\frac{d\hat{K}}{dt}=\frac{i}{\hbar}[\mathcal{H}_e,\hat{K}]=\frac{-ie}{m\hbar c}(\mathbf{p}\cdot\mathbf{A}+\mathbf{A}\cdot\mathbf{p})\hat{K}\ . \tag{2.31c}$$

This result for $g(\mathbf{q},\Omega)$ and therefore $K_2^b(\mathbf{r}_1,\mathbf{r}_2)$, in Eq. (2.15), is completely general (in the weak-coupling limit) and true for any level of impurities or any strength of the magnetic field. The effect of the magnetic field (or breaking of time-reversal symmetry) resides entirely in $\hat{K}(t)$. Equation (2.31) cannot be calculated in general. However, in the dirty limit, where the motion of the electrons is diffusive on a scale of the magnetic orbit, $g(\mathbf{r}_1,\mathbf{r}_2,\Omega)$ can be shown to satisfy a diffusion equation (see de Gennes, 1966) with the consequence that the H_{c2} line [or Eq. (2.23)] is valid all the way to $T=0$; the crossover region to $H_{c\infty}$ (see Fig. 1) disappears. Now we come to a possible misconception already alluded to in the Introduction. On the surface, this conclusion appears to be very general and valid for any $\mathbf{H}$. It is important to realize that it is not so. The diffusive propagation of the electron must persist even within the cyclotron orbit (or magnetic length). If this orbit is smaller than l_d, then Eq. (2.31a) is not the appropriate starting point. The full Landau-level structure for the states $|m\rangle$ must be used; the consequences of this will occupy much of the rest of this review.

In low-carrier-density systems, at high fields, and in particular in the quantum limit, l is comparable to the average electron separation l_e. To get to the high-field limit, the purity of the material must be such that $v_F\tau\gg l_e$; this is not particularly hard to achieve in doped semiconductors and semimetals. In the high-field limit, then, there will be a reentrance to the $H_{c\infty}$ at higher fields. So here is the possible source of confusion we want to avoid. Often one associates type-II behavior with "dirty" superconductors. In fact, perfectly pure systems with low carrier density are commonly strongly type II. But even if a particular material is type I in a pure phase and is made dirty intentionally to convert it to type II, one should not take the simplistic view that higher and higher fields (as we travel along $H_{c\infty}$) reflect a more and more type-II superconductor, implying the need for larger and larger impurity concentration. This thinking would lead us back to the situation in which the diffusive result (discussed above) for $g(\mathbf{q},\Omega)$ is appropriate and $H_{c\infty}$ would be eliminated from the phase diagram in Fig. 1. This reasoning, however, is not correct. It is important to recognize that there is in fact no direct connection between the low-field and the high-field limits of superconductivity. In the most extreme case we can even imagine a sample that has no superconducting instability at low (or zero) fields, whose effective interparticle interaction becomes attractive when $H\approx H_{\rm QL}$, thus leading to high-field-limit superconductivity (see our discussion on the effect of $\mathbf{H}$ on $v_{\rm eff}$). Consequently a given promising material can be made extremely pure, and the effect of impurities can be minimized so as to make the situation most favorable for the high-field superconducting state. This is a very important point to appreciate, since it makes the experimental "quest" for high-field superconductivity a realistic one in a proper class of materials.

In this section we have presented some general properties of a superconducting state in an external magnetic field. We have outlined what is involved in the solution of the mean-field equations and have discussed the interplay of time-reversal symmetry and impurity scattering, which is of concern in real systems. Now we turn to the explicit solution of the mean-field theory which is the source of the phase diagram in Fig. 1.

III. THE TRANSITION LINE

Let us now search for instabilities of the electron gas with no Zeeman splitting [$g=0$ in Eq. (2.1b)] in the

quantum limit, i.e., with all the electrons in the lowest Landau level (Rasolt, 1987; Tešanović, Rasolt, and Xing, 1989). We then need to consider the various cross sections of the e-h *and* e-e channels, in the lowest Landau level. In Fig. 5 we present the cross section for the e-h scattering; Fig. 3 corresponds to the e-e channel. In both cases the ladder graphs can be readily summed, and in both cases the cross section becomes singular at a critical temperature, which in weak coupling (see below for a discussion of strong-coupling corrections) is given by

$$T_c = 1.14\Omega \exp[-2\pi l^2/c_{\text{e-h (e-e)}}N_1(0)|V|] \ . \qquad (3.1)$$

Here Ω is the energy cutoff on V and $N_1(0)=m/[2\pi k_F(H)]$ is a 1D density of states at the Fermi level of left- (right-) going particles. In Eq. (3.1), Fig. 3 corresponds to a positive V and Fig. 5 to a negative V, where V is the effective e-e interaction in Eq. (2.4). Figure 5 is the well known instability towards spin-density waves, first considered by Celli and Mermin (1965). In this case we should use $c_{\text{e-h}}=2$ in the exponential of Eq. (3.1). If V is attractive, we can have a charge-density-wave instability in the e-h channel (Fröhlich and Terreaux, 1965; note that these authors consider this instability the quantum-limit analog of a superconducting state, but their superconducting state is a Fröhlich "superconductor," which is in fact a CDW state. Consequently such a state does not have the orbital frustration characteristic of a true superconductor and is different from the BCS-like state discussed in this review). However, there is also an instability in the e-e channel. Here we must use $c_{\text{e-e}}=1$.

What is somewhat unexpected in the above is that the transition temperature for the e-e instability is finite. There are two questions that naturally come to mind at this point. First, it seems that Eq. (3.1) is at odds with the familiar result that a magnetic field suppresses superconductivity through orbital frustration and an ensuing diamagnetic pair breaking. In Secs. III and IV we shall examine this "superconductivity" in great detail and show that the finite transition temperature arises through the transformed nature of orbital frustration. In fact, the diamagnetic pair breaking is effectively eliminated in these high fields, its only vestige being $c_{\text{e-e}}=\frac{1}{2}c_{\text{e-h}}$ (note that in the 1D $H=0$ case $c_{\text{e-e}}=c_{\text{e-h}}$.). As the field increases, the superconducting transition temperature is strongly enhanced through the density-of-states effect, as are CDW or SDW instabilities. This leads us to the second question: Can this superconductivity overcome other instabilities and emerge as a ground state of some suitable system? We shall postpone a detailed discussion of this question until Sec. VI. We do, however, give a preview of our answer. While for the very simplified model used in deriving Eq. (3.1) it seems that the CDW state will be a favored state for attractive V, since $c_{\text{e-h}} > c_{\text{e-e}}$, in a realistic situation, with the attraction arising from electron-phonon interaction, and in the presence of long-range Coulomb forces, the competition will most likely be between superconductivity and SDW states, with CDW states being largely disqualified by the direct Coulomb repulsion (Tešanović and Halperin, 1987). Even for finite Zeeman splitting, with $g<2$, as long as both spins are occupied, Celli and Mermin found a stable SDW state. We shall show below that the same holds true for the superconducting instability. The SDW instability has motivated considerable experimental effort, while the superconducting instability was hardly contemplated either theoretically or experimentally. There is no reason why both should not exist, and in truly 1D systems both e-e and e-h channels have been considered on an equal footing (see Sec. V). In fact, in Sec. VI we shall argue in favor of an attractive e-e interaction (V positive) in the quantum limit (Rasolt, 1987), which should result in superconductivity.

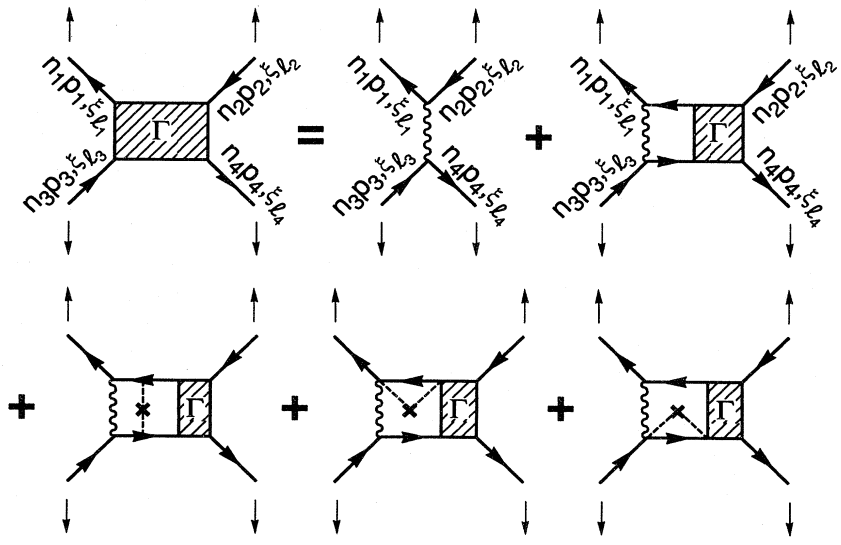

FIG. 5. The electron-hole scattering amplitude Γ of two different spin states in the ladder approximation. The wavy line is the interparticle interaction. The arrowed lines are the noninteracting single-particle propagators. The last three graphs include the effects of impurities to lowest order in impurity scattering.

A. The pure type II with no Pauli pair breaking

The transition line, for any **H**, is described as the solution of Eq. (2.15). The states $\phi(\mathbf{r})$ in Eq. (2.16) are eigenstates of $\hat{H}_e$ with $U_{\sigma v}$ and $\mathbf{a}(\mathbf{r})$ set equal to zero and $\mathbf{A}(\mathbf{r})=\frac{1}{2}\mathbf{H}\times\mathbf{r}$ (we shall always work in the symmetric gauge unless explicitly stated otherwise). Then

$$\phi_i(\mathbf{r})=\frac{e^{ik_z\zeta}}{\sqrt{L}}\phi_{n,m}(z)\ , \tag{3.2a}$$

$$\phi_{n,m}(z)=(2^{m+n})^{1/2}/(2\pi m!n!)^{1/2}\exp(\tfrac{1}{4}|z|^2)\left[\frac{\partial}{\partial z^*}\right]^m\left[\frac{\partial}{\partial z}\right]^n\exp(-\tfrac{1}{2}|z|^2)\ . \tag{3.2b}$$

in Eq. (3.2b) k_z is the momentum parallel to **H**, and L is the macroscopic length of the system along **H**, $z\equiv(x-iy)/l, \mathbf{r}=(x,y,\zeta)$. Moreover, n is the Landau-level index and m is the index for the manifold of degenerate states of number $N=A/(2\pi l^2)$, with A the area of the system perpendicular to **H**. The eigenstates ξ_i in Eq. (2.16) are $\xi_i=(n+\frac{1}{2})\hbar\omega_c+\hbar^2k_z^2/2m$. Using Eq. (3.2) in Eq. (2.16), one can write a closed form for Eq. (2.15). There are a number of different equivalent forms for this equation (depending on the gauge, etc.). Here we use the form first derived by Rajagopal and Vasudevan (1966a, 1966b) in their study of the low-field limit:

$$\Delta(\mathbf{r})=V\int\mathcal{G}(\mathbf{r}')\exp\left[\frac{i}{l^2}\hat{H}\cdot(\mathbf{r}\times\mathbf{r}')\right]\Delta(\mathbf{r}+\mathbf{r}')d^3\mathbf{r}'\ , \tag{3.3a}$$

where

$$\mathcal{G}(\mathbf{r})=\frac{1}{(2\pi l^2)^2}\sum_{n',n=0}^{\infty}\exp\left[\frac{-|z|^2}{2}\right]L_n\left[\frac{|z|^2}{2}\right]L_{n'}\left[\frac{|z|^2}{2}\right]$$
$$\times\int\int\frac{dk_z dk_z'}{(2\pi)^2}\exp[i(k_z+k_z')\cdot\zeta]\frac{\tanh[\beta\epsilon_n(k_z)/2]+\tanh[\beta\epsilon_{n'}(k_z)/2]}{\epsilon_n(k_z)+\epsilon_{n'}(k_z)}\ , \tag{3.3b}$$

where L_n are the Laguerre polynomials and

$$\epsilon_n(k_z)=(n+\tfrac{1}{2})\hbar\omega_c+\frac{\hbar^2k_z^2}{2m}\ .$$

It was first noted by Rajagopal and Vasudevan that $\Delta(\mathbf{r})=\Delta_0\exp(-|z|^2/2)$ is a solution of Eq. (3.3). It was further observed by Tešanović, Rasolt, and Xing (1989) that any holomorphic form $f(z)\exp(-|z|^2/2)$ is a solution of Eq. (3.3) for any H; this degeneracy of solutions is important in understanding the nature of the order parameter (see Sec. IV). This form of $\Delta(\mathbf{r})$ has the lowest kinetic energy of the center-of-mass motion of Cooper pairs. Other forms of $\Delta(\mathbf{r})$, having higher kinetic energy, will generally lead to much lower $T_c(H)$ in 3D. In 2D (Rasolt, 1991, 1992), however, special circumstances may arise where other channels in $\Delta(\mathbf{r})$ become competitive. For a discussion of the solutions of (3.3a) in different channels in 2D the reader should consult MacDonald *et al.* (1992) and Rajagopal and Ryan (1991).

Using $f(z)\exp(-|z|^2/2)$, we find that Eq. (3.3a) reduces to

$$1=\frac{V}{2\pi l^2}\sum_{n',n=0}^{\infty}\frac{(n'+n)!}{n'!n!}\left[\frac{1}{2}\right]^{n'+n}I_{n',n}\ , \tag{3.4a}$$

where

$$I_{n',n}=\int\frac{dk_z}{2\pi}\frac{\tanh[\beta\epsilon_n(k_z)/2]+\tanh[\beta\epsilon_{n'}(k_z)/2]}{\epsilon_n(k_z)+\epsilon_{n'}(k_z)}\ . \tag{3.4b}$$

In principle, Eq. (3.4) contains the whole range of the $H_{c2}\rightarrow H_{c\infty}$ line. Here, for simplicity, we have assumed that V is independent of H. This, of course, is generally not true, and the $V(H)$ dependence has to be studied for each particular physical situation (see our discussion of v_{eff} in the high-field limit). At first glance, it seems reasonable that $T_c(H)$ should be quite close to $T_c^{\text{AG}}(H)$. The semiclassical phase-integral approximation is correct in the limit when the number of occupied Landau levels, n_c, goes to infinity. For a typical superconductor, $n_c[H\simeq H_{c2}(0)]\simeq(E_F/T_{c0})^2\gg1$, and this should be an excellent approximation. Assuming a semiclassical-limit approximation (SCLA) $n_c\gg1$, Rajagopal and Vasudevan (1966a, 1966b) studied Eq. (3.4) along the lower part of

the H_{c2} line. The reader should note that the semiclassical-limit approximation is different from the semiclassical phase-integral approximation used by Gor'kov. In the former, the Landau-level structure is not ignored but is included approximately by using the Poisson summation formula and replacing sums by integrals. Using the Poisson summation formula, Rajagopal and Vasudevan found a small correction to the standard H_{c2} line of Fig. 1,

$$T_c^{\mathrm{SCLA}}(H)\simeq T_c^{\mathrm{AG}}(H)-T_c^{\mathrm{AG}}\left[\frac{2\omega_c}{E_F}\right]^{1/2}\times\exp\left[-\frac{2\pi^2 T_c^{\mathrm{AG}}}{\omega_c}\right]\sin\left[\frac{2\pi E_F}{\omega_c}+\frac{\pi}{4}\right], \tag{3.5}$$

where $T_c^{\mathrm{AG}}(H)$ is the Abrikosov-Gor'kov transition temperature [i.e., the semiclassical phase-integral approximation result for the $H_{c2}(T)$ line]. $T_c^{\mathrm{SCLA}}(H)$ has an oscillatory nature due to the presence of Landau levels but has, on the average, a monotonically decreasing trend as a function of H. The corrections are small and, in particular, $T_c^{\mathrm{SCLA}}[H\to H_{c2}(0)]\to 0$. Thus the nature of the superconducting state remains basically the same as in the semiclassical phase-integral approximation and is reasonably described in Eq. (2.2b) (however, see below).

Equation (3.4) contains yet another, more exotic limit: the high-field limit of Tešanović, Rasolt, and Xing (1989). To appreciate how this limit arises, one must realize that the solution to Eq. (3.4) depends very much on where one is in the H-T phase diagram. In fact, the "seed" of this new limit appears even at low fields. The first sign of serious deviation from the semiclassical phase-integral approximation occurs at a temperature T^* given by $\omega_c[H_{c2}(T^*)]=2\pi T^*$. It follows that $T^*\sim T_{c0}^2/E_F \ll T_{c0}$. If $T_c(H)<T^*$, the full Landau-level structure begins to play an essential role and Eq. (3.5) is not appropriate (Tešanović, Rasolt, and Xing, 1989). For the great majority of superconducting systems T^* is a very low temperature and is in the 1-mK range. Thus it would appear that there is little practical interest in studying this very-low-temperature regime. However, in high-temperature oxide superconductors or in Nb-Sn systems, T^* may be sufficiently high to allow for the observation of these initial deviations from the Abrikosov-Gor'kov theory (Tešanović, Rasolt, and Xing, 1989; Maniv, Rom, Vagner, and Wyder, 1991). But a dramatically different situation is obtained in the limit of very strong fields, $\omega_c \gg 2\pi T$ (the high-field limit). The extreme example of this is the situation in which only a single Landau level is occupied (the quantum limit). This happens for

$$H>H_{\mathrm{QL}}=2mcE_F/(3\sqrt{2})^{2/3}e\sim(E_F/T_{c0})^2H_{c2}(0)\ ,$$

where $H_{c2}(0)$ refers to the standard result. In this limit, the integral equation (3.3) reads

$$\frac{1}{V}\Delta(z,z^*)=\beta^{-1}\sum_{\omega}\sum_{k_z}\frac{1}{\omega^2+(\epsilon_{k_z}+\frac{1}{2}\omega_c)^2}\int d^2r'\frac{1}{(2\pi l^2)^2}\exp(-|z|^2/2-|z'|^2/2+zz'^*)\Delta(z',z'^*)\ . \tag{3.6}$$

We have neglected the Zeeman splitting ($g=0$) and assumed that Δ is uniform along $\mathbf{H}$.

In Eq. (3.6) we can decouple the (x,y) plane from the ζ axis. There is an infinite degenerate manifold of solutions, given by $\Delta(z,z^*)=\Delta f(z)\exp(-|z|^2/2)$, where $f(z)$ is an arbitrary holomorphic function, while

$$T_c(H>H_{\mathrm{QL}})=1.14\Omega\exp\left[-\frac{2\pi l^2}{N_1(0)V}\right]$$

[Eq. (3.1)]. This result, of course, is also contained in Eq. (3.4). The approximation of the constant density of states in the k_z integration of Eq. (3.6) is accurate for weak coupling, i.e., $\Omega \ll E_{F0}$, where E_{F0} is the Fermi energy for the lowest Landau level. As $\mathbf{H}$ increases, one eventually gets into a strong-coupling regime where $\Omega > E_{F0}$. This situation will be discussed shortly. The above result seems puzzling, since $T_c(H>H_{\mathrm{QL}})$ is comparable to $T_c(H=0)$ [T_c's for $H=2.13H_{\mathrm{QL}}$ and $H=0$ are equal if one assumes that $V(H_{\mathrm{QL}})\cong V(H=0)$, i.e., that V is independent of H; recall the discussion of Eq. (2.3)] and it grows with the field: $2\pi l^2/N_1(0)\propto H^{-2}$ as shown in Fig. 6. (Of course, T_c cannot grow indefinitely, and the strong-coupling effects will renormalize it back to zero for $H\gg H_{\mathrm{QL}}$. The simplest source of reduction in T_c will be the change in the cutoff frequency from Ω to E_{1F}, where E_{1F} is the quasi-one-dimensional Fermi energy, once $\Omega<E_{1F}$ (Rasolt, 1987). This situation is also depicted in Fig. 6.) Furthermore, to understand the solution of Eq. (3.4) when the number of occupied Landau levels $n_c>1$, we note that Eq. (3.4) has two types of terms: *diagonal*, for which the Landau-level index is the same, and *off-diagonal*, where the Landau-level indices differ. Only diagonal terms possess a Cooper singularity, and, for $H\le H_{\mathrm{QL}}$, when n_c is not "too large," one expects that neglecting the off-diagonal terms will be a good approximation. We call this the quantum-limit approximation (QLA). In this approximation we obtain

$$T_c^{\mathrm{QLA}}(H)=1.14\Omega\exp\left[-\frac{2\pi l^2}{V}\left[\sum_{n=0}^{n_c}N_{1n}(0)\frac{(2n)!}{2^{2n}(n!)^2}\right]^{-1}\right], \tag{3.7}$$

where $N_{1n}(0)$ is the 1D density of states for the nth Landau level. (In the above equation it was assumed that $\Omega\ll\omega_c$ and that the Fermi level is $\sim\Omega$ away from the

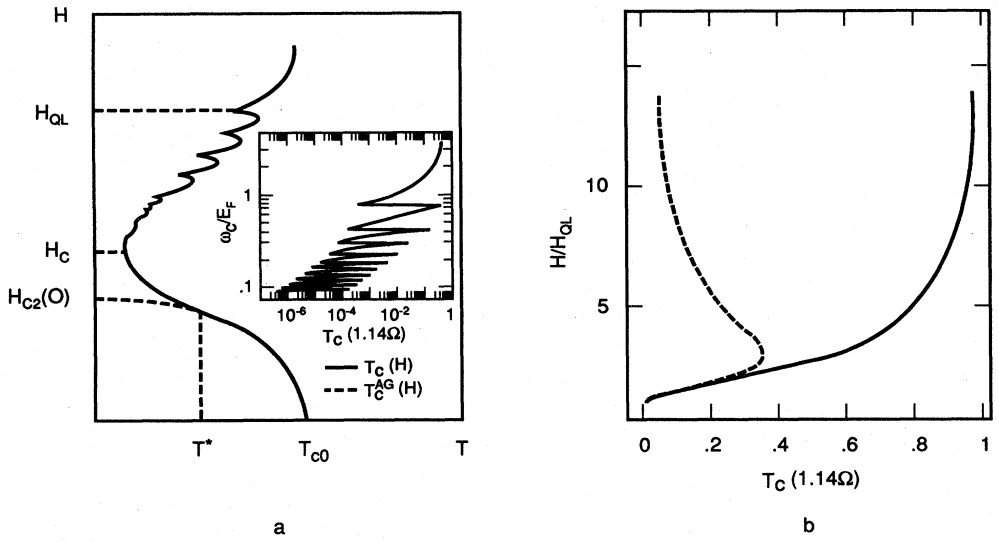

FIG. 6. A more detailed presentation of Fig. 1. (a) The solid line is an artist's rendering of the $T_c(H)$ curve for a BCS-like type-II superconductor. The dashed line is the Abrikosov-Gor'kov result. The physical significance of H_C, H_{QL}, and T^* is explained in the text. The inset shows T_c evaluated in the high-field limit, including up to 11 Landau levels [we have chosen $N(0)V=0.6$ and have used the standard Coulomb cutoff to round off divergencies in the density of states (see text for discussion of this point)]. Actually, for low-carrier-density materials in the high-field limit, $T_c(H)$ shown here represents a lower bound for a BCS superconductor. Further enhancement of the coupling constant will arise due to a reduction in the average Coulomb repulsion when $k_F^{-1} \simeq l$ (see text). However, see Secs. III and VI for discussion of strong-coupling effects. (b) $T_c(H)$ of a BCS superconductor in the quantum limit. $\lambda(H=H_{QL})$ is set to 0.18. Note the rapid rise of T_c as H increases. Such a rise is unphysical for $\Omega > E_{1F}$ when Ω has to be replaced by E_{1F} as the cutoff in the BCS formula. This is illustrated by the dashed line. We have chosen Ω to be $\sim 10\%$ of the 3D Fermi energy.

singularities in the density of states. Clearly, this approximation becomes increasingly unreliable as one moves to lower fields.) $T_c^{\mathrm{QLA}}(H)$ displays an oscillatory behavior reflecting the Landau-level structure and has a monotonically *increasing* trend (on the average) as a function of H. Consequently the quantum-limit approximation can never recover the Abrikosov-Gor'kov low-field limit. The inset of Fig. 6 shows $T_c^{\mathrm{QLA}}(H)$. As the number of Landau levels increases (H decreases) T_c^{QLA} decreases rapidly. As the Fermi level crosses each Landau level the density of states in Eq. (3.7) diverges. This is an unphysical divergence and it can be removed in one of two ways: (a) by a more accurate evaluation of the BCS equation for T_c (in other words, without making a constant-density-of-states approximation once $E_{Fn} < \Omega$, where E_{Fn} is the quasi one-dimensional Fermi energy for the nth Landau level); (b) by more physical effects of strong-coupling renormalization and thermal and/or disorder broadening of the density of states. Effectively, the Landau level crossing the Fermi energy is "turned off," and it does not contribute to T_c. In Fig. 6 a Coulomb "cutoff" $\mu^* = \mu/[1+\mu \ln(E_{Fn}/\Omega)]$ was included to smooth out the oscillations ($\mu = 0.15$).

The qualitative behavior of $T_c^{\mathrm{QLA}}(H)$ in Eq. (3.7) is completely opposite to $T_c^{\mathrm{SCLA}}(H)$ in Eq. (3.5). This new behavior, characteristic of the high-field limit, signals a complete breakdown of the semiclassical phase-integral approximation. The vortex lattice reaches its quantum limit, in which the orbital frustration results in the enhancement of the superconducting transition temperature. This may seem counterintuitive, since the increase in H enhances orbital frustration and time-reversal symmetry breaking. The fact is, however, that orbital frustration does not always result in a suppression of superconductivity. In low fields the Landau-level structure is thermally smeared (above T^*), and the electronic Green's function is still well represented by its plane-wave form, corrected only by the field-dependent phase factor. The order parameter is formed as a linear combination of the anomalous expectation values $\langle c_{\mathbf{k}\uparrow} c_{-\mathbf{k}+\mathbf{q}\downarrow} \rangle$. The wave vectors $\mathbf{q}$ that dominate this linear combination have the magnitude given by $\sim \pi/r_s$, where r_s is the separation between vortices. As H increases, $r_s \cong \sqrt{2}l$ decreases, and one has to reach farther and farther away from the Fermi surface in order to construct the proper $\Delta(\vec{r})$. This leads to a cost in condensation energy and destruction of the superconducting state, once $r_s \sim \xi(T)$ [$H_{c2}(T)$ is defined by $\xi(T) \cong l$]. This summarizes the traditional view of this problem. But, below T^*, or in very high fields, the Landau-level structure must be included explicitly, with the order parameter now having the form

$$\sum_{nn'}\sum_{mm'}\alpha_{mm'}^{nn'}\langle c_{k_z nm\uparrow}c_{-k_z n'm'\downarrow}\rangle \ .$$

In the high-field limit this sum is dominated by the $n=n'$ terms. This transforms the effect of orbital frustration, since now the correct form of $\Delta(\vec{r})$, with the required density of zeros, can be built without an appreciable cost in condensation energy. In fact, in the quantum limit the magnetic field acts only as an external constraint, and, once this constraint on the transverse motion is satisfied, the BCS form of the condensation energy comes from the motion along the field (if one considers a 2D problem there is really no BCS weak-coupling solution. One has to consider an infinitely degenerate Landau-level structure in the presence of a finite interaction, which leads to a very strongly coupled problem). The lowest few Landau levels, participating in the pairing correlations, "naturally" lead to the required form of $\Delta(\mathbf{r})$. This new role of orbital frustration can be understood only by considering the nature of the superconducting state below $T_c(H)$ and will be made clear in the following sections. What should be emphasized here is that T_c^{QLA} represents a completely "legitimate" limit of superconductivity in a magnetic field, in which orbital frustration leads to the elimination of diamagnetic pair breaking, in sharp contrast to $T_c^{\mathrm{SCLA}}(H)$ and the low-field limit.

To obtain the crossover from the high-field behavior given by Eq. (3.7) to the low-field limit of Eq. (3.5) and to the familiar Abrikosov-Gor'kov theory, it is necessary to include the off-diagonal terms in Eq. (3.4). Although these terms do not have the Cooper singularity, their number grows as n_c^2, as opposed to n_c for the diagonal terms, when n_c becomes large. Thus, while the diagonal terms dominate at high fields and lead to an increasing $T_c(H)$, at low fields the off-diagonal terms take over, resulting in a decreasing $T_c(H)$. Because the sign of these off-diagonal terms is always positive, they create a countereffect to the decreasing critical temperature of the diagonal terms [Eq. (3.7)]. At some field H_c the off-diagonal terms will become dominant, leading to a crossover from $T_c^{\mathrm{QLA}}(H)$ to a smooth (smooth only in some average sense, since the fast oscillations in the density of states have to be dealt with) transition to the Abrikosov-Gor'kov curve, as depicted in Fig. 1. With off-diagonal terms present, $T_c(H)$ cannot be written in a closed form and has to be evaluated numerically. The results are summarized in Fig. 6(a) in the solid line. It is, of course, clear that this solid line is an artist's rendering of the overall trend in $T_c(H)$ and that there will be rapid oscillations throughout this region due to the Landau-level structure. We find that as long as n_c is less than ~ 25 or so, Eq. (3.7) is a very good approximation to a numerical $T_c(H)$. This is because an off-diagonal term contributes only if the energy difference between two Landau levels $(n\omega_c)$ is less than Ω. For larger n_c, once $\omega_c \ll \Omega$, the off-diagonal terms become increasingly important. This now signals the breakdown of the quantum-limit approximation as one moves from the high-field limit down to low fields ($n_c \gg 1$) and indicates that some form of quasiclassical approximation should be appropriate. This crossover has been investigated in some detail by Gunther and Gruenberg (1966), Gruenberg and Gunther (1968), and, more recently, by Maniv, Markiewicz, Vagner, and Wyder (1990), and by Maniv, Rom, Vagner, and Wyder (1991) using quasiclassical approximations for the Landau levels. Using a rough approximation for the off-diagonal terms and defining H_C from $dT_c/dH=0$, we find $H_C \sim (E_F/T_{c0})H_{c2}(0)$. Since the off-diagonal terms are not singular, and therefore are not dominated by contributions around E_F, the exact shape of this crossover region would require the calculation of the off-diagonal terms $I_{n',n}$ [in Eq. (3.4)] over the full energy range of ϵ_{k_z}. Throughout the crossover region, T_c is typically extremely small ($<10^{-10}$ Ω), and only the high-field limit [in which $T_c^{\mathrm{QLA}}(H)$ is perfectly appropriate] will typically have observational significance. However, as stated earlier, in type-II superconductors with very high upper critical fields, the crossover region may be observable. In such systems the temperature T^* is a sizable fraction of $T_c(H=0)$, and one may well be able to reach the crossover region with available fields and still have an observable transition temperature. A particularly detailed study of $T_c(H)$ in the whole field range is presented by Maniv *et al.* (1991). These authors use the semiclassical approximation and demonstrate that the crossover to the high-field limit can occur in realistic circumstances, particularly in quasi-2D strongly type-II systems. One should emphasize that T_c remains finite at all fields, a result obvious from Eq. (3.4) and first explicitly stated by Gruenberg and Gunther (1968). It is important to realize, however, that finite $T_c(H)$ obtained from Eq. (3.4) *does not* imply that one has a stable superconducting ground state at all fields. Whether such a state exists can be decided only by analyzing the nature of the state below $T_c(H)$ using the Ginzburg-Landau or some other approach that allows one to study the situation with *finite* $\psi(\mathbf{r})$. For example, in type-I superconductors, even though $T_c(H)$ exists it is preempted by a first-order transition at the H_c line. The nature of the superconducting state and its stability below $T_c(H)$ must be studied simultaneously (Tešanović, Rasolt, and Xing, 1991a, 1991b).

In the above discussion, we have made several tacit assumptions. As already stated, we have assumed that V is not a function of H. An additional assumption, which was considered here for simplicity, is that in the low-field limit the system is a type-II superconductor. In that case there must be a continuous $T_c(H)$ curve joining the low- and high-field limits of BCS superconductivity (continuous only in some average sense, as is clear from our discussion). But, in accordance with the above discussion, it is perfectly possible for a high-field-limit superconductor to behave as type-I superconductor in low fields, with a reentrance at high fields. In fact, a high-field-limit superconductor may not be a low-field superconductor at all, but instead have a ground state of completely different

symmetry (SDW, CDW, Fermi liquid, etc.). If this is the case, various phase transitions will take place as the external field increases, resulting ultimately in a high-field-limit superconducting state. Study of such transitions is obviously a very complex problem, involving detailed understanding of the interacting electron systems in a varying field. Finally, these results are valid for an ideal system in the absence of Zeeman splitting and disorder. We now turn to a discussion of these two perturbations in the high-field limit.

B. Effects of Pauli pair breaking and disorder

The discussion of the previous section ignored Zeeman splitting. The effective g factor can indeed be zero if we consider the intervalley pairing in multivalley semiconductors and semimetals (Rasolt, 1990). But, even in those cases, there can be a contribution from the spin-singlet channel and it is therefore important to understand how Pauli pair breaking will affect the results of Sec. III.A. Naively, one might expect that Pauli pair breaking would simply wipe out the high-field limit of superconductivity. We know that in the low-field limit Pauli pair breaking leads to the Pauli critical field H_p, which is simply obtained by comparing the Zeeman energy with T_c. If the Zeeman splitting is larger, then no spin-singlet superconductivity is possible (this is well known as the Chandrasekhar-Clogston limit). One can go slightly above the Chandrasekhar-Clogston limit if a superconducting state with a finite linear momentum of Cooper pairs is introduced to recover the Cooper singularity (Fulde and Ferrell, 1964). Unfortunately, the region of stability of the Fulde-Ferrell state is very narrow, since one can truly have a Cooper singularity only at a single point in phase space. Consequently the critical field is still of order $T_c/g\mu_B$, but the numerical factor in front is larger by a few percent. However, in the high-field limit there is a qualitatively new possibility: due to the quasi-one-dimensional nature of the electronic dispersion relation one can choose to pair electrons with momenta along the field axis k_z and $-k_z+q_0$, where q_0 is chosen so as to offset the Zeeman splitting (Tešanović, Rasolt, and Xing, 1989). The important difference is that now a full one-half of all the phase space is available for pairing, and it contributes to the Cooper singularity, as opposed to a fraction of measure zero in the familiar Fulde-Ferrell state (Schrieffer, 1959). As a result, superconductivity exists at arbitrarily strong fields as long as both spin species are present. While, for a Zeeman splitting much larger than the thermal energy, T_c is somewhat reduced, it is still definitely observable, and thus the Pauli pair breaking is dramatically decreased. Since the above discussion is very important in the light of experimental observation of superconductivity in the high-field limit, we now consider it in detail.

The most interesting region is the quantum limit. When Zeeman splitting is present we have a situation depicted in Fig. 7. If we consider the uniform (along the field) superconducting state of the previous section and include the Zeeman splitting, we obtain the following weak-coupling equation for T_c:

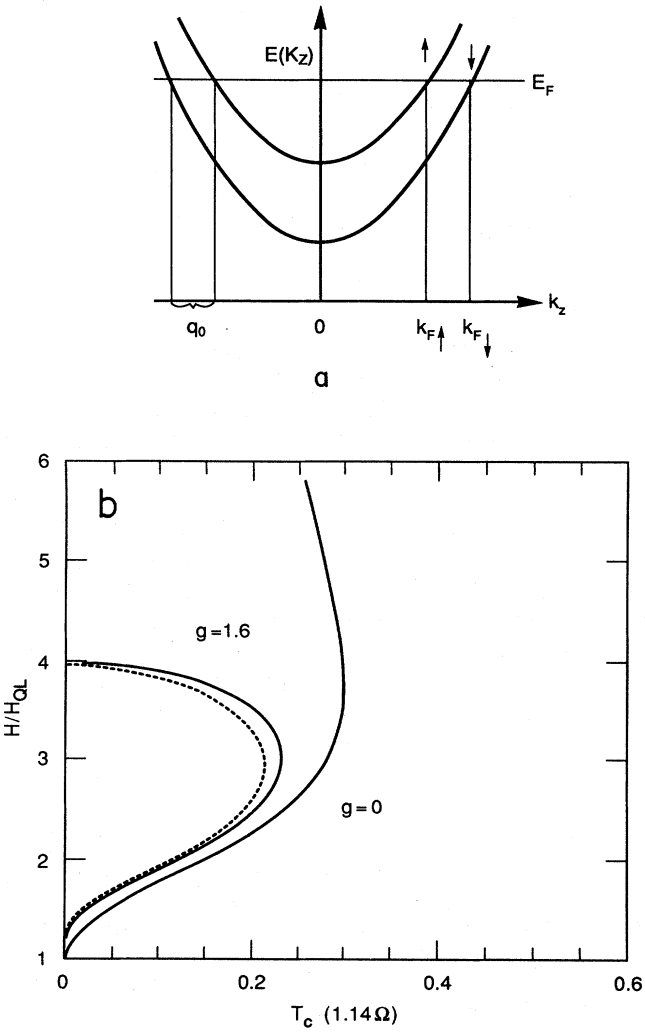

FIG. 7. Zeeman splitting in high magnetic fields. (a) Quasi-one-dimensional spin-up and spin-down bands in the quantum limit. Zeeman splitting is assumed to be small compared to the cyclotron frequency. (b) $T_c(g)$ and $T_c(g=0)$ as described in the text. The T_c vanishes at $H=H_{dep}$. The dotted line is $T_c(g)$ for a nonuniform state with disorder: $1/2\tau E_{3DOF}=10^{-3}$, which can be achieved in doped semiconductors and semimetals. Clearly, the nonuniform state compensates for the Zeeman energy over a wide range of H. Unlike the 3D Fulde-Ferrell state, in which the Cooper singularity is restored only at a single point in the 3D phase space, in the quantum limit the Cooper singularity for the nonuniform high-field-limit state is restored for a full one-half of the phase space. [When full strong-coupling corrections are included, the uniform state in Ge ($g=1.6, g_{eff}=0.13$) is completely eliminated, and the nonuniform state is essential in obtaining $T_c(g)\sim T_c(g=0)$.] The dotted curve demonstrates that impurities do not "destroy" this state.

$$\frac{1}{V}=\frac{1}{2\pi l^2}\left[\frac{2N_{1\uparrow}N_{1\downarrow}}{N_{1\uparrow}+N_{1\downarrow}}\right]\ln\left[\frac{1.14\Omega}{\max(T,A)}\right], \tag{3.8}$$

where

$$N_{1\uparrow(\downarrow)}=m/2\pi k_{F\uparrow(\downarrow)},$$

$$A=2k_{F\uparrow}k_{F\downarrow}g\mu_B H/\pi(k_{F\uparrow}+k_{F\downarrow})^2,$$

and

$$\max(T,A)\approx\sqrt{T^2+A^2}.$$

It is assumed throughout that $A\ll\Omega$, which will be true in a realistic case. There is no reduction in the coupling constant in the above equation, since

$$\frac{2N_{1\uparrow}N_{1\downarrow}}{N_{1\uparrow}+N_{1\downarrow}}=N_1(g=0)$$

and thus $\lambda(g\neq 0)=\lambda(g=0)$. This fact (which, of course, is true only in weak coupling) is, however, not of much help here, since the Cooper singularity has been cut off by A, the pair-breaking parameter of the Zeeman splitting. Obviously T_c will be reduced rather rapidly with increasing g: Eq. (3.8) is easily solved and gives $T_c^2(g)\approx T_c^2(g=0)-A^2$. In the uniform state $T_c(g)$ is suppressed to zero for $A=T_c(g=0)$, and thus Zeeman splitting of the order of the thermal energy will destroy the uniform superconducting state. (This result is similar to what occurs in the low-field limit.) Figure 7(a) seems to suggest that one should consider a nonuniform superconducting state of the type

$$\Psi(\mathbf{r})=\Psi f(z)\exp(-|z|^2/2)\exp(iq_0\xi),$$

where, for $H>H_{\rm QL}$, $q_0=2g\mu_B meH^2/\pi^2 nc$. This corresponds to relaxing the requirement of time-reversal invariance of the ground state $|\tilde{\phi}\rangle$ [in Eq. (2.26)] parallel to **H** [i.e., by creating Cooper pairs from $e^{ik_z\zeta}$ and $e^{i(q_0-k_z)\zeta}$ in Eq. (3.2)]. The point is that, in the absence of the Zeeman term, Eq. (2.1) is invariant under the time-reversal operator $\hat{K}$ [in Eq. (2.2)] restricted to k_z and $-k_z$. This "restricted time reversal" property of Eq. (2.1) is lost in the presence of Zeeman splitting. By solving Eq. (3.6) (with Zeeman splitting included) one finds

$$\frac{1}{V}=\frac{1}{4\pi l^2}\left[\frac{2N_{1\uparrow}N_{1\downarrow}}{N_{1\uparrow}+N_{1\downarrow}}\right]\times\left[\ln\left[\frac{1.14\Omega}{T}\right]+\ln\left[\frac{1.14\Omega}{\max(T,2A)}\right]\right]. \tag{3.9}$$

In this case half of the available electronic states still contribute to the logarithmic singularity. Combined with the fact that the coupling constant is unchanged as discussed above, this state appears to be far more promising. The reason is as follows: For $A\ll T_c(0)$ the uniform state still has a higher transition temperature. But for $A>T_c(0)$, when the uniform state is destroyed, the nonuniform state has a transition temperature given by $T_c(g)=1.14\Omega\exp(-1/\lambda)$, where

$$\lambda=\frac{\lambda(g=0)}{A+\frac{1}{2}\lambda(g=0)\ln[\max(T,2A)/T]}, \tag{3.10}$$

and thus, in the weak-coupling limit $(\lambda\ll 1)$, $T_c(g)\approx T_c(g=0)$. Therefore the nonuniform superconducting state can exist even for Zeeman splitting considerably larger than the thermal energy, and the transition temperature will still be of the order of $T_c(g=0)$. This is a very important result from a practical viewpoint, since it demonstrates that the spin-singlet superconductivity in the high-field limit could in principle be observable in physical systems with finite g factors. One must emphasize, however, that all the reasoning and approximations used above implicitly assume that the range of the fields in the quantum limit over which both spin states are occupied is reasonably large, since obviously no spin-singlet superconductivity can exist if one of the spin states is completely depopulated. This condition immediately rules out the great majority of standard superconductors, which have effective masses of the order of the bare electron mass and g factors of order 2, since in that case the quantum limit strictly speaking does not exist. The region of **H** for which both spin species are present and only the lowest Landau level is occupied will be either very narrow or nonexistent, and high-field superconductivity will be destroyed even for a nonuniform state. This is not of great consequence, since most of the standard superconductors are already ruled out as candidates for high-field superconductivity by virtue of their too high electronic densities, which would require enormous fields in order to reach the quantum limit. We want to emphasize, though, that it is important to have small g factors so as to have a wide region in the quantum limit where both spins are present. In many low-carrier-density systems the effective g factors are quite low, and such materials would be best suited for high-field superconductivity.

As n_c increases the situation becomes quite complicated. Pauli pair breaking will start suppressing T_c very rapidly, since now one cannot choose a single wave vector that would restore the Cooper singularity for all the occupied Landau levels. One can still argue, however, that, as long as $\Omega\ll\omega_c$ and E_{Fn} is away from singularities in the density of states, T_c will remain finite although considerably depressed. An interesting situation would arise if a g factor were very close to $2m/m_c$, where m_c is the effective cyclotron mass. In this case the Zeeman splitting would be very close to the cyclotron splitting, making the nth spin-up Landau level nearly degenerate with the $(n+1)$th spin-down one. T_c would then be revived again, although it would still be less than for the $g=0$ case. This may be the situation in $SrTiO_3$, a well known low-carrier-density superconductor. Similarly, for particular cross sections (corresponding to different field orientations) of the Fermi surface in various materials, the Zeeman splitting could be such as to make the

nth ($\uparrow$) Landau level nearly degenerate with the $(n+m)$th ($\downarrow$) one. This situation could be achieved by varying the direction of the external field relative to the principal crystalline axes (Norman, Akera, and MacDonald, 1992).

We have already discussed some general aspects of the interplay between magnetic fields and impurities [Eq. (2.31)]. As we saw, impurities change the time dependence of $\hat{K}(t)$ and have a profound effect on the $H_{c2}\rightarrow H_{c\infty}$ line. For a very large level of impurities, i.e., when the magnetic length l is bigger than the electron diffusion length l_d, there is no doubt that the $H_{c\infty}$ will disappear. It is therefore very important to maintain high purity of those materials in which one is searching for high-field-limit superconductivity. The purer the material the better. In the study of conventional superconductors one often associates very pure systems with type-I behavior, and type-II behavior can sometimes only be induced by making a system "dirty." This is not the case here. First of all, the promising materials for high-field superconductivity will have a low density of carriers and are likely to be strongly type II even when pure. But even if such a pure system does not show a type-II behavior in the low-field limit, and the H_{c2} line is replaced by the H_c line of a type-I superconductor, or, for that matter, by a nonsuperconducting state, this does not preclude superconductivity in the high-field limit. The superconductivity at this high field could in principle exist independently of the nature of the ground state in low fields.

The presence of impurities will affect high-field-limit superconductivity in several ways. In addition to simple pair breaking (which is obviously present in any realistic, $g\neq 0$ nonuniform case), thermal and quenched disorder will broaden sharp features in the density of states and may change the effective interaction, particularly the Coulomb repulsion. Here we shall consider the effect of pair breaking only; the broadening of the density of states can be simply included phenomenologically and leads to suppression of T_c for $n_c>1$, since it flattens out the jumps in the density of states but has little effect on the quantum limit. The effect of disorder on the effective electron-phonon and electron-electron interaction is a very complicated subject, even for ordinary, zero-field superconductivity, and we shall not consider it in this paper. Finally, probably the most serious problem encountered by experimentalists searching for other quasi-one-dimensional instabilities in the quantum limit, like SDW, CDW, etc., is "magnetic freezeout." This dramatic loss of carriers (due to deepening of the local impurity levels in high fields) will affect the superconducting state in a similar way. Recently, however, there has been considerable experimental progress in minimizing the effects of disorder and producing high-mobility 3D samples, particularly in so-called wide parabolic quantum wells (see Sec. IV.C.5). It appears likely that advances in artificially structured materials will soon lead to systems in which the electron-impurity interactions will be negligible.

Pair-breaking can be included by considering the effect of disorder on Eq. (3.6) (see Fig. 3). We first consider the realistic $g\neq 0$ case and use the Born approximation to derive the following expression for $T_c^{\rm dis}(H,g\neq 0)$, valid for weak disorder, $1/\tau E_F \ll 1$, where $1/2\tau$ is the scattering rate due to disorder (defined in zero field) and E_F is the zero-field Fermi energy (we only give the expression for the quantum limit, for $g\neq 0$, since the calculation is very involved when several Landau levels are included):

$$\ln\left[\frac{T_c^{\rm dis}\max(t_c^{\rm dis},2A)}{T_c\max(T_c,2A)}\right]=\pi T\sum_{\omega}\left[D_1(\omega,1/2\tau)\left[1-\frac{1}{2\tau_{Ql}}[D_1(\omega,1/2\tau)+D_2(\omega,1/2\tau)]\right]^{-1}\right]$$
$$+\pi T\sum_{\omega}\left[D_2(\omega,1/2\tau)\left[1-\frac{1}{2\tau_{Ql}}[D_1(\omega,1/2\tau)+D_2(\omega,1/2\tau)]\right]^{-1}-D_1(\omega,0)-D_2(\omega,0)\right], \tag{3.11a}$$

where

$$D_2(\omega,1/2\tau)=\frac{1}{(d_1^2+d_2^2)^{1/4}}\{\exp(-i\delta/2)\theta[\cos(\delta/2)]-\exp(-i\delta/2)\theta[-\cos(\delta/2)]\} \tag{3.11b}$$

and

$$d(\omega,1/2\tau)\equiv d_1+id_2\equiv(d_1^2+d_2^2)^{1/2}\exp(i\delta)$$
$$=\omega^2+\omega\eta[\tfrac{1}{4}\tau_\uparrow+\tfrac{1}{4}\tau_\downarrow+v_{F\uparrow}/4v_{F\downarrow}\tau_\downarrow+v_{F\downarrow}/4v_{F\uparrow}\tau_\uparrow+i(v_{F\uparrow}+v_{F\downarrow})q_0]$$
$$+\eta[\tfrac{1}{4}\tau_\uparrow\tau_\downarrow+(v_{F\uparrow}/2\tau_\downarrow-v_{F\downarrow}/2\tau_\uparrow)^2/4v_{F\uparrow}v_{F\downarrow}-v_{F\uparrow}v_{F\downarrow}q_0^2+i(v_{F\uparrow}/2\tau_\downarrow+v_{F\downarrow}/2\tau_\uparrow)q_0], \tag{3.11c}$$

with

$$1/2\tau_{\rm QL}=(2N_{1\uparrow}N_{1\downarrow}/(N_{1\uparrow}+N_{1\downarrow}))\pi W^2/4\pi l^2 . \tag{3.11d}$$

W^2 is the root mean square (RMS) value for the random potential, $\frac{1}{2}\tau_{\uparrow,\downarrow}$ are corresponding single-particle scattering rates, and

$$\eta=[1+(v_{F\uparrow}-v_{F\downarrow})^2/4v_{F\uparrow}v_{F\downarrow}]^{-1} .$$

One obtains $D_1(\omega,\frac{1}{2}\tau)$ from $D_2(\omega,\frac{1}{2}\tau)$ by setting $q_0=0$.

To get some feeling for what happens below the quantum limit, we give the result for $g=0$,

$$\ln\frac{T_c^{\rm dis}}{T_c}=-\psi\left\{\frac{1}{2}+\left[\frac{1}{2\tau E_F}\right]\left[\frac{E_F}{2\pi T_c^{\rm dis}}\right]\sum_{n=0}^{n_c}\frac{N_{1n}(0)}{2\pi l^2 N_{3D}(0)}\left[2-\frac{(2n)!}{2^{2n}(n!)^2}\right]\right\}+\psi\left\{\frac{1}{2}\right\}, \tag{3.12}$$

where T_c is given in Eq. (3.7). In the above equations the Born approximation should be reasonable in the quantum limit as long as the field is not too high, making k_F^{-1} too long. When this occurs, one must go beyond the Born approximation, which is quite a complicated issue. Furthermore, as the field becomes very strong, l grows shorter and eventually becomes less than the typical range of the impurity potential, resulting in reduced pair breaking. Below the quantum limit the Born approximation is less valid, since the density of states oscillates faster and faster as the field decreases. The pair breaking increases and disorder will eventually suppress T_c to zero, resulting in a crossover region where superconductivity does not occur even for $T=0$. Eventually there could be a reentrant transition to the low-field regime. In the quantum limit for a disorder such that $1/2\tau E_{3D,F}=10^{-3}$, which can be achieved in low-carrier-density systems, using Eq. (3.11) we find a small correction [Fig. 7(b)] to the $H_{c\infty}$ line [Fig. 6(b)]. We should mention here that there exists an opposing point of view, which argues that in a high field and in the quantum limit superconductivity can never be observed in nature, due to the effects of Pauli pair breaking and disorder (Rieck, Scharnberg, and Klemm, 1990; Norman, 1991; Scharnberg and Rieck, 1991). The proponents of this view argue that Pauli pair breaking and disorder always "destroy" the $H_{c\infty}$ line (Fig. 1) and consider the possibility of superconductivity in the high-field limit unrealistic. Explicit calculations for Ge-type systems, however, reveal that $T_c(H)$ is appreciable in the quantum limit with both disorder and Pauli pair breaking present (Tešanović, Rasolt, and Xing, 1991a). One must realize here that the general conditions on the Zeeman splitting and the strength of disorder are similar for superconducting and the SDW state in the quantum limit (Tešanović and Halperin, 1987, and references therein). Thus a low effective g factor is needed to have a relatively wide region in the quantum limit where both spin states are occupied, and a low level of impurities is necessary. We shall say more about how such conditions can be met in real systems at the end of the next section and in Sec. VI.A.

In summary, we have given here a detailed solution for the mean-field $T_c(H)$ line in a BCS superconductor. We have shown how the familiar $H_{c2}(T)$ line crosses over into $T_c(H)$, which is an increasing function of the field, once the Landau-level structure is properly included. The high-field limit was then discussed in detail and the effects of Zeeman splitting and impurity scattering on this unusual limit of superconductivity were studied.

IV. THE NATURE OF THE SUPERCONDUCTING STATE

As shown in the previous section, two opposite regions of the $H_{c2}\rightarrow H_{c\infty}$ line, the high-field limit and the familiar low-field $H_{c2}(T)$ line, could be discussed very accurately. The crossover region, in which the contribution from diagonal pairing was of a similar order to the contribution from off-diagonal terms, could also be analyzed using semiclassical methods. In particular, the origin of this crossover, from $T_c(H)$ being an increasing function to its being a decreasing function of H, is, in our opinion, now well understood in terms of the effect of the Landau-level structure within the mean-field approximation. The next step, which is probably more revealing and important, is to achieve a similar understanding of the actual superconducting state below the $H_{c2}\rightarrow H_{c\infty}$ line. In this section we should like to elucidate the nature of orbital frustration in the high-field limit and to examine how diamagnetic pair-breaking is circumvented in such strong fields. First, in Sec. IV.A, we discuss some general properties of the BCS wave function in the quantum limit. In Sec. IV.B we then discuss the nonlinear Ginzburg-Landau theory and the full BCS theory. Both can be solved exactly in the quantum limit and to a very good approximation in the quantum-limit approximation, where off-diagonal pairing terms are neglected. We also discuss the crossover to low-field behavior within the Ginzburg-Landau theory. Furthermore, we explore the relationship of the superconducting order parameter and the "induced" vector potential which, in very low fields, leads to the Meissner effect. Finally, in Sec. IV.C, we present a general discussion of transport properties in this new state and their evolution from the low-field limit.

A. The ground-state wave function in the quantum limit

Nothing can provide more information and insight into what is going on than the ground-state wave function and low-energy excited states. This will become particularly clear, for example, when we consider the nature of dissipation and current flows. For arbitrary H, guess-

ing the form of $|\tilde{\phi}\rangle$ [as in Eq. (2.25) or (2.26)] is hopeless; the mean-field approach presented in Sec. II.B.2 is a very important simplification. Typically, however, one cannot find the ground-state wave function and the excited states for $H\neq 0$ even within the BCS theory. The fact that the superconducting order parameter is nonuniform makes this a nasty nonlinear "band-structure" problem. In the quantum limit, where all the electron states reside in the lowest Landau level [i.e., Eq. (3.2) with $n=0$], things turn out to be far more promising. Now $|\tilde{\phi}\rangle$, in the most general form, can be written as

$$|\tilde{\phi}\rangle=\sum_N \sum_{\kappa_z,M} \alpha^N_{\kappa_z M} \prod_i^N C^\dagger_{k_{zi},m_i}|\text{vacuum}\rangle \ , \tag{4.1}$$

where the coefficient $\alpha^N_{\kappa_z M}$ depicts the various configurations $(k_{z1}m_1)\cdots(k_{zN}m_N)$ [coefficients $m=0,1,\ldots,m_c$ denote the degenerate manifold of the states in Eq. (3.2) in the lowest Landau level for N particles; m_c is given by $\Omega/2\pi l^2$, where Ω is the cross-sectional area of the system, assumed to be a cylinder of radius $R=\sqrt{\Omega/\pi}$ and length L_z.]

From Eq. (3.2)

$$\phi_{n=0,m}(z)=\frac{1}{\sqrt{2\pi m!2^m}} z^m e^{-|z|^2/4} \ . \tag{4.2}$$

In Eq. (4.1) we have extended $|\tilde{\phi}\rangle$ to a varying number of particles N for the same reasons discussed in Eq. (2.25). Again this is done for the convenience of defining the order parameter in Eq. (2.6a), which is at $T=0$

$$\Delta(\mathbf{r})=V\langle\tilde{\phi}|\psi(\mathbf{r}\uparrow)\psi(\mathbf{r}\downarrow)|\tilde{\phi}\rangle \ . \tag{4.3}$$

Using Eq. (4.1), we can write $\Delta(\mathbf{r})$ in the quantum limit in the most general form as

$$\Delta(\mathbf{r})=V\sum_{m=0}^{2m_c}\gamma_m(\zeta)z^m e^{-|z|^2/2} \ . \tag{4.4}$$

The excited states are all still in the lowest Landau level (at finite temperature) and do not change this form; they only introduce a temperature dependence in $\gamma_m(\zeta)$. Thus the confinement to the lowest Landau level provides a severe restriction on the form of $\Delta(\mathbf{r})$. Apart from the overall exponential, $\Delta(\mathbf{r})$ is a general holomorphic function of z. This restriction leads to a significant simplification of the whole problem. Here we make a few general comments about Eq. (4.4), which are important to keep in mind in what follows and which illustrate the special role of the quantum limit: (a) The ζ dependence describes fully the spatial variation of $\Delta(\mathbf{r})$ parallel to $\mathbf{H}$. (b) Equation (4.4) is not restricted to the mean-field approximation; it is *completely general.* (c) Equation (4.4) is not restricted to being close to the $H_{c\infty}$ line. Therefore, in the quantum limit the form of $\Delta(\mathbf{r})$ in Eq. (4.4) is an exact solution of the full problem, at any temperature and any field, provided one knows the exact γ's. (d) In the quantum limit the task left is to calculate the $\gamma_m(\zeta)$ within some approximate scheme. We shall consider these $\gamma_m(\zeta)$ in the mean-field approximation shortly. We shall also discuss, in Sec. V, how the fluctuations modify the mean-field results. (e) The change in the form of the exponential form $\exp(-|z|^2/4)$ for the electronic wave functions to $\exp(-|z|^2/2)$ (which is the signature of the Cooper pairing; i.e., $l\rightarrow l^*$) and the extension of the sum to $2m_c\equiv m_c^*$ provides the correct complete basis set for $\Delta(\mathbf{r})$ in Eq. (4.4). [Note that $\Delta(\mathbf{r})$ is confined to the lowest Landau level itself, if we think of $\Delta(\mathbf{r})$ as representing bosons of charge $e^*=2e$. These "bosons" are Cooper pairs, and their Landau levels correspond to the center-of-mass motion. Also, note that $2\pi l^2 m_c=2\pi l^{*2}m_c^*=\Omega$.] (f) As we go along the $H_{c2}\rightarrow H_{c\infty}$ line to a finite number of electronic Landau levels, it is evident that the form of Eqs. (4.1) and (4.4) will no longer hold true, as higher Landau levels start being involved in the pairing correlations. This makes the discussion of the order parameter close to the transition line more difficult. However, as we saw in Sec. III, Eq. (4.4) continues to be a solution to Eq. (3.3) for all Landau-level occupation. Furthermore, even below $T_c(H)$ the form (4.4) still represents the dominant part of the exact $\Delta(\mathbf{r})$. (g) Above the true transition temperature [which, in general, is different from $T_c(H)$ found in the mean-field approximation], $\Delta(\mathbf{r})\rightarrow 0$ corresponding again to arbitrary phases in $|\tilde{\phi}\rangle$. Things, however, are a bit more subtle and will be discussed in Sec. V.

As emphasized above, Eq. (4.1) is very general. It can also include a glassy superconducting state, etc. In fact, for totally arbitrary form of $\alpha^N_{k_z M}$ there will be random phase changes in Eq. (4.1); there will be no zero-entropy state, and therefore $\Delta(\mathbf{r})$ will be zero. We can restrict Eq. (4.1) to include explicitly at least coherence along $\mathbf{H}$, i.e.,

$$|\tilde{\phi}\rangle=\prod_{k_z,m}\sum_{m'}(u^{m,m'}_{k_z}+v^{m,m'}_{k_z}C^\dagger_{k_z m\uparrow}\underline{C}^\dagger_{k_z m'\downarrow})|\text{vacuum}\rangle \tag{4.5}$$

with

$$|u^{m,m'}_{k_z}|^2+|v^{m,m'}_{k_z}|^2=1 \ .$$

For the nonuniform, spin-split Zeeman case discussed in Sec. III.B, we need only to shift $-k_z\rightarrow -k_z+q_0$ in Eq. (4.5).

B. The mean-field theory in a very high magnetic field

The form of $\Delta(\mathbf{r})$ in Eq. (4.4) is completely general. Consequently, in the mean-field approximation and in the quantum limit we can solve for $\gamma_m(\zeta)$ exactly (Tešanović,

Rasolt, and Xing, 1991)! The generalization to nonuniform ζ dependence along $\mathbf{H}$ is straightforward and well defined, at least for small g factors. In the quantum limit all it does is change $\Delta(\mathbf{r})$ to $\Delta(\mathbf{r})\exp(\pm iq_0\zeta)$; see Sec. III.B. Therefore we consider only the uniform case. This amounts to the exact solution of the full BCS theory for arbitrary H and T, as long as one is in the quantum limit. We are not familiar with any other example of an exact solution to the BCS theory in a finite magnetic field. This makes this example of the quantum limit very valuable and the starting point for a detailed understanding of the BCS theory in high fields.

1. The order parameter in the quantum limit

Before we discuss the full solution of the BCS theory let us first consider what happens right below $H_{c\infty}$, using the nonlinear Ginzburg-Landau expansion. This will prove useful a little later; particularly in the discussion of the induced currents in the quantum limit; see end of Sec. IV.B.3. We start with Eq. (2.21). The kernels $K_2(\mathbf{r}_1,\mathbf{r}_2)$, $K_3(\mathbf{r}_1,\mathbf{r}_2)$, and $K_4(\mathbf{r}_1,\mathbf{r}_2,\mathbf{r}_3,\mathbf{r}_4)$, defined in Eqs. (2.17d), (2.17e), and (2.20c), can be written in closed form (Tešanović, Rasolt, and Xing, 1989). Using the quantum limit form for $G_{0\sigma}$ of Eq. (2.18a), we get

$$G_{0\sigma}(w,\mathbf{r}_1,\mathbf{r}_2)=\frac{1}{2\pi l^2}\sum_{k_z}\frac{\exp(z_1z_2^*-|z_1|^2/4-|z_2|^2/4)}{iw-\xi_{k_z}}\ , \tag{4.6}$$

$$K_2(\mathbf{r}_1,\mathbf{r}_2)=\frac{\alpha'(T)}{(2\pi l^2)^2}\exp(-z_1^*z_1/2-z_2^*z_2/2+z_1z_2^*)\ , \tag{4.7}$$

$$K_4(\mathbf{r}_1,\mathbf{r}_2,\mathbf{r}_3,\mathbf{r}_4)=\frac{\beta'(T)}{(2\pi l^2)^4}\exp[-z_1^*z_1/2-z_2^*z_2/2-z_3^*z_3/2-z_4^*z_4/2+(z_1+z_3)(z_2^*+z_4^*)/2]\ , \tag{4.8}$$

and

$$K_3(\mathbf{r}_1,\mathbf{r}_2)=\frac{\gamma'(T)}{(2\pi l^2)^3}\exp(-z_1^*z_1/2-z_2^*z_2/2+z_1z_2^*/2)\times\int d^3r_3\exp(-z_3^*z_3/4+z_1z_3^*/2)h(z_3,z_3^*)\exp(-z_3^*z_3/4+z_3z_2^*/2)\ , \tag{4.9}$$

where

$$h(z,z^*)\equiv\frac{e}{2imc}\left[\left[a^*,\frac{\partial}{\partial z^*}\right]_+ + \left[a,\frac{\partial}{\partial z}\right]_+\right]+\frac{e^2}{2mc^2}(A^*a+Aa^*)\ ,$$

with $a(A)\equiv a_z(A_z)+ia_y(A_y)$ and where

$$\alpha'(T)=\frac{1}{\beta}\sum_{k_z,w}\frac{1}{(iw-\xi_{k_z})(iw+\xi_{k_z})}\ , \tag{4.10a}$$

$$\beta'(T)=\frac{1}{\beta}\sum_{k_z,w}\frac{1}{(iw-\xi_{k_z})^2}\frac{1}{(iw+\xi_{k_z})^2}\ , \tag{4.10b}$$

and

$$\gamma'(T)=\frac{2}{\beta}\sum_{k_z w}\frac{1}{(iw-\xi_{k_z})}\frac{1}{(iw+\xi_{k_z})^2}\ . \tag{4.10c}$$

We now consider the physics described by the various kernels in the Ginzburg-Landau form of the free energy. First we note that all the kernels entering the Ginzburg-Landau free energy are fully nonlocal and no gradient expansions are possible, since the order parameter varies over the same length scale as the kernels. The quadratic kernel K_2 projects $\Delta(\mathbf{r})$ to the "lowest bosonic Landau level," i.e., $K_2(\mathbf{r}_1,\mathbf{r}_2)$ is proportional to the Green's function of charge-2e bosons restricted to the lowest Landau level, in accord with our discussion following Eq. (4.4). Thus, if we consider contributions to K_2 coming only from the lowest electronic Landau level, all $\Delta(\mathbf{r})$ have to be of the form $f(z)\exp(-z^*z/2)$ [again in agreement with Eq. (4.4)] and have the same T_c, while all other functional forms of the order parameter (coming from higher "bosonic" Landau levels) do not contribute at all. This simple situation illustrates the important physical point already mentioned in previous sections: the diamagnetic pair-breaking effect of the magnetic field is basically eliminated, and there is no frustration characterizing the low-field superconducting state [the only effect is that K_2 leads to $c_{\text{e-e}}=\frac{1}{2}c_{\text{e-h}}$, as mentioned below Eq. (3.1)]. The electronic wave functions constrained to the lowest Landau level naturally produce the order parameter describing charge-2e bosons (Cooper pairs) in their corresponding lowest Landau level.

This property is shared by the quartic term as well. One can easily see that K_4 also acts as a projection operator by rewriting the quartic part of Eq. (2.21a) as

$$\int d^2r\exp(-2z^*z/2)\int d^2r_1\exp(-z_1^*z_1/2+z_1z^*)\Delta^*(\mathbf{r}_1)\times\int d^2r_2\exp(-z_2^*z_2/2+z_2^*z)\Delta(\mathbf{r}_2)\int d^2r_3\exp(-z_3^*z_3/2+z_3z^*)\Delta^*(\mathbf{r}_3)\int d^2r_4\exp(-z_4^*z_4/2+z_4^*z)\Delta(\mathbf{r}_4)\ , \tag{4.11}$$

which is clearly nonzero only for the above "holomorphic" form of $\Delta(\mathbf{r})$. There is an important consequence of this projection property: First we note that K_4 and $F_{\text{s-b}}$ select $\Delta(\mathbf{r})$ that minimize F. Finding such configurations involves a variation of F with respect to $\Delta(\mathbf{r})$ and $a(\mathbf{r})$. For $T_c \ll E_F$ the coupling between $\Delta(\mathbf{r})$ and $a(\mathbf{r})$, given by $\gamma'(T)$, can be shown to be of order T_c/E_F, which translates to order $(T_C/E_F)^2$ for $F_{\text{s-b}}$. Thus, in weak coupling, we can ignore the "Meissner effect," and the minimization of F reduces to minimization of F_a with respect to $\Delta(\mathbf{r})$ at a fixed external $\mathbf{H}$. (It is clear that this is an excellent approximation, since the external field in the high-field limit will be far stronger than any field that can be created by the motion of Cooper pairs.) Consequently we can immediately conclude that $\Delta(\mathbf{r})=\Delta_0 f(z)\exp(-z^*z/2)$ must be the form of the exact solution of the nonlinear Ginzburg-Landau equation. This equation reads

$$V^{-1}\Delta(\mathbf{r})=\frac{\delta F_s}{\delta\Delta(\mathbf{r})}=\alpha'(T)\int d^2r_2 K_2(\mathbf{r},\mathbf{r}_2)\Delta(\mathbf{r}_2)+\beta'(T)\int d^2r_2 d^2r_3 d^2r_4 \Delta(\mathbf{r}_2)K_4(\mathbf{r},\mathbf{r}_2,\mathbf{r}_3,\mathbf{r}_4)\Delta^*(\mathbf{r}_3)\Delta(\mathbf{r}_4)\ . \tag{4.12}$$

There are many possible solutions of Eq. (4.12), depending on the choice of $f(z)$. From variational calculations in the low-field limit it is known that a triangular lattice gives particularly low free energy. So we can simply take the variational Abrikosov solution (which *is* confined to the lowest bosonic Landau level) for a triangular vortex lattice and check whether this is a solution of Eq. (4.12). After some algebra one finds that indeed it is! In fact, every function of the above form with a periodic $\Delta(\mathbf{r})$ such that there is a flux quantum per zero is an exact solution of (4.12), i.e., the correct choice of the γ_m's in Eq. (4.4) leads to (in the symmetric gauge)

$$\Delta(\mathbf{r})=\Delta_0\Pi_i e^{-|z|^2/2}(z-z_i^0)^\lambda\ , \tag{4.13}$$

where z_i^0 are the position of the periodic array of zeros of power λ. The flux per plaquette is $\lambda\hbar c/2e$. Therefore we have now obtained an exact solution of the nonlinear Ginzburg-Landau equation which, for $\lambda=1$, is likely to be the absolute minimum of the mean-field free energy.

The above form of $\Delta(\mathbf{r})$ provides an important clue to the physics of the superconducting state. The holomorphic function is fully specified by the position of its zeros, $\{z_i\}$. The total number of zeros is $\Omega/2\pi l^{*2}$. The quadratic kernel does not prefer any particular arrangement of zeros; all configurations are equivalent. This is a consequence of the fact that $\Delta(\mathbf{r})$ itself belongs to the lowest Landau level for charge $e^*=2e$. Which configuration has the lowest free energy is decided by the quartic term. We can consider Δ_0 and $\{z_i\}$ as variational parameters and minimize the free energy with respect to their variation. For some fixed position of $\{z_i\}$, the minimization with respect to Δ_0 leads to $F_{\text{GL}}(\{z_i\})$, the free energy for that particular configuration of zeros. Finally, minimization with respect to $\{z_i\}$, $\partial F_{\text{GL}}/\partial z_i=0$, leads to a solution. Note that this equation is in fact Eq. (4.12) in disguise. Thus Eq. (4.12) is nothing else but the D'Alembert condition for the static equilibrium. Consequently an arbitrary regular lattice of $\{z_i\}$, such that every zero corresponds to a center of symmetry resulting in cancellation of forces arising from other zeros, will be an exact solution of the nonlinear Ginzburg-Landau theory in the quantum limit.

2. BCS theory and the excitation spectrum in the quantum limit

An inspection of the higher-order terms in the Ginzburg-Landau expansion of the mean-field free energy reveals that, in the quantum limit, all kernels (of order six and higher) act as projectors in a way similar to K_2 and K_4. Thus the form $\Delta(\mathbf{r})=\Delta_0 f(z)\exp(-z^*z/2)$, with proper periodicity, is indeed the exact solution of the full BCS mean-field theory in the quantum limit at any temperature and any field (Tešanović, Rasolt, and Xing, 1991b). Again, we can consider Δ_0 and $\{z_i\}$ as variational parameters. The argument presented above goes right through, and we simply have to replace F_{GL} by F_{BCS}. There are numerous solutions, all representing regular lattices of $\{z_i\}$ in D'Alembert static equilibrium. The condition for this static equilibrium, $\{z_i\}, \partial F_{\text{BCS}}/\partial z_i=0$, is in fact the BCS self-consistency condition (2.10).

To find which of these solutions has the lowest free energy we need an explicit solution of Eqs. (2.9). Here we follow Tešanović, Rasolt, Andreev, and Dukan (1991) and Rasolt (1991, 1992). Using the Landau gauge $[\vec{A}=H(-y,0,0)]$ for convenience, we can write the gap parameter as

$$\Delta(\mathbf{r})=\Delta_0\sum_n c_n\exp\left[\frac{2\pi i n}{a}x\right]\exp\left[-\frac{1}{2}\left[\frac{y}{l^*}+\frac{bn}{l^*}\right]^2\right]\ ,$$

where $ab=2\pi l^{*2}$ fixes the flux per elementary plaquette. To solve Eqs. (2.9) we exploit the generalized Bloch theorem by noticing that (as an example, we consider a rectangular lattice but our discussion can be easily generalized to a triangular lattice)

$$u(x+a,y)=e^{iq_x a}u(x,y)\ ,$$

$$u(x,y+2b)=\exp\left[iq_y b-\frac{2i\pi}{a}x\right]u(x,y)$$

and

$$v(x+a,y)=e^{iq_x a}v(x,y)\ ,$$

$$v(x,y+2b)=\exp\left[iq_y b+\frac{2i\pi}{a}x\right]v(x,y)\ .$$

Now, by defining $u_{\mathbf{q}}(\mathbf{r}),v_{\mathbf{q}}(\mathbf{r})$, $[\mathbf{q}=(q_x,q_y)]$, consistent with the generalized Bloch theorem,

$$u_{\mathbf{q}}=\frac{1}{\sqrt{L_x}}\frac{1}{(\sqrt{\pi}l)^{1/2}}\left[\frac{b}{L_y}\right]^{1/2}u_{k_z\mathbf{q}}(\zeta)\sum_n\exp(-2inq_y b)\exp\left[i\left[q_x+n\frac{2\pi}{a}\right]x\right]\exp\left\{-\frac{1}{2}\left[\frac{y}{l}+\left[q_x+\frac{2\pi n}{a}\right]l\right]^2\right\}\ ,$$

$$v_{\mathbf{q}}(\mathbf{r})=\frac{1}{\sqrt{L_x}}\frac{1}{(\sqrt{\pi}l)^{1/2}}\left[\frac{b}{L_y}\right]^{1/2}v_{k_z\mathbf{q}}(\zeta)\sum_n\exp(-2inq_y b)\exp\left[i\left[q_x-n\frac{2\pi}{a}\right]x\right]\exp\left\{-\frac{1}{2}\left[\frac{y}{l}-\left[q_x-\frac{2\pi n}{a}\right]l\right]^2\right\}\ ,$$

we find that Eqs. (2.9) become

$$\begin{aligned}E_{k_z\mathbf{q}}u_{k_z\mathbf{q}}&=\left[\xi_{k_z}+\frac{\hbar\omega_c}{2}-E_F\right]u_{k_z\mathbf{q}}+\Delta(\mathbf{q})v_{k_z\mathbf{q}}\ ,\\ -E_{k_z\mathbf{q}}v_{k_z\mathbf{q}}&=-\Delta^*(\mathbf{q})u_{k_z\mathbf{q}}+\left[\xi_{k_z}+\frac{\hbar\omega_c}{2}-E_F\right]v_{k_z\mathbf{q}}\ ,\end{aligned}\tag{4.14a}$$

yielding the self-consistency condition and the quasiparticle spectrum

$$1=\frac{Vb}{\sqrt{2\pi l^2}}\frac{1}{L_xL_yL_z}\sum_{k_z}\sum_{\mathbf{q}}\frac{D(\mathbf{q})}{2E_{k_z\mathbf{q}}}\tanh\left[\frac{E_{k_z\mathbf{q}}}{2K_BT}\right]\ ,\tag{4.14b}$$

where

$$D(\mathbf{q})\equiv d\prod_j|\tilde{q}-\tilde{q}_j|^2e^{-|\tilde{q}|^2/2}\ ,$$

with d depending on the choice of lattice constant and

$$E_{k_z\mathbf{q}}=\pm\left[\left[\xi_{k_z}+\frac{\hbar\omega_c}{2}-E_F\right]^2+|\Delta(\mathbf{q})|^2\right]^{1/2}\ .\tag{4.14c}$$

Here

$$\Delta(\tilde{q})=\frac{\Delta_0}{\sqrt{2}}\prod_j(\tilde{q}-\tilde{q}_j)e^{-|\tilde{q}|^2/4}$$

with $\tilde{q}\equiv 2(q_y+iq_x)l^*$. In the last step (4.14c) we have now transferred $\Delta(\tilde{q})$ back to the symmetric gauge which we tend to favor in this paper.

This form makes it particularly clear that the gap $|\Delta(\tilde{q})|$ has zeros located at $\{\tilde{q}_j\}$ which are directly related to the zeros of $\Delta(\mathbf{r}),\{z_i\}$, via

$$2q_{yj}l^*=x_i/l^*,\quad 2q_{xj}l^*=y_i/l^*\ .$$

Equations (4.14) illustrate a particularly transparent relationship between the behaviors in real and momentum space. This is another manifestation of the simple form that orbital frustration takes in the quantum limit. The compact form of Eqs. (4.14) indicates that the quantum limit is, in fact, a "natural" limit in which to study the effect of a magnetic field on a superconductor. Note that the Cooper pairs are formed by electrons in states of equal and opposite "crystalline" momenta $\vec{q}$, corresponding to the magnetic translation group determined by the initial choice of the vortex lattice in real space. These states are not related by time-reversal operation, since time-reversal symmetry does not exist in the quantum limit.

The zeros in real space are here directly transferred to the points $\{q_j\}$, where the gap in the quasiparticle excitation spectrum vanishes. This gapless behavior at a set of points in the magnetic Brillouin zone is an essential feature of the excitation spectrum in a very high magnetic field. The existence of these zeros has profound consequences for the thermodynamic behavior of a high-field-limit superconductor. For example, the specific heat at low temperatures goes as $C_V\propto T^3$, $[\Delta(T)-\Delta(0)]/\Delta(0)\propto -T^4$, etc. Similarly, the transport properties will be affected as discussed later. The self-consistency equation has to be solved numerically and yields temperature dependence for Δ_0 different from the standard BCS one, owing to these zeros in the gap. Numerical calculation of the BCS condensation energy is quite delicate, but it seems that the triangular lattice of $\{z_i\}$ results in the lowest energy at all T and H in the quantum limit.

3. BCS theory and the order parameter below the quantum limit

If several Landau levels are occupied, the above results can be easily generalized as long as we use the quantum-limit approximation discussed in Sec. III. Two necessary conditions are $\Delta\ll\omega_c$ and $H>H_C$. In particular, the BCS theory can again be solved (Dukan, Andreev, and Tešanović, 1991), leading to an excitation spectrum of Bogoliubov quasiparticles, which is a straightforward generalization of Eq. (4.14c) with the gap for the nth branch (arising from the nth Landau level) given by

$$\Delta_{nn}(\tilde{q})\propto[\Pi^\dagger]^{2n}\Delta_{00}(\tilde{q})\ ,$$

where $\Delta_{00}(\tilde{q})$ is the gap in the quantum limit given below Eq. (4.14c) (one should remember that in the quantum-limit approximation we include only the diagonal pairing terms). The operator $\Pi^{\dagger}$ is

$$\Pi^{\dagger}=\frac{1}{2l}\left[-i\frac{\partial}{\partial q_y}-\frac{\partial}{\partial q_x}+2q_x l^2\right].$$

The spectrum is gapless at the same set of points in the magnetic Brillouin zone as in the quantum limit, since all $\Delta_{nn}(\tilde{q})$ vanish at these points. Again, the gapless spectrum will have observable consequences and is the signature of the high-field limit. We should mention that the result for a quasiparticle spectrum presented here differs from that found by Stephen (1991), who concluded that the energy bands are almost flat.

The above form also represents the exact solution of a BCS theory in two dimensions in the quantum limit. The problem of orbital frustration is the same, and the only difference is that one now does not have the motion along the field. Moreover, the superconducting solution will now not appear for arbitrarily small attractive V, but for some critical value of the interaction that is larger than the Zeeman splitting. The density of states is now a set of delta functions (broadened by thermal and impurity scattering) corresponding to different Landau levels. Because of these sharp features in the density of states, the effect of Landau quantization is even more pronounced than in 3D (Maniv *et al.*, 1991). This makes layered systems (Tešanović, Rasolt, and Xing, 1989), like high-temperature and organic superconductors, likely candidates for the observation of quantum oscillations in the superconducting state in the vicinity of $H_{c2}(0)$ and above. Very recently Akera *et al.* (1991) have studied the high-field limit in a 2D system. They consider pairing in several possible channels, including the case in which the effective attraction has a finite range, and find that for pairing involving several electronic Landau levels, the order parameter at low T has a more complicated form than that given by Eq. (4.13). These issues could become relevant in light of the possibility that a "superconducting" state may be found in semiconducting heterostructures typically used in quantum Hall effect experiments.

There is, however, an important difference between 2D and 3D. In a 2D case there is no weak-coupling parameter T_c/E_F, and the validity of the mean-field approximation in the high-field limit is highly questionable. In this limit the average separation between vortices is of the order of the average separation between the electrons, and the quantum fluctuations could be so strong as to destroy the mean-field vortex lattice solution at any temperature (even at zero temperature). After all, it is well known that for repulsive interactions the ground state involves correlations that are not of the Hartree-Fock type (Laughlin, 1983a). This is a serious concern, which is addressed further in Sec. V.C. However, this does not preclude a possibility that some signature of high-field superconductivity could be seen in 2D heterojunctions and other layered systems.

As the field is lowered further below the quantum limit, the approximation used above eventually fails, as was discussed in Sec. III. The contribution from off-diagonal pairing terms increases with an increasing n_c suppressing gapless behavior, and now the diagonalization of the "band-structure" problem presented above becomes an increasingly hopeless task. An interesting study that addresses this problem by considering a disordered array of vortices has been recently carried out by Stephen (1992). However, we can still learn about the nature of the superconducting order by studying the Ginzburg-Landau theory in and around the crossover region. If many Landau levels are occupied, the Ginzburg-Landau free energy can be found in a similar fashion. The kernels K_2 and K_4 are not projectors any more, and the exact solution for $\Delta(\mathbf{r})$ will now have a contribution from higher bosonic Landau levels. The insight that we gained in the quantum limit concerning the nature of orbital frustration can now be used to construct a solution to Ginzburg-Landau equations at lower fields. Maniv and Tešanović (1991) consider an ordinary (low-field in the sense of Fig. 1) strongly type-II superconductor ($\kappa \gg 1$), with a large $H_{c2}(0)$. The Ginzburg-Landau expansion for the free energy in an external field can be written to zeroth order in the fluctuating part of the vector potential, exploiting $\kappa \gg 1$, but otherwise in analogy with Eq. (2.21a) with K_3 set equal to zero. Let us start with the low-field region, where the semiclassical phase-integral approximation applies, i.e., Eq. (2.23a) with $\mathbf{a}(\mathbf{r})$ set equal to zero. The linearized equation (2.23a) has the form of the Schrödinger equation for bosons of charge $e^*=2e$ and mass $m^*=2m$ in an external magnetic field (but not projected to the lowest Landau level, unlike in the quantum limit). The eigenvalues are $\alpha(T)=\hbar\omega_c(n+\frac{1}{2})$, where $\omega_c=e^*H/m^*c$, and a complete orthonormal set of eigenfunctions of Eq. (3.26) modified for $e\rightarrow e^*$, i.e., $\phi'_{nm}=2\phi_{nm}(\sqrt{2}z)$. The highest T_c corresponds to $n=0$. This leads to an infinitely degenerate manifold of solutions, which can be represented as $\Delta'(\mathbf{r})=\Delta_0 f(z)\exp(-|z|^2/2)$, where the superscript prime indicates the solution of the linearized Ginzburg-Landau equation. The Abrikosov variational solution consists of a linear combination of the eigenfunction from within the lowest, $n=0$, Landau level with coefficients so selected as to produce a regular lattice of zeros in $f(z)$. The density of zeros has to match the average magnetic induction $\langle \mathbf{B}(\mathbf{r})\rangle$. This form of solution we denote by $f_A(z)$. It is easy to see that $\Delta'_A(\mathbf{r})$ [with $\mathbf{B}(\mathbf{r})=\mathbf{H}$] is not a solution of Eq. (2.23a); thus the exact solution does not lie entirely in the lowest Landau level, as in the quantum limit. Yet, at temperatures sufficiently close to $T_c(H)$, the continuity of $\Delta(\mathbf{r})$ at T_c should guarantee that $\Delta'_A(\mathbf{r})$ represents a significant part of this exact solution.

To separate the exact solution into parts belonging to the lowest and higher Landau levels we now can use what we have learned in the quantum limit. We also use the lowest-order gradient expansion for kernels K_2 and K_4.

It is very important to emphasize that this is only for the sake of brevity. The procedure below can be carried through with fully nonlocal K_2 and K_4 as well, and the reader should consult Maniv *et al.* (1991) for details concerning the crossover regime. We project Eq. (2.23a) to the lowest Landau level:

$$\tilde{\alpha}\phi(\mathbf{r})+\beta\int d^2r' P(\mathbf{r},\mathbf{r}')|\phi(\mathbf{r}')|^2\phi(\mathbf{r}')=0 \tag{4.15a}$$

where

$$P(\mathbf{r},\mathbf{r}')=\sum_{m=0}^{\infty}\phi'_{0m}(\mathbf{r})\phi'_{0m}(\mathbf{r}')$$
$$=\frac{1}{\pi}\exp(-|z|^2/2-|z'|^2/2+zz'^*) \tag{4.15b}$$

is the projection operator on the subspace formed by the lowest Landau level, with

$$\phi(\mathbf{r})=\int d^2r' P(\mathbf{r},\mathbf{r}')\psi(\mathbf{r}') ,$$

where $\psi(\mathbf{r})$ is the standard Ginzburg-Landau order parameter,

$$\psi(\mathbf{r})\equiv\left[\frac{7\xi(3)n}{8(\pi K_B T_c)^2}\right]^{1/2}\Delta(\mathbf{r}) ,$$

and $\tilde{\alpha}=\alpha+\frac{1}{2}\hbar\omega_c$.

This projected equation is closely related to Eq. (2.21a). It has a continuous set of exact solutions, which can be written as

$$g(z)=\sum_{-\infty}^{\infty}a_n\exp[-(\pi n/a_x)^2+(2\pi i n z/a_x)] ,$$

where a_x is an arbitrary real constant, determining the period $a_x l$ along the x axis, and

$$g(z)\equiv f(z)\exp(-|z|^2/2) .$$

The coefficients $\{a_n\}$ are given by

$$a_n=\exp[(i\pi b_x/a_x)n^2] , \tag{4.16}$$

where b_x is an arbitrary real number, and the amplitude ψ_0 is

$$\psi_0^2=-\tilde{\alpha}\sqrt{2}/\beta s(2b/a_x) . \tag{4.17}$$

Here

$$s(\rho)=|\Theta_3(0|\rho)|^2+|\Theta_2(0|\rho)|^2$$

and $\Theta_{3,2}(\zeta|\rho)$ are the Jacobi theta functions, and b is defined as $b=b_x+ib_y$, where $b_y=\pi/a_x$. The corresponding entire function, $f(z)$, is given by

$$f(z)=\exp(|z|^2/2)\Theta_3(\pi z/a_x|b/a_x) ,$$

whereas the corresponding order parameter

$$\psi(\mathbf{r})=\psi_0\exp(-|z|^2/2)f(z)$$

coincides with the Eilenberger eigenfunction on an arbitrary periodic lattice (Eilenberger, 1967), whose primitive unit vectors are a_x and b. The above relation between b_y and $a_x, a_x b_y=\pi$ fixes the flux through each unit cell to be one elementary flux unit ϕ_0. It can be readily shown that the resulting order parameter is directly related to the familiar Abrikosov form, except for a different gauge.

The fact that $\phi(\mathbf{r})$ is a solution of Eq. (4.15a) enables us now to solve the original Ginzburg-Landau equation (2.23a) exactly: We write the exact solution of Eq. (2.23a) as

$$\psi(\mathbf{r})=\phi(\mathbf{r})+\delta\psi(\mathbf{r})$$

and then expand $\delta\psi(\mathbf{r})$ in the complete set of eigenfunctions $\{\phi'_{nm}\}$ as

$$\delta\psi(\mathbf{r})=\psi_0\sum_{n=1}^{\infty}\sum_{mk}b_{nm}\phi'_{nm}(\mathbf{r}) .$$

Since $\phi(\mathbf{r})$ is a projection to the lowest Landau level, it can be written as

$$\phi(\mathbf{r})=\psi_0\sum_m b_{m0}\phi'_{m0}(\mathbf{r}) .$$

Now, we project the Ginzburg-Landau equation (2.23a) to higher Landau levels ($n>0$) by applying the operator $\delta(\mathbf{r}-\mathbf{r}')-P(\mathbf{r},\mathbf{r}')$. This leads to a nonlinear equation for the coefficients $\{b_{nm}\}$, which can be solved by iteration, assuming $\{b_{nm}\}$ are small. To the lowest order, appropriate for H not too far from H_{c2}, one gets

$$b_{nm}=-(\beta/\psi_0\hbar\omega_c)\int d^2r|\phi(\mathbf{r})|^2\varphi(\mathbf{r})\phi^*_{nm}(\mathbf{r}) . \tag{4.18}$$

Similarly, the lowest-order correction to F arising from higher Landau levels can be written

$$\Delta F=-\hbar\omega_c\psi_0^2\sum_{n=1}^{\infty}n|b_n|^2 , \tag{4.19}$$

suggesting that excitations to higher Landau orbitals induce attractive forces between vortices.

There are a number of other related questions which we shall consider in Sec. V. For example, an interesting issue is whether the triangular lattice of simple zeros remains the lowest free-energy configuration at all fields. In the high-field limit, one could imagine "Peierls"-type instability, leading to deformation of the lattice and possibly overlap of zeros. Also, thermal and quantum fluctuations should be included.

To study qualitatively the crossover region, where many Landau levels are occupied, is more difficult. However, the important feature to appreciate is that close to the $H_{c2}\rightarrow H_{c\infty}$ line the order parameter $\Delta(\mathbf{r})$ is almost entirely represented by the basis set restricted to the lowest Landau level, no matter where we are on the $H_{c2}\rightarrow H_{c\infty}$ line. This follows directly from the form of Eq. (4.15a). Since higher Landau levels will produce a finite change in $\tilde{\alpha}$, the cubic term cannot compensate, and the effect of higher Landau levels in $\Delta(\mathbf{r})$ must go to zero close to the transition line [i.e., go to zero faster than $\Delta'(\mathbf{r})$]. Starting then from the quantum limit, as H decreases towards the low-field limit the vortex lattice in

the Ginzburg-Landau region simply expands, keeping the area of the elementary hexagonal plaquette equal to $2\pi l^{*2}$. This continuous monotonous crossover might seem in contradiction with our insistence (see, in particular, the Introduction) that the nature of the superconductivity in the quantum limit is different from that in the semiclassical phase-integral approximation. We therefore discuss next in some detail what is going on.

The fact that $\Delta(\mathbf{r})$ in mean-field approximation looks very much the same all along the $H_{c2}\rightarrow H_{c\infty}$ line *does not* mean that the properties of the superconducting states are similar. In particular, the response of the system in the presence of $\mathbf{H}$ is characterized by the induced currents (which, for example, lead to diamagnetic pair breaking in the semiclassical phase-integral approximation, as discussed in the Introduction) and not by $\Delta(\mathbf{r})$. It is difficult to write down in a transparent way the relation between the induced current $\mathbf{j}(\mathbf{r})$ and $\Delta(\mathbf{r})$ everywhere on the transition line [although in principle Eq. (2.21a) does contain the full information].

Two extreme regions are accessible. For the semiclassical phase-integral-approximation region, $\mathbf{j}(\mathbf{r})$ is given by Eq. (2.23b),

$$\mathbf{j}(\mathbf{r})=\frac{-e\hbar}{im}[\psi^*(\mathbf{r})\nabla\psi(\mathbf{r})-\psi(\mathbf{r})\nabla\psi^*(\mathbf{r})] - \frac{4e^2}{mc}\psi^*(\mathbf{r})\psi(\mathbf{r})\,\mathbf{A}(\mathbf{r}) \ . \tag{4.20}$$

For the quantum limit using Eqs. (2.21b) and (4.9) we get, after a bit of algebra,

$$\frac{\partial b}{\partial z}(z,z^*)=-\frac{V^2e^2H}{\pi l^2mc^2}\frac{\beta}{2}\gamma'(T)z^*e^{-|z|^2/2}\int d^2r_1\int d^2r_2\Delta^*(z_1,z_1^*)\Delta(z_2,z_2^*) \times\exp\left[+\left[\frac{-|z_1|^2}{2}-\frac{|z_2|^2}{2}+\frac{z_1z_2^*}{2}+\frac{z_1z^*}{2}+\frac{zz_2^*}{2}\right]\right], \tag{4.21}$$

where $\gamma'(T)$ is given in Eq. (4.10c); of course, $(4\pi/c)\mathbf{j}(\mathbf{r})=\nabla\times\mathbf{b}(\mathbf{r})$. Let us now see the difference between Eqs. (4.20) and (4.21).

Suppose we produce the same disturbance (due to, say, some external potential) in the quantum limit and the low-field limit by setting

$$\psi(\mathbf{r})\equiv\Delta(z,z^*)=e^{-|z|^2/2} \ . \tag{4.22}$$

From Eq. (4.20) we get that $\mathbf{j}(\mathbf{r})$ in the low-field limit is

$$\mathbf{j}(\mathbf{r})\approx e^{-|z|^2}\mathbf{H}\times\mathbf{r} \ . \tag{4.23}$$

From Eq. (4.21) we get that $\mathbf{j}(\mathbf{r})$ in the quantum limit is

$$\mathbf{j}(\mathbf{r})\approx e^{-|z|^2/2}\mathbf{H}\times\mathbf{r} \ . \tag{4.24}$$

Aside from differences in proportionality constants, Eqs. (4.23) and (4.24) differ by a factor of 2 in $e^{-|z|^2}$; this actually is a signature of the difference between the two regimes.

The induced current in Eq. (4.23) is the response of a *macroscopic* order parameter made up of *many* Cooper pairs. To get the current response for such a $\psi(\mathbf{r})$ we must square it [i.e., $\psi^*(\mathbf{r})\psi(\mathbf{r})$] and multiply it by $\mathbf{A}(\mathbf{r})$. On the other hand, the response in the quantum limit can be traced to a current carried only by the two local Landau orbitals making up the Cooper pair. These local currents are simply the result of these orbitals [i.e., Eq. (4.2)] being eigenstates of electrons in a magnetic field. For example, the wave function of Cooper pairs that leads to Eq. (4.22) is, from Eq. (4.5),

$$|\tilde{\phi}\rangle=\prod_{k_z}(u_{k_z}+v_{k_z}C^\dagger_{k_zm=0\uparrow}C^\dagger_{k_zm=0\downarrow})|\text{vacuum}\rangle \ . \tag{4.25}$$

In Eq. (4.25) the concept of magnetic frustration is clearly irrelevant. As already discussed in the Introduction, the frustration energy in the low-field limit is a consequence of the expense in energy due to the displacement (by $\mathbf{H}$) of the momenti transverse to $\mathbf{H}$. This leads to current flows perpendicular to $\mathbf{H}$ and to "frustration energy." It is the underlying essence of Eq. (4.20). There is no analogous frustration in the quantum limit.

The crossover between these two regimes can now be understood as well. As the field $\mathbf{H}$ gets stronger, the transverse frustration loss in energy is regained by stronger and stronger pairing along $\mathbf{H}$. The crossover region contains a mixture of the current responses of Eqs. (4.20) and (4.21). The order parameter, however, still looks the same while the underlying properties continue to change smoothly to the quantum limit.

While the coupling between the order parameter and $\mathbf{a}(\mathbf{r})$ can be ignored in the above discussion, it is still important conceptually. This coupling can be treated perturbatively in the above exact solution of the Ginzburg-Landau equations. The magnetic field induced by superconductivity itself is very small compared to the external field. This is also true when the induced $\mathbf{a}(\mathbf{r})$ is coupled to the order parameter in strongly type-II superconductors (i.e., $\kappa\gg1/\sqrt{2}$). Therefore, to some extent, we can think of high-field-limit superconductivity as a manifestation of extreme type-II behavior. The two coupled equations (2.23a) and (2.23b) can be solved perturbatively, resulting in a variational solution to the problem. The effect of the induced $\mathbf{a}(\mathbf{r})$ scales like $1/\kappa\ll1$ and can be ignored for most purposes. It is important to keep in mind that the effect of the induced vector potential is always significant at very large distances ($\gg\lambda$), and so one should be careful about ignoring it. In the high-field lim-

it the effective λ will typically be longer than the size of a sample, and thus our neglect of $\mathbf{a}(\mathbf{r})$ is justified.

C. Transport properties

1. General remarks

We next turn to transport properties in the mean-field approximation. Although the magnetic response of a superconductor, discussed above (and, in fact, the response of the normal Fermi-liquid state as well), share many similarities with transport properties (i.e., the response to an electric field), they are not the same. Before we turn to our primary interest here, which is the superconducting transport properties in the quantum limit, we want to illustrate this difference in the linear-response region. It is certainly true that both an applied electric field and a magnetic field produce currents in the system. When the velocity of the current in the superconducting state exceeds some critical value, dissipation starts. This is true for currents induced by both magnetic (see the Introduction) and electric fields. However, the two are not exactly the same. The response of electrons (superconducting or normal) to an external magnetic field is a ground-state property; not so, the response to an electric field.

The most general formulation of these ground-state properties has been presented in recent papers by Vignale and Rasolt (1987, 1988 for the continuum and Rasolt and Vignale, 1990 for the lattice). Unlike the normal case, however, the case of superconductivity, requires the addition of the self-consistent correction discussed in Sec. VII of Vignale and Rasolt (1988). We should also point out that below the H_{c1} line (and certainly in the linear-response region) the magnetic field is totally expelled from the bulk, and therefore the bulk ground-state properties are unaffected by $\mathbf{H}$. However, around the H_{c2} line this new theory of Vignale and Rasolt can have important implications, which are presently being exploited (see also Olivera, Gross, and Kohn, 1988). This is even more relevant to the effect of quantum fluctuations (see Sec. V) around the $H_{c\infty}$ line (in particular in the quantum limit), where the Abrikosov lattice reflects more microscopic many-body effects perpendicular to $\mathbf{H}$ [see the discussion below Eq. (4.24)].

Coming back to a simple illustration of the difference between responses to magnetic and electric fields, consider Fig. 8, where we present the current-current response function $\chi_{jj}(\mathbf{q},\omega)$ in the normal states. The more complex set of graphs of Fig. 9 represent the same response in the superconducting state. Both cases incorporate the effects of disorder to lowest order in impurity scattering. These contributions are equivalent to Fig. 3, now for the current-current response χ_{jj}. In other words, Fig. 3 represents the effect of impurities (for weak disorder) on K_2 [of Eq. (2.16)] and therefore on the creation of the superconducting condensate [or equivalently $\Delta(\mathbf{r})$]. Figure

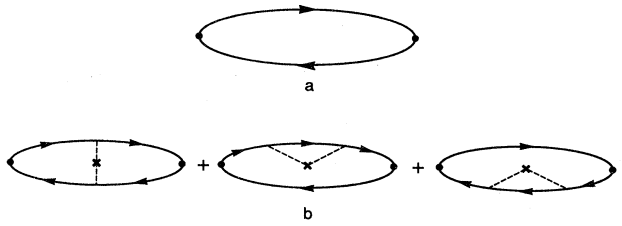

FIG. 8. Current-current response in the normal state: (a) Current-current response function of the pure normal state; (b) response to lowest order in impurity scattering.

9 represents the effect of impurities (for equivalent disorder) on the response to either magnetic or electric fields, once the condensate has been created (i.e., below the H_{c2} line or above the $H_{c\infty}$ line). The induced current $\mathbf{j}(\mathbf{q},\omega)$ is given by the Kubo relation

$$\mathbf{j}_\alpha(\mathbf{q},\omega)=\left[\chi_{jj}^{\alpha\beta}(\mathbf{q},\omega)-\frac{\rho e^2\delta_{\alpha\beta}}{mc}\right]A^\beta(\mathbf{q},\omega)\ . \tag{4.26}$$

Equation (4.26) assumes that the response of the system is translationally invariant after the average over impurities has been taken.

From the spatial isotropy,

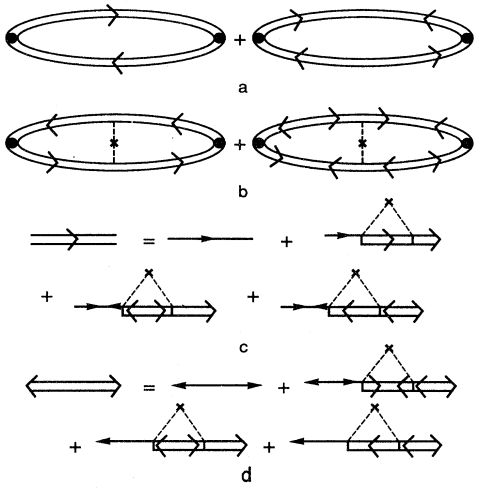

FIG. 9. Current-current response in the superconducting state. (a) Current-current response function in the superconducting state ignoring impurity vertex corrections. The double-line arrowed propagators represent the normal and anomalous propagators in the superconducting states defined in (c) and (d). (b) Including vertex corrections. (c) The normal propagator, in the superconducting state, to lowest order in impurity scattering. In contrast to Figs. 3 and 5, the single-line arrowed propagators include electron-electron interactions. This, of course, is the reason why the single-line arrowed anomalous propagator is nonzero. (d) The anomalous propagator to lowest order in impurity scattering.

$$\chi_{jj}(\mathbf{q},\omega)=B_L(\mathbf{q},\omega)\frac{q_\alpha q_\beta}{q^2}+B_T(\mathbf{q},\omega)\left[\delta_{\alpha\beta}-\frac{q_\alpha q_\beta}{q^2}\right] . \tag{4.27}$$

From gauge invariance,

$$\lim_{\omega\to 0} B_L(\mathbf{q},w)=\frac{\rho e^2}{mc} , \tag{4.28}$$

so

$$\lim_{\omega\to 0}\chi_{jj}^{\alpha\beta}(\mathbf{q},\omega)=\frac{\rho e^2}{mc}\frac{q_\alpha q_\beta}{q^2}+B_T(\mathbf{q},\omega\to 0)\left[\delta_{\alpha\beta}-\frac{q_\alpha q_\beta}{q^2}\right] . \tag{4.29}$$

In the normal state

$$\lim_{\mathbf{q}\to 0}\lim_{\omega\to 0} B_T(\mathbf{q},\omega)=\frac{\rho e^2}{mc} . \tag{4.30}$$

In the superfluid (or superconducting) state the superfluid density ρ_s (remember that ρ_s is not simply $|\psi|^2$ but is related to the helicity modulus) is

$$\rho_s=\lim_{\mathbf{q}\to 0}\lim_{\omega\to 0}[B_L(\mathbf{q},\omega)-B_T(\mathbf{q},\omega)] . \tag{4.31}$$

[Note that according to Eqs. (4.28), (4.30), and (4.31) $\rho_s=0$ in the normal state.] Now let us return to Figs. 8 and 9 and start with the normal state. In the absence of impurities, only Fig. 8(a) contributes. Figure 8(a) in conjunction with Eq. (4.29) then leads to the noninteracting Landau dimagnetism,

$$\chi_L^0=\frac{-k_F e^2}{2\pi^2 mc^2} . \tag{4.32}$$

On the other hand, the response of the system to an electric field (i.e., transport) is given by reversing the limits in Eq. (4.29). Including impurities, the conductance σ is given by the famous Drude form,

$$\sigma\approx\lim_{\omega\to 0}\lim_{\mathbf{q}\to 0}\frac{\chi_{jj}(\mathbf{q},\omega)}{i\omega}=\lim_{\omega\to 0}\frac{\rho e^2 i}{m(\omega+i/\tau)}=\frac{\rho e^2\tau}{m} . \tag{4.33}$$

When we take, however, the pure system, then $\tau\to\infty$ and σ goes to infinity as it should. The difference between transport and ground-state properties reduces to an emphasis on temporal or spatial responses, respectively.

In the superconducting state, χ_{jj} of Fig. 9 can also be calculated. It is found that now, due to the presence of a gap, both χ_L and σ become infinite even in the presence of impurities (see below). [Incidentally, the terms presented in Fig. 9 will not yield the gauge-invariant form of Eq. (4.29). As is well known, additional corrections (vertex corrections) beyond the mean-field approximation need to be included. At finite ω these lead to the Anderson-Higgs Goldstone mode (for Coulomb e-e interaction to a plasmon), which is a collective Cooper pair–Cooper pair excitation present beyond the single quasiparticle excitation $\epsilon_n\equiv(\xi_n^2+\Delta^2)^{1/2}$, the only excitation available in the mean field.] Perhaps we should add one more remark about the Meissner effect. In the linear-response region the magnetization $\mathbf{M}$ (in the superconducting state) equals $-\mathbf{H}/4\pi$, the definition of the Meissner effect. This is a direct consequence of χ_L's going to infinity, because

$$H=\frac{\partial F}{\partial M}=\frac{\partial}{\partial M}\left[+\frac{1}{2\chi_L}M^2-2\pi M^2\right] . \tag{4.34}$$

Therefore in the superconducting state $M=-(H/4\pi)$, while in the normal state, where $|\chi_L|\ll 1/4\pi$, $M=\chi_L H$.

The relation between transport and ground-state properties in the superconducting state (and in linear response) can be made more general by considering Fig. 9 for arbitrary $\mathbf{q}$ and ω. For completeness, we list the final result:

$$\mathbf{j}_\alpha(\mathbf{r})=\int d^3r'\left\{\frac{\hbar}{2\pi c}\int d\xi\, d\xi' L(\xi,\xi')\mathrm{Re}\left[\sigma_{\alpha\beta}\left[\mathbf{r},\mathbf{r}',\frac{\xi-\xi'}{\hbar}\right]\right]-\frac{\rho e^2}{mc}\delta(\mathbf{r}-\mathbf{r}')\delta_{\alpha\beta}\right\}A_\beta(\mathbf{r}') , \tag{4.35a}$$

where

$$L(\xi,\xi')=\frac{\Delta^2+\xi\xi'-\epsilon\epsilon'}{\epsilon'\epsilon(\epsilon'+\epsilon)} \tag{4.35b}$$

and $\epsilon=(\xi^2+\Delta^2)^{1/2}$ and $\sigma_{\alpha\beta}$ is the transport response. We then see that even for arbitrary variations of $E(\mathbf{r})$ there is a close relation between transport and ground-state properties, though the two are not the same. Finally, we should mention that Eq. (4.35) can be derived, as well, by expanding Eq. (2.9) to linear order in $\mathbf{A}(\mathbf{r})$.

2. Transport properties of the normal state in the high-field limit—linear response

To understand the transport properties of the superconducting state in the high-field limit we start with the normal state in this limit. This problem has been thoroughly investigated by Abrikosov (1969). We list the relevant aspects of his study below.

The response to a weak electric field is given again in Fig. 8. The single-particle propagators are now given in terms of the Landau levels; it is an extension of Eq. (4.6) to many such levels,

$$G_0(\omega,\mathbf{r}_1,\mathbf{r}_2)=\sum_{m,n}\frac{\phi^*_{nm}(\mathbf{r}_1)\phi_{nm}(\mathbf{r}_2)}{i\omega-\xi_{n\pm}(k_z)}\ , \tag{4.36a}$$

where ϕ_{nm} are given in Eq. (3.26) and where

$$\xi_{n\pm}(k_z)=\frac{eH}{m_c c}(n+\tfrac{1}{2})\mp\frac{geH}{2mc}+\frac{\hbar^2k_z^2}{2m_z}-E_F \tag{4.36b}$$

(we are keeping the Zeeman splitting).

The Fermi momentum (along **H**) for each occupied Landau level is given by

$$k_{Fn\pm}=\left[\left[E_F-\frac{eH}{m_c c}(n+\tfrac{1}{2})\pm\frac{geH}{2m_z c}\right]2m_z\right]^{1/2}. \tag{4.36c}$$

Now introducing Eq. (4.36) for the electron propagator into Fig. 10, we get the following form for the Green's function in the presence of pointlike impurities of amplitude U_0:

$$G=\sum_{m,n}\frac{\phi^*_{nm}(\mathbf{r}_1)\phi_{nm}(\mathbf{r}_2)}{i\omega-\xi_n(k_z)-\Sigma} \tag{4.37a}$$

where

$$\Sigma=N_i U_0\left[1+i\,\mathrm{sgn}\omega U_0\frac{eHm_c}{2\pi c}\sum_n\frac{1}{k_{Fn\pm}}\right]^{-1} \tag{4.37b}$$

and where N_i is the impurity concentration, the sum in Eq. (4.37b) is over the occupied Landau levels, and Eq. (4.37b) is restricted to zero temperature. The result of Eq. (4.37b) is rigorous when $(\tau k_{F0}^2)/(2m_z)\to\infty$, with $1/\tau=-2\,\mathrm{Im}\Sigma$. Since the impurities are nonmagnetic, there is no communication between the two spins, and the effect of the Zeeman splitting is to introduce the $\pm$ signs according to Eq. (4.36b). As we shall see below in considering superconducting transport, it is important to note that the imaginary part of Σ [in Eq. (4.37b)] is nonzero *only* due to scattering from states of momentum k_z and Landau index n to k_z' and n' all sitting at the Fermi energy E_F. If a gap appears in the $\xi_n(k_z)$ at E_F the imaginary part of Σ must vanish.

Now introducing G [Eq. (4.37)] into Fig. 8, we get the various current responses depending on the orientation of **E** relative to **H** (or equivalently the z axis); for **E** along z,

$$\sigma_{zz}=(\rho_+\tau_+ +\rho_-\tau_-)e^2/m_z,\quad \sigma_{zx}=0,\quad \sigma_{zy}=0\ , \tag{4.38}$$

where $\rho_\pm$ and $\tau_\pm$ are the two spin densities and lifetimes, respectively.

For **E** along y the longitudinal Hall conductance is

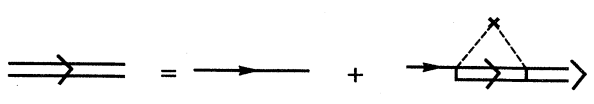

FIG. 10. The normal propagator in the normal state to lowest order in impurity scattering.

$$\sigma_{yy}=\frac{e^2m_c}{2\pi^2}\left[\frac{1}{\tau_+}\sum_n\frac{n+\frac{1}{2}}{k_{Fn+}}+\frac{1}{\tau_-}\sum\frac{n+\frac{1}{2}}{k_{Fn-}}\right], \tag{4.39a}$$

and the transverse Hall conductance is

$$\sigma_{xy}=\rho_\pm ec/H\ . \tag{4.39b}$$

3. Transport properties of a superconductor in the high-field limit—linear response

We can carry out the same calculation for Fig. 9 as we did for Fig. 8. The calculation is more tedious, due to the presence of the anomalous propagator $F(i\omega,\mathbf{r}_1,\mathbf{r}_2)$. Not only that, but in the mean-field approximation the order parameter has a lattice structure (see Sec. IV.B). This requires the calculation of $G(i\omega,\mathbf{r}_1,\mathbf{r}_2)$ and $F(i\omega,\mathbf{r}_1,\mathbf{r}_2)$ in the presence of a nonuniform $\Delta(\mathbf{r})$, which is very difficult. What will happen to Eqs. (4.38) and (4.39) in the superconducting state, however, can be understood without such a calculation.

Let us turn, then, to the wave function given in Eq. (4.5) (for simplicity we restrict the discussion to the quantum limit). Whatever the coefficients u and v do, as a function of m and m', as long as the coherence is maintained between k_z and $-k_z$ the lifetimes τ_+ and τ_- [in Eqs. (4.38) and (4.39)] must go to infinity. This we can see by defining a new set of operators $D^\dagger_{k_z m}$ and $D_{k_z m}$ such that

$$D_{k_z m}=\sum_{m'}A^{k_z}_{m,m'}C_{k_z m'}\ , \tag{4.40}$$

where the matrix A diagonalizes $v^{m,m'}_{k_z}$ in Eq. (4.5). The ground-state wave function in the mean-field approximation, given in Eq. (4.5), now reads

$$|\tilde{\phi}\rangle=\prod_{k_z,m}(\tilde{u}^m_{k_z}+\tilde{v}^m_{k_z}D^\dagger_{k_z m\uparrow}D^\dagger_{-k_z m\downarrow})|\text{vacuum}\rangle\ . \tag{4.41}$$

The Bogoliubov operators introduced in Eq. (2.8) are now

$$\gamma^\dagger_{k_z m\uparrow}=\tilde{u}^m_{k_z}D^\dagger_{k_z m\uparrow}-\tilde{v}^m_{k_z}D_{-k_z m\downarrow}\ . \tag{4.42}$$

These can be shown to create the quasiparticle excitation of Eq. (4.41). These excitations have a gap as long as $\tilde{u}_{k_z}\neq 0$ [i.e., as long as the coherence along k_z and $-k_z$ is maintained; see, however, Eq. (4.14)]. We then conclude from Eq. (4.38) and (4.39) that in the superconducting state in high fields, the longitudinal resistance ρ_{zz} parallel to the field vanishes and ρ_{yy} perpendicular to the field also shows a significant drop. Such dramatic drops in resistance make this state experimentally *distinct* from all the other instabilities (for example, SDW, CDW) and other transport properties (like magnetic freezeout). In using Eqs. (4.38) and (4.39) we did not take into account the spatial nonuniformity of $\Delta(\mathbf{r})$ perpendicular to **H** (nor parallel to **H** in the case of Zeeman splitting). This should not, however, change our discussion; we come

back to this in a more general discussion shortly. It might be tempting to suggest that the transport properties perpendicular to **H** should resemble the quantum Hall effect; this is not entirely true. There are many reasons for this. We list a few: (a) In Eq. (4.39b) there is no relation between the carrier density $\rho_{\pm}$ and **H**, as there is, for example, in the integer quantum Hall effect without impurities, which is certainly very well understood. (b) The general gauge arguments by Laughlin for the case of impurities depend on the 2D geometry of the quantum Hall effect. (c) Localization and the corresponding plateaus are not strong in 3D. (d) Any finite temperature leads in the quantum Hall effect to opening of the gap and some low-level dissipation. Here the gap remains up to T_c except for single points in the zone [see Eq. (4.14)].

We want to conclude this discussion with a few more remarks about $|\tilde{\phi}\rangle$ of Eq. (4.5). For arbitrary u's and v's Eq. (4.5) describes any spatial form of the order parameter $\Delta(\mathbf{r})$. Another useful form for $\tilde{\phi}$ which leads to an approximate vortex structure in the mean field approximation is

$$|\tilde{\phi}\rangle=\prod_{k_z,i}(\tilde{u}_{k_z,i}+\tilde{v}_{k_z i}D^{\dagger}_{k_z i\uparrow}D^{\dagger}_{-k_z i\downarrow})|\text{vacuum}\rangle\ , \tag{4.43}$$

where the $D^{\dagger}_{k_z i}$ creates single-particle states of momentum k_z and index i in the basis set introduced by Maki for the Wigner lattice ground state of the quantum Hall effect,

$$\phi_{k_z i}(\mathbf{r},z)=\frac{e^{ik_z\zeta}}{\sqrt{L}}e^{-|z|^2/4}e^{-|z_i|^2/4}e^{zz_i^*/2} \tag{4.44}$$

where $z_i=R_x+iR_y$ are distributed in a hexagonal Abrikosov structure of R_x and R_y. Such a $|\tilde{\phi}\rangle$ resembles a set of tubes (depicted in Fig. 11) filled up with many Cooper pairs of k_z and $-k_z$ momentum, with the same $\phi_{k_z i}$ per tube.

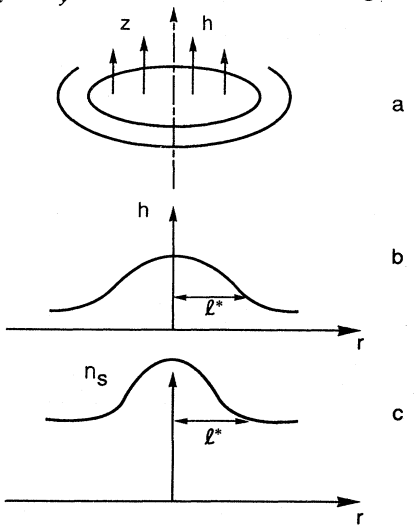

FIG. 11. Induced magnetic and current profiles in the quantum limit: (a) The superconducting "tube" in the quantum limit; (b) the induced part of the magnetic field h associated with a single tube (note $h \ll H$); (c) in contrast to Fig. 2, the radius of the tube is governed by the magnetic length l^*. Note also that there are no diamagnetic superconducting currents (a) circling in the tube, since they are extremely small.

4. Transport properties of a superconductor in the high-field limit—general considerations

We can go beyond linear response. We can take our superconductor and push a current through it, with some superfluid velocity v_s, and ask what happens to its dissipation. Let us start with zero temperature. When there is coherence in the wave function (4.5), the system has a gap [see, however, the discussion of Eq. (4.14)]. We can now change this wave function to a current-carrying one by multiplying $|\phi\rangle$ by $\exp i\mathbf{Q}\cdot\sum_i \mathbf{r}_i$,

$$\tilde{\phi}_{v_s}(\mathbf{r}_1\cdots\mathbf{r}_i)=\exp\left[i\mathbf{Q}\cdot\sum_i \mathbf{r}_i\right]\tilde{\phi}(\mathbf{r}_1\cdots\mathbf{r}_i)\ , \tag{4.45}$$

where $\mathbf{v}_s=\hbar\mathbf{Q}/m$. We should remark that for $\mathbf{Q}\|\mathbf{H}$ $\tilde{\phi}_{v_s}(\mathbf{r}_1\cdots\mathbf{r}_i)$ is an eigenstate of $\hat{H}$ in Eq. (2.4) [with $U_{\sigma v}(\mathbf{r})$ and $\mathbf{a}(\mathbf{r})$ set to zero in Eq. (2.1b)]. On the other hand, for $\mathbf{Q}\perp\mathbf{H}$, Eq. (4.45) is an eigenstate of $H+(v_s Hy)/c$, where the y axis is perpendicular to the current flow. This is just as it should be, the appropriate Hall voltage. As long as v_s is not so large that $\tilde{\phi}(\mathbf{r}_1\cdots\mathbf{r}_2)$ will itself be modified by the currents, then the superconducting order parameter remains the same; i.e., the fact that it is nonuniform both along z, due to Zeeman splitting, and perpendicular to **H**, due to the vortex lattice structure, does not interfere in the nondissipative flow. This is true all along the $H_{c2}\to H_{c\infty}$ line, although a remark should be made about the effect of finite temperature. At finite temperature, a gap continues to exist in the usual way (except for single points in the zone) below the whole $H_{c2}\to H_{c\infty}$ line. A zero-entropy mode always exists in the presence of quasiparticle excitations and, in the usual way, the superflow and the stationary normal fluid stabilize at a maximum entropy.

Thermal and quantum fluctuations can also melt the vortex structure. The wave functions are now random superpositions of $|\tilde{\phi}\rangle$'s of Eq. (4.5) and therefore coherence is lost (e.g., $u\to 0$) and no zero-entropy mode survives. See Sec. V for discussion of fluctuation effects.

5. Transport properties of a superconductor in the quantum limit within a wide parabolic quantum well

In order for superconductivity in donor-doped semiconductors to exist in the quantum limit, it is preferable (or perhaps even essential) to keep donor impurities out of the conducting region (e.g., magnetic freezeout is one serious concern; see Sec. VII). Wide parabolic quantum wells are one solution to this experimental problem (Gos-

sard, Halperin, and Westervelt, 1987; Gwinn *et al.*, 1989; Sajoto *et al.*, 1989). Here we discuss the expected transport behavior in such a restricted geometry. As already stressed in the Introduction and in later sections, there is a strong similarity between SDW instabilities and superconducting instabilities in the quantum limit. This will become even clearer here. In fact, to discuss the transport properties in a wide parabolic quantum well, all we need is to "invert" the discussion of Brey and Halperin (1989) in the same geometry for a spin-density wave; by "invert" we mean that whenever a gap at E_F, due to the SDW, occurs, conductivity parallel to **H** is reduced, while whenever the same occurs for spin-singlet superconductivity the conductivity increases.

The geometry we consider is a thick (>1000 Å) and uniform layer of high mobility; we choose the y direction to be perpendicular to the layer, and we place **H** along the z axis. We also choose a carrier density such that only the lowest level of the quantum well is occupied. The Fermi surface without the superconducting instability is illustrated in Fig. 12(a) and with the instability in Fig. 12(b). Here is what we are looking at: the flat portion of the Fermi surface represents the fact that, when the Landau states (in the lowest Landau level) are far from the two boundaries of the parabolic quantum well (along y), the eigenvalues as a function of k_x are dispersionless. (Here it is more convenient to switch to the Landau gauge, where the k_x's represent the usual center of the localized wave functions in the y direction). The curvature of the Fermi surface for larger $|k_x|$ represents the effect of the boundary of the wide parabolic quantum well (i.e., so called edge states). The curvature at positive k_x and negative k_x represents the edge state at the two quantum well boundaries.

When a superconducting instability occurs, the flat regions of the Fermi surface acquire a gap, and excitations over that part of the Fermi surface are eliminated (see Fig. 12). The group velocity **v** of an electron with wave vector (k_z,k_x) is given by the gradient of the dispersion with respect to (k_z,k_x). It is clear that the edge states at E_F with $k_x>0$ all have $v_x>0$, while states at the opposite edge have $v_x<0$. The value of v_z depends on k_z, and both signs of v_z may be found at each edge of the layer. Now suppose we set the state in motion. The impurity potential will scatter electrons at E_F, on either side of the wide parabolic quantum well, from one value of k_z to another. If the quantum well is thick compared to the magnetic length, there is little overlap between the states from opposite sides of the layer, so that the impurities should produce very little scattering between these two sets of states. Since the states at a given edge carry a current of a definite sign in the x direction, they cannot be localized in that direction, and this probably implies that they must also be extended in the z direction.

In order for a current to be carried by the sample in the x direction, one must establish a difference in the electrochemical potential between the two sides of the electron layer (essentially a Hall voltage). The electrical current is then carried by a combination of two effects: an excess in charge carriers at the edge, corresponding to a positive group velocity, and a contribution from the $E\times B$ drift of electrons in the center of the layer, arising from the induced electrostatic field E_y. In order for the current to relax, it is necessary for electrons near the Fermi energy to be scattered from one side of the electron layer to the other and thus restore the equilibrium population. Since there is little overlap between the two sets of states, this scattering rate should be relatively small, and the resistivity ρ_{xx} for currents in the x direction, at low temperatures in the spin-singlet superconducting state, should be smaller than the values at temperatures above the spin-singlet superconducting transition.

By contrast, current in the z direction is carried equally by extended states at both sides of the electron layer; it is not necessary to scatter electrons across the layer to restore equilibrium in this case. We expect that the resistivity ρ_{zz} for currents in the z direction will be significantly lower in the spin-singlet superconducting state than at temperatures above the spin-singlet superconducting transition, because electrons near the center of the parabolic well cannot scatter due to the superconducting gap. We note, however, that for a layer of finite thickness the values of both ρ_{zz} and ρ_{xx} should be finite.

In this section we have studied high-field superconductivity below the transition line. We have shown how the BCS theory in the high-field limit can be solved exactly and have discussed the nature of the superconducting state. We found the excitation spectrum of Bogoliubov quasiparticles to be gapless at a set of points in the magnetic Brillouin zone. The consequences of this solution of the BCS theory were then discussed, with particular emphasis on differences from and similarities to the low-field limit and transport properties.

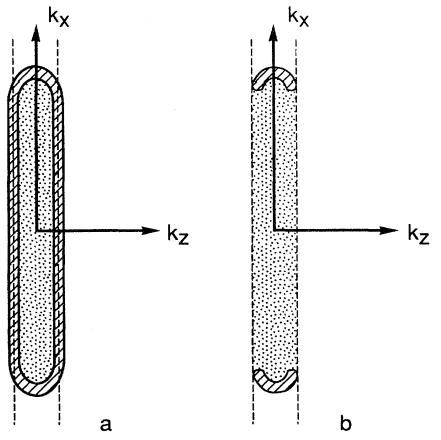

FIG. 12. Fermi surface of a wide parabolic quantum well: (a) schematic of Fermi surface in the absence of superconductivity; (b) schematic of Fermi surface in the presence of superconductivity. From Brey and Halperin, 1989.

V. FLUCTUATIONS

A. General remarks

All of what we have said up to now follows one crucial simplification of the exact thermodynamics as given by Eq. (2.5). This simplification is presented in Eq. (2.7) and is exactly what is meant by the mean-field approximation. To go beyond the mean-field approximation (for a superconductor in a magnetic field) is a very nontrivial matter, and exact results are scarce. This is particularly true in the quantum limit, where both thermal and quantum fluctuations could potentially play an important role.

First, we discuss what would be required to solve the problem exactly [i.e., calculate Z in Eq. (2.5a)] throughout the whole $\mathbf{H}$-T plane. Since at this point our discussion is totally general, we go back even further and start with $\hat{H}$ in Eq. (2.1).

1. Fluctuations outside the superconducting transition

Here the free energy is given exactly by the famous linked-cluster expansion. We illustrate in Fig. 13 a low-order fluctuation contribution to the free energy, which includes the remainder of the superconducting state inside the transition. We have already seen these ladder graphs in Fig. 3, representing the effect of superconducting fluctuations in the normal state (Aslamasov-Larkin fluctuations). To get the full contribution to the free energy, we need to sum all contributing graphs. It is not uncommon to divide fluctuations into thermal and quantum types. For example, in Fig. 14, to get thermal fluctuations only (in the order parameter) we set ω_α to zero

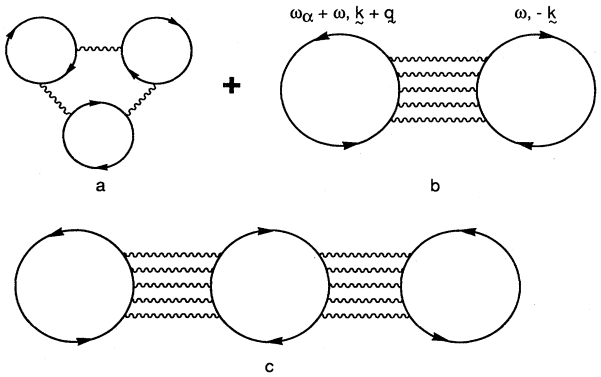

FIG. 13. Fluctuation contributions to the free energy above T_c. (a) Example of nonsuperconducting fluctuations (or equivalently correlations) contributing to the free energy in the normal state. (b) Contribution of a single superconducting fluctuation to the free energy in the normal state. When ω_α is set to zero we commonly think of it as a "thermal" fluctuation. (c) Contribution of the interaction of two such superconducting fluctuations to the free energy in the normal state. When the ω_α's are set to zero such nonlinear contributions correspond to quartic and higher contributions in the Landau-Ginzburg expansion of the free energy.

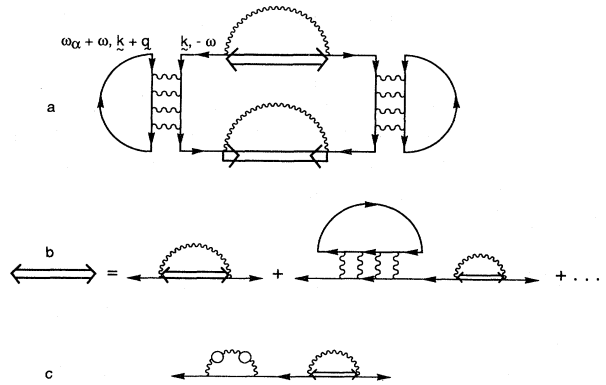

FIG. 14. Fluctuation contributions to the free energy below T_c: (a) example of fluctuation-corrected free energy in the superconducting state; (b) example of the effect of superconducting fluctuations on the order parameter; boot strap effects (see text); (c) example of normal fluctuations and their effect on the order parameter.

and keep $\mathbf{q}$ finite. These fluctuations should, to a good approximation (although not rigorously), be viewed as additional to the thermal excitations of quasiparticles across the gap. The quantum fluctuations are associated with finite ω_α. This separation, however, is a bit artificial, particularly in the quantum limit; the full answer is a hybrid of both.

Another way of carrying out exactly the same calculation is to decouple the quartic interaction in Eq. (2.5) using the Hubbard-Stratonovich fields $\Delta(\mathbf{r},\tau)$. Equation (2.5a) now includes an integral over $D\Delta(\mathbf{r},\tau)D\Delta^*(\mathbf{r},\tau)$, and in Eq. (2.7) $\Delta(\mathbf{r})\rightarrow\Delta(\mathbf{r},\tau)$ and

$$d^3\mathbf{r}\rightarrow\frac{1}{\beta}\int_0^\beta d\tau\, d^3\mathbf{r}\ .$$

Again the thermal fluctuations are associated with neglecting the τ dependence (or equivalently ω_α; see above), and again this separation is artificial.

Calculating the fluctuation contributions this second way leads to direct contact with the Ginzburg-Landau expansion for thermal fluctuations. It corresponds to approximating Eq. (2.5) by

$$Z=\int D\Delta(\mathbf{r})D\Delta^*(\mathbf{r})D\mathbf{a}(\mathbf{r})e^{-\beta F} \tag{5.1}$$

with F given in Eq. (2.17). It is exact all along the $H_{c2}\rightarrow H_{c\infty}$ line when quantum fluctuations are neglected and when we describe a second-order phase transition with the expectation that no higher than quartic contributions in $\Delta(\mathbf{r})$ are required. Incidentally, this is true for some things (like universal exponents) but not true for the shape of the transition line. In the quantum limit the transition line (and even the nature of the transition) can be strongly affected by thermal as well as quantum fluctuations (see below).

2. Fluctuations inside the superconducting transition

In the superconducting state the free energy of Fig. 13 needs to include symmetry-breaking corrections. This, as we saw, is illustrated in Fig. 14. In the Hubbard-Stratonovich field the same calculation involves introducing tadpole graphs for the broken symmetry of $\Delta(\mathbf{r},\tau)$ in the superconducting phase.

Finally we remark on the case in which the transition of $\Delta(\mathbf{r})$ is first order (such as perhaps the melting of the Abrikosov lattice; see below). For a first-order phase transition, Eq. (2.17) [inserted into Eq. (5.1)] is not appropriate for studying the transition line. Contributions like Fig. 14 must be calculated without any assumption of the magnitude of $\Delta(\mathbf{r})$. The free energy must be also calculated for the normal phase (Fig. 13). The equality of the two phases will then give the correct transition line; this is an enormously complex route. It is not, for example, as simple as calculating a melting curve of, say, sodium. The point is that the gap itself is crucially bootstrapped to the fluctuations. One can think of the melted lattice as a collection of vortices that have lost their spatial long-range order. This implies that the "normal" phase loses the true, static ($\omega=0$) gap in the quasiparticle excitation upon vortex melting (see Sec. IV.A), but the remnant contributions from the superconducting phase remain very strong. The free energy of the "fluid" phase in the vicinity of the transition is therefore particularly complicated.

B. One-dimensional phase transitions and the quantum limit

Although in principle methods do exist to handle the quantum limit rigorously, in reality this is an impossible task. As we shall see, even the treatment of thermal fluctuations in the low-field region is a highly nontrivial problem. The nonuniformity of $\Delta(\mathbf{r})$, due to magnetic frustration, makes such calculations much more difficult than the spatial isotropic Ginzburg-Landau-Wilson renormalization-group treatment. However, quantum and thermal fluctuations can be handled with some rigor in truly 1D systems. These calculations do provide some useful insights into fluctuations in the quantum limit; we take a few pages to discuss this.

Both Fig. 5 for spin-density waves and Fig. 3 for superconducting instabilities can be reduced to a one-dimensional form [see Eq. (3.6)]. The remaining one-dimensional variable is the momentum k_z along the magnetic field. Does that imply that a 3D electron gas in the presence of a very strong magnetic field (where all the electrons occupy the lowest Landau level) is truly one dimensional? Of course not. The one-dimensional form in the case of spin-density waves, as well as for off-diagonal superconducting instabilities, is a consequence of degeneracy in the eigenstates of different momenta k_y. This permits the elimination of k_y by summing over this variable (i.e., summing over the phase space perpendicular to the magnetic field or, in the cylindrical gauge, over m). Such a sum, however, does not make the system *truly* one dimensional. In fact, precisely this degeneracy was resolved below T_c to give the Abrikosov lattice discussed in Sec. IV, which is a three-dimensional configuration.

Above T_c the three-dimensional nature of the phase transition will appear at once, the moment we consider contributions beyond the ladder graphs of Fig. 5 for the spin-density wave state or Fig. 3 for superconductivity. For example, contributions from cross terms in the irreducible vertex (see Fig. 15) will not permit its transformation to 1D.

We can reduce the quantum limit to a *truly* 1D problem by replacing the interparticle interaction in Eq. (2.4) by a delta function interaction $w(\mathbf{q})$,

$$w(\mathbf{q})=g(q_z)\delta(q_x)\delta(q_y)\ . \tag{5.2}$$

This interaction is a constant in real space, perpendicular to the magnetic field, i.e., very long range and highly unphysical. In any event, the initial momentum k_{y1} and k_{y3} now remain the same across any intermediate states *for any scattering processes* (see Fig. 15). The problem is now truly 1D.

In 1D there is strong competition between superconductivity, spin-density waves and charge-density waves. The phase diagram for this 1D case has been studied previously. We discuss briefly the conclusions of these studies with particular attention to their implication for the mean-field predictions made in Secs. III and IV in the case of a realistic interparticle interaction (i.e., a short-range interaction in real space).

The interaction of Eq. (5.2) leads to scattering only along the z direction. Now in the weak-coupling limit the singular nature in the electron-electron or electron-hole scattering occurs around the Fermi surface. In 1D, then, there are only two possible scattering processes. Either the two electrons scatter in the forward direction

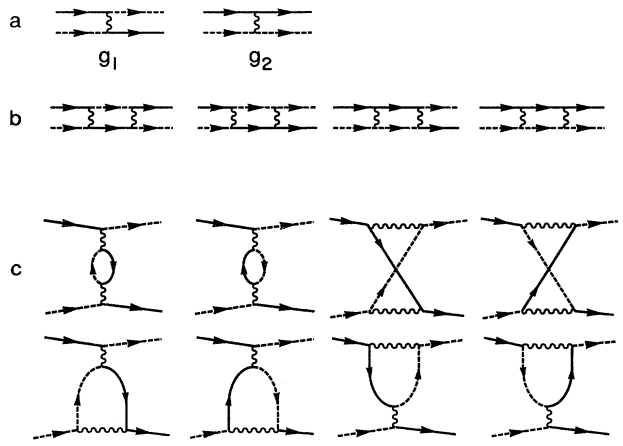

FIG. 15. Low-order scattering processes (to second order) (b,c) in 1D Fermi systems, in terms of the backward (g_1) and forward (g_2) elements. From Sólyom, 1979.

[i.e., $g(p_z=0)\equiv g_2$] or they scatter in the backward direction [i.e., $g(p_z=2k_F)\equiv g_1$]. Of course, there is a small range of intermediate momentum $|k_0|$ (or energy $E_0=\hbar^2 k_F|k_0|/m$) around k_F, whose contributions to the singular scattering amplitude is important. In this small range, however, we expect $g(p_z)$ to remain relatively constant. In addition to the electron and holes' being close to k_F, in both the e-e channel and e-h channel, the states must lie on opposite sides of the Fermi surface. [Incidentally, we are not interested in the pathological case of a half-filled band, in which case an Umklapp process is possible and an additional $g(p_z=4k_F)$ must be included.] The phase transition, in 1D, is then described by collecting all the singular contributions to, say, the electron-electron scattering amplitude (see Fig. 15). In Fig. 15(a), g_1 and g_2 are defined. The arrowed line is an electron state with momentum k_F, and the dashed arrowed line is an electron with momentum $-k_F$. The contributions to the e-e scattering amplitude Γ, to second order in the couplings g_1, and g_2, are presented in Fig. 15(b). Note that this collection of terms allows only for forward and backward momentum exchange. Moreover, the intermediate electron-electron and electron-hole lines are always on opposite sides of the Fermi surface, in accordance with the above discussion.

Suppose we consider two electrons with different spins. Two different cross sections can then be identified: $\tilde{\Gamma}_2(\omega,E_0)$, where the two electrons emerge with the same initial spins, and $\Gamma_1(\omega,E_0)$, where the spin is interchanged,

$$\Gamma(\omega,E_0)=\Gamma_1(\omega,E_0)\delta_{\alpha\gamma}\delta_{\beta\delta}-\Gamma_2(\omega,E_0)\delta_{\alpha\delta}\delta_{\gamma\beta}\ . \tag{5.3}$$

It is easy to identify these two distinct cross sections in the collection of terms in Fig. 15. [The reason for the dependence of $\Gamma(\omega,E_0)$ on E_0 can be found in Eqs. (5.4) and (5.5)]. Each one of these diagrams contains logarithmic singularities in 1D. These arise from the product of the e-e Green's functions,

$$-i\int_{k_F-|k_0|}^{k_F+|k_0|}\frac{dk'}{2\pi}\int\frac{d\omega'}{2\pi}G_+(k',\omega')G_-(-k',\omega-\omega') =\frac{m}{\hbar 2\pi k_F}\left[\ln\left[\frac{\hbar\omega}{E_0}\right]-\frac{i\pi}{2}\right] \tag{5.4}$$

and the e-h,

$$-i\int_{k_F-|k_0|}^{k_F+|k_0|}\frac{dk'}{2\pi}\int\frac{d\omega'}{2\pi}G_+(k',\omega')G_-(k'-2k_F,\omega'-\omega) =\frac{m}{\hbar 2\pi k_F}\left[\ln\left[\frac{\hbar\omega}{E_0}\right]-\frac{i\pi}{2}\right], \tag{5.5}$$

where G_+ and G_- are the 1D noninteracting Green's functions for k_F and $-k_F$, respectively.

One can continue to write infinite sets of such diagrams, with leading logarithmic singularities; these are the so-called parquet graphs. Such sets of graphs have great resemblance to the ladder graphs already considered in Figs. 3 and 5. However, what is crucial to 1D is that the e-h products [Eq. (5.5)] and e-e products be maintained consistently in the SDW, CDW, and superconductivity response functions; we did not do this in Secs. III and IV. When this is done correctly, no phase transition can occur in 1D. It is instructive to see how this happens in 1D and then to reconsider the implications for a short-range interparticle interaction (i.e., the physically meaningful situation) discussed in Secs. III and IV.

A very elegant way to sum this set of graphs is the multiplicative renormalization group developed by Sólyom (1979), and others. The idea is to demand scale invariance of the two amplitudes $\Gamma_1(\omega,E_0)$ and $\Gamma_2(\omega,E_0)$ when E_0 (or equivalently k_0) is scaled from E_0 to E_0'. The result is the usual flow equations for the couplings g_1 and g_2, as a function of x (where $x\equiv E_0'/E_0$). The two flow equations are

$$\frac{dg_1(x)}{dx}=\frac{1}{x}\left[\frac{m}{\hbar k_F\pi}g_1^2(x)+\frac{m^2}{(\hbar k_F)^2 2\pi^2}g_1^3(x)+\cdots\right] \tag{5.6}$$

and

$$\frac{dg_2(x)}{dx}=\frac{1}{x}\left[\frac{m}{2\pi\hbar k_F}g_1^2(x)+\frac{m^2}{(\hbar k_F)^2 4\pi^2}g_1^3(x)+\cdots\right]. \tag{5.7}$$

In Eqs. (5.6) and (5.7) we have included third-order contributions in the couplings, which are not shown in Fig. 15.

The flow equations can be easily analyzed. If we neglect the third-order terms, then

$$g_1(x)=g_1/(1-g_1 1nx) \tag{5.8}$$

and

$$g_2(x)=g_2-\tfrac{1}{2}g_1+\tfrac{1}{2}g_1(x)\ . \tag{5.9}$$

To that order, there is a singularity in the renormalized coupling for $g_1<0$, corresponding to a phase transition at finite temperature. If we replace E_0' by k_BT, then the critical temperature, in the weak-coupling limit, is given by $k_BT_c=E_0e^{+1/g_1}$. This, of course, is closely related to the phase transitions discussed in Sec. III. If we include the third-order terms in Eqs. (5.6) and (5.7), then the singularities in $g(x)$ are removed. Therefore, as should be the case in 1D, there can be a phase transition only at $T=0$. The point is that uniquely in 1D *both* the e-e and e-h products must be consistently maintained to give the correct physics. One can also use the flow equations to construct response functions of appropriate symmetry. The well known phase diagram, at $T=0$, is presented in Fig. 16. Clearly the competition between the different phases in 1D is very strong.

What does this all mean for the case of short-range interparticle interactions? As already discussed above, for such physical interparticle interaction many of the terms

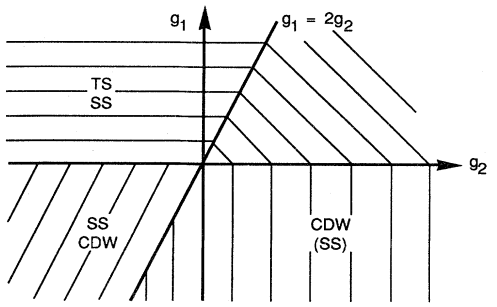

FIG. 16. Phase diagram of the 1D Fermi gas obtained in the second-order scaling approximation. The response functions corresponding to the phases indicated in parentheses have a lower degree of divergence than the others (from Sólyom, 1979). SS and TS correspond to singlet superconductivity and triplet superconductivity, respectively.

(e.g., the cross terms in Fig. 15) cannot be reduced to 1D. On the other hand, the ladder-type contributions are similar to those of one dimension and are singular both in the e-e and in the e-h channels. Therefore the situation in the quantum limit is a kind of mixture of 3D with strong 1D features. Significant progress along these lines has been made by Brazovskii (1971) and, more recently, by Yakovenko (1987). These authors have used the parquet equations to study the growth of CDW, SDW, and superconducting correlations as the temperature is reduced. They found that unretarded attractive interactions seem to favor a CDW over a superconducting instability. It is clear, however, that the realistic interactions, consisting of the short-range retarded attraction and the long-range Coulomb repulsion, could qualitatively affect their results. The long-range Coulomb part will strongly suppress the CDW instability and favor a SDW (Tešanović and Halperin, 1987), while the retarded attraction will help superconductivity (Zimanyi, Kivelson, and Luther, 1988). (The issue of the most likely ground state with a realistic interaction is further discussed in Sec. VI.) Moreover, it is most likely that the superconducting transition is discontinuous (see the discussion in the following section), and thus the approach of relying on similarity to the more familiar purely 1D case may not lead to a quantitatively reliable phase diagram. Certainly the precise interplay between e-e and e-h contributions, which led to nonsingular behavior in the renormalized couplings, is not expected to occur for the case of a physical interparticle interaction in the presence of high magnetic fields. Phase transitions to SDW, CDW, and superconductivity are expected at finite T, but the phase diagram is expected to be modified considerably from the mean-field results presented in Secs. III and IV. Unfortunately, a rigorous study of this phase diagram to our knowledge has not been carried out. When cross diagrams are included, intermediate sums over the manifold of states m [in Eq. (4.2)] remain explicitly in the renormalization-group recursions [Eqs. (5.6) and (5.7)]. The scattering cross sections [Eq. (5.3)] need to be made invariant now with the additional dependence on m (or equivalently $z \equiv x + iy$). We are pursuing such a study; the analysis is very complicated, and it is not clear whether it can be carried out at all. It does, however, share similarities with a study (Brézin, Nelson, and Thiaville, 1985) restricted to the effect of thermal fluctuations on the superconducting phase transition. We turn to this next.

C. Thermal fluctuation near $T_c(H)$

Assuming a continuous transition along the H_{c2} line, Brézin, Nelson, and Thiaville (1985) studied Eq. (5.1) with F of Eq. (2.23a), and applied renormalization-group expansion techniques to the calculation of fluctuation effects. Very briefly, what they do is write $\psi(\mathbf{r})$ in Eq. (2.23a) as

$$\psi(\mathbf{r}) = \phi(z, \mathbf{r}_\perp) \exp(-|z|^2/2) , \tag{5.10}$$

where $\phi(z, \mathbf{r}_\perp)$ is holomorphic in z. Introducing this into Eq. (2.23a), they find that the corresponding F is given by

$$F = \int d^{d-2}\mathbf{r}_\perp \int dz \int dz' \left[(|\nabla_\perp \phi|^2 + \tilde{\alpha}|\phi|^2) \exp\left[\frac{-|z|^2}{2} \right] + \tfrac{1}{2}\beta |\phi|^4 e^{-|z|^2} \right] , \tag{5.11}$$

where $\tilde{\alpha} = \alpha + \frac{1}{2}\hbar\omega_c$. The propagator of the quadratic term of Eq. (5.11) is (after Fourier transforming the $\mathbf{r}_\perp$ coordinate)

$$G(\mathbf{q}_\perp z^*, z') = \frac{1}{2\pi} \frac{1}{(q_\perp^2 + \tilde{\alpha})} e^{-z^* z'/2} . \tag{5.12}$$

Carrying out the standard renormalization-group rescaling along $\mathbf{q}_\perp$, Brézin, Nelson, and Thiaville (1985) could not find the same form for the rescaled F; they concluded that thermal fluctuations cause the transition across the H_{c2} line to be first order. It might be that in fact the Abrikosov lattice does not disappear continuously (as envisioned by Abrikosov from the mean-field approximation), but rather melts through a first-order phase transition (see Sec. V.A). [Incidentally, Halperin, Lubensky, and Ma (1974) find a first-order fluctuation-driven phase transition for Eq. (2.23a) due to the fluctuation in $\mathbf{a}(\mathbf{r})$.] This possibility gives further credibility to the various attempts to understand the melting of the Abrikosov lattice in high-T_c superconductors (Nelson, 1988; Houghton, Pelcovits, and Sudbo, 1989; Nelson and Seung, 1989; Xing and Tešanović, 1990; Brandt, 1991). For example, Nelson and Seung (1989) apply continuum elastic theory and the Lindemann criterion to the displacement free en-

ergy of an Abrikosov lattice,

$$\delta F(\mathbf{u}(\mathbf{r}))=\tfrac{1}{2}\int d^3r\left[2\mu u_{\alpha\beta}^2+\lambda u_{\delta\delta}^2+K\left[\frac{\partial\vec{u}}{\partial z}\right]^2\right], \quad (5.13a)$$

where

$$u_{\alpha\beta}(\mathbf{r})=\tfrac{1}{2}\left[\frac{\partial u_\alpha}{\partial r_\beta}+\frac{\partial u_\beta}{\partial r_\alpha}\right]_{\alpha,\beta=x,y} \quad (5.13b)$$

is the symmetrized two-dimensional strain matrix, μ and λ are Lamé coefficients, and K is a tilt elastic constant. For high-T_c material, where K is very small, they find that melting preempts the continuous transition along the H_{c2} line.

It is physically clear from the above approaches that the true superconducting transition $T_{sc}(H)$, defined as the point where the resistivity vanishes, is different from $T_c(H)$ found in the mean-field approximation. Thermal fluctuations act to reduce $T_{sc}(H)$ relative to $T_c^{MFA}(H)$. However, the renormalization-group technique cannot be used to treat what is, most likely, a first-order transition. Furthermore, the elastic theory uses the Lindemann criterion to locate $T_{sc}(H)$. This is clearly unsatisfactory, since the Lindemann criterion is entirely *ad hoc* and certainly does not represent a theory of melting of the vortex lattice. Finally, the elastic theory has one further principal difficulty: it cannot describe the vortex "liquid" phase above $T_{sc}(H)$.

Recently there has been some further progress in understanding the true superconducting transition $T_{sc}(H)$, by Tešanović and Xing (1991) and by Tešanović (1991). Tešanović and Xing consider the case of "ordinary" low-field quasi-2D superconductors—thin films, superlattices, and layered systems—but their approach can be generalized to 3D (Tešanović, 1991) and to the high-field limit (Tešanović, Rasolt, Andreev, and Dukan, 1991), which is of interest here. Let us review this approach, which, in fact, leads to a unified description of both vortex "solid" and "liquid" phases and leads to a quantitative result for $T_{sc}(H)$ in very good agreement with experiments in "low-field" superconductors.

Physically, the idea of Tešanović and Xing is that fluctuations of the superconducting order parameter $\psi(x,y,\zeta)$ are dominated by two factors: First, the external magnetic field places a constraint on the form of $\psi(x,y,\zeta)$. Near $T_c^{MFA}(H)$ we can expand

$$\psi(x,y,\zeta)=\sum_{nm} b_{nm}(\zeta)\phi_{nm}(z,z^*),$$

where $\phi_{nm}(z,z^*)$ are the Landau eigenfunctions (for particles of charge $e^*=2e$) in an arbitrary gauge. As we have discussed earlier, the dominant contribution comes from the lowest "bosonic" Landau level, $n=0$. The fluctuations from higher Landau levels, $n\neq 0$, have a gap of order ω_c and can be ignored "near" T_c^{MFA}. These fluctuations will "smoothly" renormalize the Ginzburg-Landau expansion for the lowest Landau-level contribution to $\psi(\mathbf{r})$. Thus the problem is now reduced to a study of fluctuations in $\{b_{0m}\}$. The second important point is that the problem of fluctuations in type-II (and high-field-limit) superconductors is "low dimensional," even in 3D, and particularly in 2D (Lee and Shenoy, 1972; Tešanović, 1991). This is because the upper critical dimension in the sense of the renormalization group, D_c, is $D_c=6$ for this problem (Brézin, Nelson, and Thiaville, 1985). Here, a parallel is suggested with the $\mathbf{H}=0$ case for $D\ll D_c$, in which it is often beneficial to write $\psi(\vec{r})=A(\vec{r})\exp i\phi(\vec{r})$ and to study the fluctuations in amplitude and phase separately, since their nature can be quite different. This is particularly important in low dimensions, far from D_c; one example is a 2D Kosterlitz-Thouless transition. In this case the amplitude fluctuations are effectively suppressed, and the important contribution comes from the singular part of the phase fluctuations, describing the motion of vortices and antivortices. Similarly, for $\mathbf{H}\neq 0$, and as long as the fields are comparatively low, we can use the same approach and concentrate on these singular phase fluctuations, except now only vortices will be present. Near $T_c^{MFA}(H)$, however, while one can still separate the amplitude and the phase as above, confinement to the lowest Landau level provides a stringent constraint on the fluctuations in A and ϕ. They cannot fluctuate independently. Tešanović and Xing show that this constraint can be enforced exactly in the symmetric gauge by writing

$$\psi(x,y,\zeta)=\sum_{m=0}^{N} b_m(\zeta)\phi_{0m}(z,z^*)$$
$$=\Phi(\zeta)\prod_{i=1}^{N}\left[z-z_i(\zeta)\right]e^{-|z|^2/4}, \quad (5.14)$$

where now $\Phi(\zeta)$ and $\{z_i(\zeta)\}$ are allowed to fluctuate freely. The fluctuations in Φ and $\{z_i\}$ near $T_c^{MFA}(H)$ are the "natural" way of representing two distinct tendencies in $\psi(\vec{r})$: Φ describes the "global" superconducting correlations, while the motion of vortices $\{z_i\}$ emulates "local" amplitude and phase fluctuations, coupled together by confinement to the lowest Landau level.

In the mean-field approximation, Φ becomes finite, and the $\{z_i\}$ order into a triangular lattice at the same point, $T_c^{MFA}(H)$, as was discussed previously. Tešanović and Xing demonstrate that, when thermal fluctuations are properly included, Φ and $\{z_i\}$ behave very differently. Vortices $\{z_i\}$ still form a liquid long after the fluctuations in Φ have subsided, and its value is dominated by the mean-field saddle point. They find that the growth of Φ provides an effective interaction between the vortices $\{z_i\}$ and ultimately leads to the formation of the vortex "solid." This solidification, or melting point, is identified with $T_{sc}(H)$. Tešanović and Xing also show that $T_{sc}(H)$ is *always far* from $T_c^{MFA}(H)$, in some universal sense, as will become clear below.

We now illustrate how this works in a 2D "low-field" case, following Tešanović and Xing. Equation (5.1) can be written as

$$Z=\int Db_{0m}Db_{0m}^{*}\exp[-\beta F(b_{0m},b_{0m}^{*})]\ . \tag{5.15}$$

The measure of the functional integral in Eq. (5.15) can be transformed, after some algebra, to

$$\propto\frac{1}{N!}\int\prod_{i=1}^{N}\frac{dz_i dz_i^{*}}{2\pi}\prod_{i<j}^{N}|z_i-z_j|^2\int d\Phi\, d\Phi^{*}(\Phi\Phi^{*})^{N}$$

by the evaluation of the Jacobian for

$$\prod_m db_{0m}db_{0m}^{*}\rightarrow d\Phi\, d\Phi^{*}\prod_i dz_i dz_i^{*}\ .$$

This change of variables contains important physics. The eigenmodes of the quadratic part of $F,\{b_{0m}\}$, describe an infinitely degenerate manifold. As one approaches $T_c^{\mathrm{MFA}}(H)$ these modes are so strongly mixed by the quartic term that they completely lose their initial identity. But general linear combination of these eigenmodes is exactly (5.14). Furthermore, the additional, and essential, benefit of these new variables becomes obvious when we note that the integral over Φ in the partition function can be carried out exactly in the thermodynamic limit. This is significant since this integral contains contributions from the nonperturbative sector of Eq. (5.15). After integration one obtains

$$Z\propto\int\prod_{i=1}^{N}\frac{dz_i dz_i^{*}}{2\pi}[C]^{-(N+1)/2}\prod_{i<j}^{N}|z_i-z_j|^2 \times\exp[\tfrac{1}{2}NB^2-\tfrac{1}{2}NB\sqrt{B^2+2}-N\sinh^{-1}(B/\sqrt{2})]\ , \tag{5.16a}$$

where

$$C(\{z_i\})\equiv\int\frac{dzdz^{*}}{2\pi N}\exp(-z^{*}z)|f(z,\{z_i\})|^4\ ,$$

$$f(z,\{z_i\})=\prod_i(z-z_i)\ ,$$

$$B(\{z_i\})\equiv g\frac{\int\frac{dzdz^{*}}{2\pi N}\exp(-z^{*}z/2)|f(z|\{z_i\})|^2}{\left[\int\frac{dzdz^{*}}{2\pi N}\exp(-z^{*}z)|f(z|\{z_i\})|^4\right]^{1/2}}\ , \tag{5.16b}$$

and

$$g=\tilde{\alpha}(2\pi l^2 d/2\beta k_B T)^{1/2}\ .$$

Z describes a two-dimensional classical system of particles with density fixed at $(2\pi l^2)^{-1}$ interacting through a long-range multiple (2,3,...) body potential $B(\{z_i\})$. These long-range "gauge" forces arise from the confinement to the lowest Landau level, much as in the quantum Hall effect. The introduction of Φ and $\{z_i\}$ as basic variables was crucial, since it is the integration over Φ that enables Tešanović and Xing to extract the interaction among vortices $\{z_i\}$ which dominates the low-temperature behavior. Note that this interaction becomes the Abrikosov mean-field free energy when the $\{z_i\}$ freeze. This interaction is inherently nonperturbative and cannot be detected in large-order perturbation theory (where the quartic term in the free energy is treated as a perturbation; Ruggeri and Thouless, 1976; Brézin, Fujita, and Hikami, 1990). The thermodynamics of this dense vortex plasma is equivalent to the original problem of superconducting fluctuations in 2D.

As an example of cooperative phenomena, Tešanović and Xing consider the melting transition. Once the dense vortex plasma freezes, by conventional wisdom, disorder will pin this vortex solid and result in dissipationless flow for weak currents. Thus the melting point of the dense vortex plasma can be identified as $T_{\mathrm{sc}}(H)$. The "gauge interaction" $B(\{z_i\})$ is scale invariant. Therefore the thermodynamics of the plasma in Eq. (5.16) does not depend on its density. It is entirely determined by the dimensionless coupling constant g. In particular, we can write down the equation for the melting line, $H_M(T)$ [or $T_{\mathrm{sc}}(H)$], in the H-T phase diagram as

$$g(T,H)=g_M^{2\mathrm{D}}\ , \tag{5.17}$$

where $g_M^{2\mathrm{D}}<0$ is a pure number (note that the mean-field transition corresponds to $g=0$). The melting line derived from Eq. (5.17) has the qualitative form shown in Fig. 17 as $H_M(T)$. This line signifies the transition to a true superconducting state. It exhibits the following "universal" feature: If experimentally determined T_M are plotted versus $g^2(T_M,H_M)k_B T_M$ for a variety of quasi-2D and $\kappa\gg1$ superconductors, the data should all fit on the same straight line, with the slope given by $(g_M^{2\mathrm{D}})^2$ (see Fig. 18).

The number $g_M^{2\mathrm{D}}$ is therefore of considerable significance. To determine $g_M^{2\mathrm{D}}$, Tešanović and Xing per-

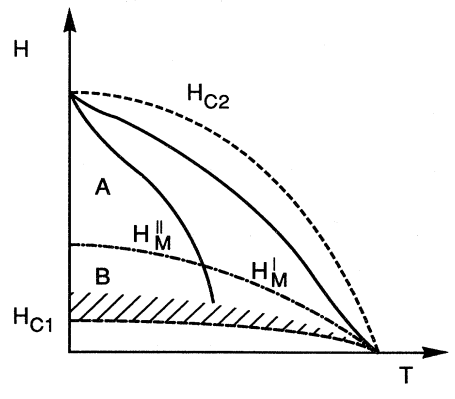

FIG. 17. A schematic H-T phase diagram for layered and thin-film type-II superconductors. The dense vortex regime (A) is separated from the dilute vortex regime (B) by a dot-dashed crossover line. For most systems θ_M is small and $H_M(T)$ behaves as $H_M^{\mathrm{I}}(T)$ (see text). As θ_M increases, $H_M^{\mathrm{I}}(T)$ evolves from $H_M^{\mathrm{I}}(T)$ to $H_M^{\mathrm{II}}(T)$. The dashed region is the London regime, where $H_M^{\mathrm{I}}(T)$ turns toward $H_{c1}(0)$ from Nelson, 1988.

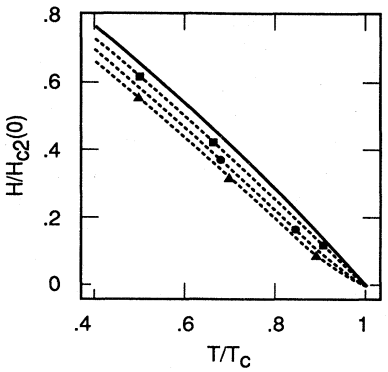

FIG. 18. $H_M(T)$ for three different thicknesses in thin films of Nb_3Ge. The data points are from Berghuis *et al.* (1990). The dashed lines are obtained from Eq. (5.17) with $g_M^2=67$, and the experimental parameters from Berghuis *et al.*

formed a numerical Monte Carlo simulation of the dense vortex plasma of Eq. (5.16). They found $(g_M^{2D})^2=63\pm12$. The origin of the uncertainty in $g_M^{2D}\sim-8$ is the softness of the potential $B(\{z_i\})$, requiring very long equilibration times.

The size of g_M^{2D} testifies to the validity of Tešanović and Xing's approach. For such large negative values of g^{2D}, Φ already has a "mean-field"-like behavior, and the superconducting transition is completely dominated by the motion of $\{z_i\}$. In fact, the leading terms in the $g\ll-1$ limit of the exponential in Eq. (5.16) are equivalent to the saddle-point approximation for Φ. For g^{2D} around zero or positive, the form of the effective interaction among $\{z_i\}$ is different and much weaker (see Tešanović, 1991). Thus, near the mean-field transition $T_c^{MFA}(H)$, which is given by $g^{2D}=0$, the system of $\{z_i\}$ is a weakly interacting liquid, far from the solidification transition. This universal large distance of $T_{sc}(H)(g^{2D}=g_M^{2D}\ll-1)$ from $T_c^{MFA}(H)$ is the consequence of the infinite degeneracy of the lowest "bosonic" Landau level and the effective low dimensionality as postulated by Tešanović and Xing.

We now consider the implications of all of this for the quantum limit. If we neglect quantum fluctuations, then the results of Tešanović and Xing can be readily extended to the 3D quantum limit. Of course, both $\tilde{\alpha}$ and β in Eq. (5.11) must be replaced by the appropriate kernels, Eqs. (4.7) and (4.8). However, the important transformation to the coordinates of the z_i [Eq. (5.14)] stands, and the analogy with plasma melting remains. Unfortunately, in 3D one cannot carry out the integration over $\Phi(\zeta)$ exactly, due to the presence of gradient terms (along **H**). However, the integration can be carried out approximately (see Tešanović, 1991) and results in a "quantized" version of this 2D dense vortex plasma. The scaling remains, except now g_{2D} goes into g_{3D} when one replaces d by $\xi_z(T,H)$, where ξ_z is the coherence length along **H**. The melting line is again determined by the 3D version of Eq. (5.17). The value of g_M^{3D} is difficult to determine with the same precision as g_M^{2D}, but it seems to be $\sim-3.5\ll-1$ (note that one is comparing the squares of g) from the fit to the experimental data on $YBa_2Cu_3O_{6.9}$, a high-temperature superconductor (Tešanović, 1991). Thus the 3D case is also "low dimensional," with $T_{sc}(H)$ dominated by the fluctuations of $\{z_i(\zeta)\}$, while the fluctuations of $\Phi(\zeta)$ have basically subsided. Furthermore, $|g_M^{3D}|<|g_M^{2D}|$, which should not be surprising since, as one goes toward dimension 6, g_M should move toward 0, its mean-field value.

As outlined above $T_{sc}(H)$ can be obtained from $g_{3D}(T,H)=g_M^{3D}$, where now

$$g_{3D}=\tilde{\alpha}'[2\pi l^2\xi_z(T,H)/2\beta' k_B T]^{1/2} .$$

Inserting the quantum limit expressions for $\tilde{\alpha}',\beta'$, and $\xi_z(T,H)$, one finally obtains

$$T_{sc}(H)\simeq\frac{1}{(g_M^{3D})^2}T_c^{QLA}(H) .$$

The value of $g_M^{3D}\simeq-3.5$ is universal and is the same for the high-field limit and "low-field" ordinary 3D superconductors (Tešanović, 1991). Thus the true $T_{sc}(H)$ is reduced to about 10% of its mean-field value $T_c^{QLA}(H)$. This illustrates that thermal fluctuations are quite significant in the high-field-limit superconductor, but they still leave $T_{sc}(H)$ observable. It is important to stress here that an analysis of the fluctuations demonstrates that high-field-limit superconductivity is a truly 3D state, despite a deceptive quasi-1D appearance at the mean-field level. The approach of Tešanović and Xing enables one to extract this important "lateral" interaction among vortices which is not found in other approaches. These lateral correlations can now be included on an equal footing with the fluctuations along **H** (Brézin, Nelson, and Thiaville, 1985). It is essential that both be included, since it is the "lateral" correlations that drive the superconducting transition both in the quantum limit and in low fields in 3D, as well as in 2D. Using the results of Tešanović and Xing, one can now address issues like the shape of the (probably first-order) transition line, the mechanism of melting of the vortex "solid," etc. Therefore the analysis of Tešanović and Xing, applied to the high-field limit, provides us with a quantitative understanding of the effect of thermal fluctuations on the superconducting transition.

Now we turn to the effect of quantum fluctuations in the quantum limit. First, if we again ignore the propagation along **H** and consider the 2D case, then the wave functions in Eqs. (4.5) and—even more explicitly—Eq. (4.43) share a lot of similarities with a boson version of the Wigner crystal phase of the quantum Hall effect. The process of melting of such a crystal to a fluid state (e.g., a ring exchange of vortices?) would probably be relevant here. We must, however, bear in mind that the density of zeros in $\Delta(\mathbf{r})$ "per plane" (next to the H_{C_∞} line) is of the

order of electron-electron separation and the tendency for melting due to such quantum fluctuations will be strong. For a complete treatment of both quantum and thermal fluctuations, we need to consider the contributions of Figs. 13 and 14. The thermal fluctuations will continue to be modified by the small q_z of the ladder graphs. We believe that the quantum fluctuations will be modified by terms like Fig. 13(a). In other words, the mean-field condensate is modified by nonsuperconducting quantum fluctuations.

The solution to the BCS theory found in Sec. IV will experience significant effects from thermal and quantum fluctuations. These effects were discussed in this section. We find that, in 3D, thermal fluctuations reduce the transition temperature in very high fields, but the superconducting state still appears at an observable temperature range. The mean-field theory is therefore a reasonable starting point at low temperatures. In 2D the effect of fluctuations is much stronger, and it may be that the mean-field theory is not a valid starting point for any temperature. The effect of quantum fluctuations is more complicated and at present remains an open issue. These fluctuations will be discussed further in the next section, with regard to the issue of competition among different types of ground states.

VI. APPLICATIONS

A. Model calculations

In Sec. III we presented some of the qualitative features of the transition temperature in high-field-limit superconductivity. Here we present several model calculations which illustrate these qualitative features. First, we specify the type of system in which high-field superconductivity can be a realistic possibility. As already mentioned before, low-carrier-density systems are probably the most suitable materials. We consider two examples, Ge and GaAs. We emphasize that we are not predicting high-field superconductivity in Ge and GaAs. We simply use their material parameters as an illustration of what range of these parameters will be favorable for superconductivity. The model based on Ge parameters we call model I, while the corresponding model for GaAs is called model II. Models I and II represent systems in which the quantum limit can be reached with reasonable laboratory fields and in which the existence of a relatively wide region between $H_{\rm QL}$ and the spin-depopulation field H_d is well established. In fact, in n-doped Ge, a spin-density wave is expected to exist in the quantum limit. This is due to a modest g factor of ~ 1.6 and large valley anisotropy. The conduction band consists of four equivalent valleys, which are ellipsoids of revolution about the $\langle 111 \rangle$ crystal axes. The longitudinal mass m_l along the $\langle 111 \rangle$ axis is 1.64 in units of electron mass, while the transverse mass m_t is only 0.08. Thus, for a field along one of the $\langle 111 \rangle$ directions, the cyclotron mass $m_c \approx m_t$, leading to an effective g factor $g^* = g m_t = 0.12$. The small effective g factor results in both spin states' being present considerably above $H_{\rm QL}$ and, combined with strong valley anisotropy, favors spin-density waves relative to other high-field quasi-one-dimensional instabilities like charge-density waves and valley density waves. Since general conditions regarding the availability of both spin states are similar for SDW and high-field spin-singlet superconductivity, we take Ge parameters for our model I. We shall also assume that **H** is applied along the $\langle 111 \rangle$ axis of one of the valleys and that Ge is simultaneously being subjected to a uniaxial stress along the same direction. The stress leads to a situation in which only this one valley is occupied, with $H_{\rm LQL} \approx 5.6T$ for a carrier density 6×10^{17} cm^{-3}. Note that in our calculations density does not appear explicitly; one can use our results for various carrier concentrations by scaling appropriate quantities. Furthermore, Ge is rich with experimental possibilities since, in the unstressed case, all four valleys will be degenerate and an intervalley pairing in the spin-triplet case becomes a possibility (which we shall not investigate in detail here). A discussion of this point is presented in Rasolt (1987). The basic idea is that valley degeneracy plays the role of the spin and makes possible the formation of the orbital s-wave state. Similarly, in GaAs the cyclotron mass is ~ 0.07, which, combined with $g = 0.32$, leads to $g^* \sim 0.02$, providing an example of a system with very small Zeeman splitting (relative to the cyclotron frequency). Finally, we choose $m_c = 0.075$, $m_l = 1.0$, and $g = 1.5$ as our model III, illustrating the values of parameters that can be found in doped semiconductors and semimetals which will be favorable for the high-field superconducting state.

The formulas of Sec. III were obtained using a simple weak-coupling BCS approximation. While this approximation is expected to be qualitatively correct, one of the important characteristics of the quantum limit is a rapid rise in the density of states (and coupling constants) with increasing field ($\propto H^2$). This is accompanied by a corresponding drop in the Fermi energy. Thus conditions for the validity of the weak-coupling BCS theory will be violated at high fields. Consequently we use here a strong-coupling theory, based on a solution of the two-square-well model for kernels of the electron-phonon and electron-electron interactions. This results in a familiar reduction of the coupling constant due to the effects of a Coulomb pseudopotential μ^* and the quasiparticle renormalization factors:

$$\lambda_{\rm sc} = \frac{\sqrt{Z_\uparrow Z_\downarrow}}{\lambda - \mu^*} , \tag{6.1}$$

where $Z_\uparrow$ ($Z_\downarrow$) are the spin-up (-down) quasiparticle renormalization factors, λ is the electron-phonon coupling constant, and

$$\mu^* = \frac{\mu}{1 + \mu \ln(\sqrt{E_{F\uparrow} E_{F\downarrow}}/\Omega)} .$$

In the above we are restricting our consideration to the lowest Landau level. The cutoff of the frequency integration is equal to Ω. The above form is applicable for $\Omega \ll \sqrt{E_{F\uparrow}E_{F\downarrow}}$. In the opposite limit, $\Omega \gg \sqrt{E_{F\uparrow}E_{F\downarrow}}$, which occurs as the field increases, the same two-square-well model leads to

$$\lambda_{sc} = \frac{\sqrt{Z_\uparrow Z_\downarrow}}{\lambda^* - \mu} , \tag{6.2}$$

where now

$$\lambda^* = \frac{\lambda}{1 - \lambda \ln(\sqrt{E_{F\uparrow}E_{F\downarrow}}/\Omega)} ,$$

and the cutoff in frequency space is replaced by $\sqrt{E_{F\uparrow}E_{F\downarrow}}$. The solution in this limit should not be taken too seriously, since many of the physical concepts of the standard Eliashberg theory fail for a Fermi energy comparable to or much smaller than the typical phonon energy. Still, the solution in this limit does have the qualitative feature of a vanishing retardation effect and the corresponding rapid loss of the effective attraction. We therefore use this form to illustrate the drop in the transition temperature, which should be a qualitative feature of the $\Omega \gg E_{F\uparrow}F_{F\downarrow}$ limit. (Here we do not consider the possibility of various bipolaronic instabilities that may occur for low Fermi energies.)

The results are plotted in Figs. 19–21. We have used $\lambda = 0.6$ and $\mu = 0.1$ for $H = H_{QL}$ in all cases, as well as $\Omega \sim 10\%$ of the 3D Fermi energy. T_c is calculated for both uniform and nonuniform states along **H** (due to Zeeman splitting) of Sec. III. Several qualitative features are apparent from our results. First, the uniform state gives $T_c = 0$ for models I and III (for model II, with its very small effective g factor, there is a region where the uniform state is competitive). Thus the nonuniform state is essential in obtaining a finite transition temperature. Furthermore, all transition temperatures are uniformly suppressed relative to weak coupling. As the coupling

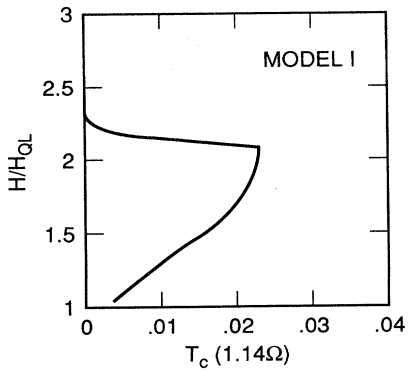

FIG. 19. $T_c(H)$ in strong coupling, for a nonuniform state. $T_c(H)$ for a uniform state is zero for models I and III, while it is smaller for model II. Model I: $m_t = 0.08$, $m_l = 1.64$, and $g = 1.6$.

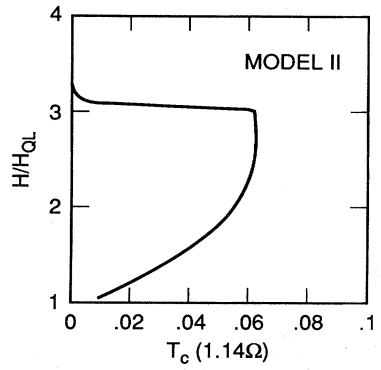

FIG. 20. Model II: $m_t = m_l = 0.07$ and $g = 0.32$.

constant increases ($\lambda \propto H^2$), the quasiparticle renormalization factors reduce T_c considerably, particularly for higher fields. One should not look for high-temperature superconductivity in the high-field limit, at least not in low-carrier-density systems like doped semiconductors and semimetals. In these systems T_c's are likely to be in the ~ 10 mK to ~ 1 K range. The break present in all $T_c(H)$ curves occurs for $\Omega \sim \sqrt{E_{F\uparrow}E_{F\downarrow}}$ and will disappear in a more realistic calculation including modifications of the Eliashberg theory for a Fermi energy comparable to the average phonon frequency. Finally, while the reduction in T_c due to Zeeman splitting is not negligible and is more significant than in weak coupling, the nonuniform state still leads to T_c's of the same order as $T_c(g = 0)$. For models I–III we find that $T_c(g)$ is typically ~ 30–80% of $T_c(g = 0)$. This qualitatively confirms the analysis of Sec. III and leads to the conclusion that the Zeeman effect does not destroy the nonuniform superconducting state in the quantum limit. All examples studied here (models I–III) indicate that if $T_c(g = 0)$ is itself observable, $T_c(g)$ will be too.

Models I–III have the parameters characteristic of low-carrier-density semiconductors and semimetals. As we have mentioned earlier, the Landau-level structure affects particularly systems with a high upper critical

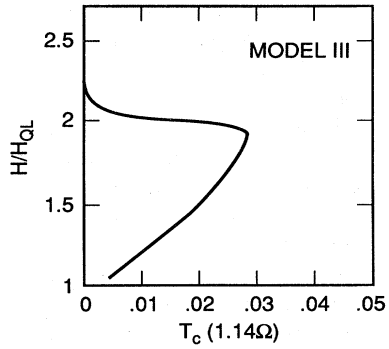

FIG. 21. Model III: $m_t = 0.075$, $m_l = 1.0$, and $g = 1.5$. For further discussion, see text.

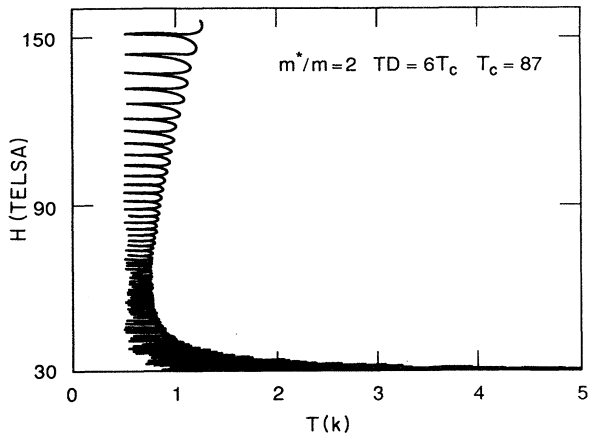

FIG. 22. H-T phase diagram for $Bi_2Sr_2CaCu_2O_8$-type systems with $m^*/m=2, T_{c0}=87$ K. The Landau-level structure results in deviations from the standard theory around $T\sim 2$ K and $H\sim 30$ Tesla and leads to the crossover to the high-field limit for $T\sim 0.8$ K and $H\sim 50$ Tesla. From Maniv *et al.*, 1991.

field, like some of the recently discovered high-temperature superconductors. While the quantum limit will be out of reach in these systems, the initial deviations from the Abrikosov-Gor'kov theory should be observable and are further enhanced by the 2D character of these systems. The effect of Landau quantization on the transition temperature at high fields has been recently calculated by Maniv *et al.* (1991) and is shown in Fig. 22. Their results show a particularly clear crossover to the high-field limit taking place at $T\sim 0.8$ K and $H\sim 50$ Tesla (this crossover occurs at a temperature much higher than in 3D systems). While the results in Fig. 22 are very sensitive to Zeeman splitting, one could tune the Zeeman splitting by tilting the direction of the field to maintain degeneracy between Landau levels (Norman, Akera, and MacDonald, 1991).

B. Interactions in real systems

So far we have assumed some BCS effective attraction, V, which is a weak function of the external field, and have focused primarily on the questions of orbital frustration and various forms of pair breaking, i.e., on how superconductivity survives in the high-field limit. But there are other issues, as well, of great practical importance for high-field superconductivity: what is the origin of V? how does it change with the external field in real systems? what is the likelihood of superconductivity's being the ground state in the quantum limit as opposed to a spin-density, charge-density, or other state? Some of these issues have been briefly touched upon in earlier sections (e.g., Sec. V); we now discuss them in some detail.

First of all, as we already mentioned in the Introduction and in Sec. III, an important piece of physics, first noted by Rasolt (1987), concerning the H dependence of V, may make spin-singlet superconductivity favorable in the H_{QL} over SDW, etc. It is the observation that a very strong magnetic field will tend to favor an attractive piece of the interparticle interaction. It is important to emphasize that this clearly may or may not be true, depending on which physical system is under consideration. The point is that in low-carrier-density systems the effect of the field is such as to actually enhance the effective attraction V (Rasolt, 1987). This important point is discussed below.

Doped semiconductors and semimetals do not make "good" superconductors. The transition temperatures that one can expect in these systems are unlikely to be very high, due to the low carrier density. The low carrier density reduces the metallic screening, and the Coulomb interaction is thus often too strong to permit any superconductivity. In addition, in low-carrier-density systems the density of states at the Fermi level will be small, which again results in low T_c's. Therefore it is very important to realize that the application of the magnetic field $\simeq H_{QL}$ may *enhance* the superconductivity already present at $H=0$ or even induce high-field superconductivity in systems that are not superconductors at $H=0$. The reason is that V, which is a simplified BCS representation for an effective attraction arising from the combined effect of electron-phonon and electron-electron interactions, is likely to increase from its $H=0$ value or to change sign from repulsive to attractive, when the field $\gtrsim H_{QL}$ is applied (Rasolt, 1987).

The physical origin of this phenomenon is the following. Even including screening, the e-e interaction has a much larger range than the phonon part. The e-e interaction drops rapidly for Fourier components $\mathbf{q}$ larger than something like the Thomas-Fermi screening wave vector of the free carriers. Now, for two carriers without a magnetic field, the states are very extended and the long-range e-e repulsion matrix element is large. The presence of the magnetic field squeezes these states perpendicular to $\mathbf{H}$ and reduces this repulsion; the phonon part remains largely unchanged. This is because in low-carrier-density systems there is a very fortuitous hierarchy of length scales: $r_s \approx l \gg a$, where r_s is the average separation between the carriers and a is the lattice constant. Of course, it is exactly this property which enables one to reach the quantum limit with reasonable fields. But, *at the same time*, this hierarchy of length scales is responsible for the electron-phonon interaction, which is why the BCS attraction remains largely unaffected by the field. H of the order of H_{QL} is very "large" as far as the carriers are concerned, but it is "low" for phonons in low-carrier-density systems. The phonon spectrum and the corresponding "ionic" part of the dielectric function are determined by *all* of the electrons in the system. The influence of the small number of carriers on this part of the dielectric function is, in fact, negligible. It is important to appreciate this since, as is well known, the polarizability of the low-density carriers is radically changed by the magnetic field, as Celli and Mermin (1965) have

shown. Furthermore, the plasmon of the low-density carriers in a polar semiconductor is known to interact with the optical phonons. All these effects are proportional to the density of carriers and should be a small correction to the effective electron-electron interaction arising from the phonon exchange. (For example, even if the optical phonons are modified due to their coupling to the plasmon of low-density carriers, what enters in the Eliashberg theory is the integral over the whole frequency range of the phononic spectral function. This quantity will still be dominated by the part in which the carriers are ignored.) To significantly modify the contribution to the dielectric function one would have to apply fields that have a magnetic length of the order of the lattice constant. Such enormous fields (10^3-10^4 T) are much, much larger than $H^{\rm QL}$ in doped semiconductors or semimetals. Furthermore, even the dramatic change in wave functions of the carriers at these high fields does not affect the effective electron-electron attraction due to phonon exchange. This interaction is short ranged, with a range of the order of one lattice constant, and has a far shorter range than the Coulomb repulsion because, contrary to what one may usually think, acoustic long-wavelength phonons play only a very minor role in the superconductivity of low-carrier-density systems. The dominant contribution comes from phonons with large wave vectors, comparable to the zone size, and, in particular, from the multivalley electron-phonon coupling (see Cohen, 1969).

The relative insensitivity of the effective attraction, arising from electron-phonon coupling, as well as the reduction of the Coulomb repulsion as the field is increased from zero to the neighborhood of $H_{\rm QL}$, means that V increases as a function of H, and the effective BCS interaction can change from being repulsive to being attractive. This effect and the orbital effect, which as we saw changes from depressing to enhancing, are what drives superconductivity in the high-field limit; they represent the two essential ingredients of superconductivity in high magnetic fields. To see how this change from repulsive to attractive works explicitly we return to Eq. (2.3). In the static approximation Eq. (2.3) gives

$$V(H)\approx\frac{-\Omega_0}{M}\frac{\bar{V}^2(Q_D)\hbar^2Q_D^2}{(\hbar\omega_{Q_D})^2}+\frac{4\pi e^2}{\epsilon Q_D^2}\ , \tag{6.3}$$

where ϵ is the dielectric constant of the semiconductor and $Q_D\simeq 1/l$. Q_D is a cutoff on the $\mathbf{q}$ components due to the Gaussian envelopes of the Landau levels. It corresponds exactly to the squeezing, perpendicular to $\mathbf{H}$, of the spread-out wave functions discussed above. To see the effect of this magnetic-field dependence in $V(\mathbf{H})$ we apply Eq. (6.1), now to a simple model of Si (we apply it to the uniform state $g=0$). For the ionic potential $\bar{V}(\mathbf{q})$ we choose

$$\bar{V}(q)=\frac{a_1(q^2-a_2)}{\exp[a_3(q^2-a_4)]+1}\ , \tag{6.4}$$

where $a_1=0.342$, $a_2=2.221$, $a_3=0.86334$, and $a_4=1.5345$, and $\bar{V}(q)$ is equal to $V(q)/\Omega_0$. Our results are displayed in Fig. 23 (Rasolt, 1987; 1990).

The next important issue is competition with other types of broken-symmetry ground states. As has already been pointed out, even an effective attraction in the Cooper channel, i.e., making our V positive and sufficiently large, does not insure that superconductivity will be a preferred state. The quasi-1D nature of the quantum limit is also very favorable for other instabilities, such as spin-density waves, charge-density waves, etc., and these states may very well have a lower free energy than the superconducting state. The competition between these various instabilities and the nature of the phase diagram is a very difficult problem to solve with realistic interactions (see discussion in Sec. V). However, we can still reach important conclusions concerning this question based on the Hartree-Fock, "weak"-coupling consideration. While such considerations are almost certainly quantitatively invalid, since low-carrier-density materials are moderately to strongly interacting systems, they should still provide qualitative guidance in charting the phase diagram in the quantum limit. We now assume that both spin levels are occupied in the quantum limit and that the Zeeman splitting is small. Under these circumstances the CDW state is always strongly disfavored in the Hartree-Fock approximation (Tešanović and Halperin, 1987). This is due to a large cost in direct, electrostatic energy that one has to pay for setting up a long-wavelength ($q=k_{F\uparrow}+k_{F\downarrow}$) first-order charge-density inhomogeneity. The strong long-range Coulomb interaction in low-carrier-density systems makes this cost sufficiently great that the system will generally avoid any state having such an inhomogeneity [for stronger fields, when the spins are polarized, a CDW or Wigner crystal may be the ground state of the system (Fukuyama, 1978)]. Thus the Coulomb repulsion alone will favor a spin-density wave or a valley density wave, composed of the "out-of-phase" CDW from different valleys in a multivalley system, with the first-order charge-density inhomogeneity canceled out (Tešanović and Halperin, 1987).

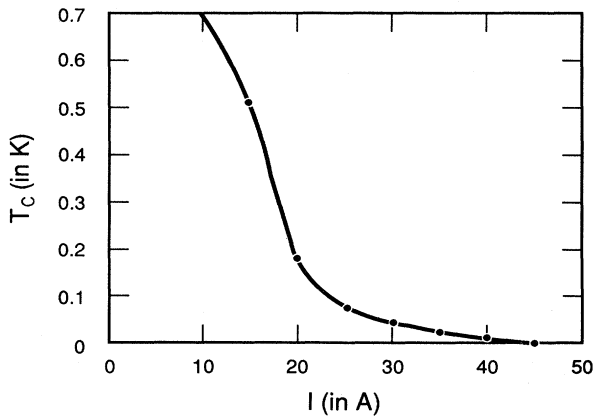

FIG. 23. Critical temperature T_c vs the magnetic length l at carrier density $\approx 10^{17}/\text{cm}^3$.

The inclusion of the short-range retarded attraction arising from phonon exchange will now introduce superconductivity into the picture (this short-range retarded attraction does not help the CDW, since the cost in electrostatic energy is always overwhelming).

The competition between superconductivity and spin-density waves (or valley density waves) will be decided by the strength of the electron-phonon coupling, degree of retardation (i.e., the size of the characteristic phonon frequency Ω relative to E_F), the strength of the Coulomb repulsion as it enters the Coulomb pseudopotential μ, etc. In a purely 1D model with only short-range interactions, the retarded attraction *always* wins over the repulsive part (even if the repulsive coupling constant is much larger) and drives the system away from a spin-density-wave state toward the superconducting state (Zimanyi, Kivelson, and Luther, 1988). It is clear that we cannot simply generalize this result to our case: After all, we have just spent considerable effort arguing that the problem in the quantum limit is not purely 1D. But this 1D analog does provide a qualitatively similar example of a superconducting state's winning over a spin-density-wave state. Thus, at least within this Hartree-Fock-type analysis, superconductivity will compete with the spin-density wave and, provided the electron-phonon coupling is sufficiently strong and retarded and the carrier density is not too low, is likely to be the ground state in the quantum limit, by the above qualitative argument. Clearly, materials of low carrier density that are superconductors at zero field are the most promising candidates for this new state. The competition between these two states must be considered in the presence of Zeeman splitting, however small. We must stress here that the problem of the phase diagram in the quantum limit with realistic interactions is still unsolved, and other possibilities, like the triplet superconductor, etc., may play a role.

Finally, we insert a word of caution about searching for this state in semiconductors (not so much in semimetals). Donors in the conduction region will contribute to magnetic freezeout. It is therefore crucial to keep impurities out of the conducting region. Modulation doping gives promising possibilities for producing regions >1000 Å of high mobility, where the electron density is fairly uniform. The transport properties of these wide parabolic quantum wells were discussed in Sec. IV.C.

To summarize, we have presented here a discussion of some of the experimental constraints and "facts of life" that will have considerable bearing on the eventual observation of high-field superconductivity in real systems. We have considered a strong-coupling correction in several representative model systems. We have also considered the validity of the BCS theory and the structure of the effective interaction in systems of low carrier density. Particularly important is the question of the competition of superconductivity with other types of broken-symmetry ground states (SDW, CDW, etc.). While this problem remains unsolved, we have presented qualitative arguments that indicate that superconductivity should be a ground state in a system with optimized, but not unrealistic, characteristics.

VII. CONCLUSIONS

In this review a new superconducting state was proposed in high magnetic fields. Such a superconducting state must be considered on an equal footing with all other possible instabilities (like charge-density waves, spin-density waves, valley density waves, etc.) believed also to be enhanced in the high-field limit. Which broken symmetry will occur in which particular material will ultimately depend on the nature of the electron-phonon and electron-electron interaction.

The main results are as follows: (i) In the very-high-field limit, and in particular in the quantum limit (when all the carriers are in the lowest Landau level, i.e., $H > H_{\rm QL}$), there is a phase transition to a new superconducting state with T_c enhanced by the external field H. (ii) The vortex lattice reaches its quantum limit; the nature of orbital frustration is completely changed from its low-field limit so that it now enhances superconductivity through a density-of-states effect. In many ways this is *the* simple limit, which provides a paradigm for studying the interaction of superconductivity with a magnetic field. In particular,

$$\Delta(\mathbf{r}) = \Delta_0 \prod_{i=1}^{N} (z - z_i) e^{-|z|^2/4}$$

is the *exact* solution of the full BCS theory, resulting in a gapless excitation spectrum. The relationship of the supercurrent with the vector potential, Meissner effect, etc. are similarly elucidated. (iii) As long as both spin states are occupied in the quantum limit, Pauli pair breaking can be largely circumvented by the nonuniform (along H) order parameter, which takes advantage of quasi-one-dimensional nesting (much like the SDW), and a novel triplet state can exist for even higher fields. (iv) Both spin states are occupied in the quantum limit only if the effective g factor g^* is less than 2, and it is preferable to have g^* considerably less than 2. (v) Low-carrier-density semiconductors and semimetals, in which the quantum limit can be readily achieved and in which often $g^* < 0.1$, are probably the best experimental candidates. Also, low-dimensional systems like layered semiconductor heterojunctions may be suitable in this respect. In particular, a superlattice made of a candidate material and a suitable high-temperature superconductor and subjected to a perpendicular magnetic field is a promising experimental geometry, since the Abrikosov lattice in the high-temperature superconducting layer would have the effect of reducing vortex fluctuations in the neighboring candidate layer. (vi) The quantum-limit approximation for $T_c(H)$, which works very well in the high-field limit, can be extended by the inclusion of off-diagonal Landau-level pairing terms to provide a unified description of the crossover from the high-field to the low-field limit ($H \sim H_{c2}$), but otherwise these two superconducting regimes are independent. (vii) Therefore the material can

be exceptionally clean, exhibit high-field superconductivity, and not be a type-II superconductor (nor, in fact, a superconductor at all) for low fields. (viii) The effect of Pauli pair breaking and impurities becomes very pronounced as the number of occupied Landau levels increases, therefore suppressing $T_c(H)$ prior to a possible reentrance at low fields. and (ix) The high magnetic field in systems of low carrier density may actually favor the effective attraction responsible for superconductivity. This is a consequence of an interplay between the electron-phonon and electron-electron interactions in the quantum limit.

As emphasized in the Introduction, this review focuses on theoretical aspects of this unusual part of the superconducting H-T phase diagram. We have attempted to provide the reader with an up-to-date coverage of the theoretical activity in this field. This activity continues, at a pace that may be faster than at any time before. The reader should realize that many important theoretical problems relevant to this subject are still unsolved. Probably the most interesting, and most difficult, is the problem of the full phase diagram in the high-field limit, including all the competing states (SDW, CDW, superconductivity of the spin-singlet and spin-triplet variety, etc.). We have presented some qualitative arguments based on the Hartree-Fock theory which give an outline of a realistic system in which the superconducting instability will dominate, but clearly much additional work in this direction is needed. Furthermore, while we have spent much effort discussing low carrier systems, like doped semiconductors and semimetals, one should also think about other possibilities: organic superconductors, artificially structured systems, etc. Also, the effect of fluctuations, particularly at very low temperatures and in 2D systems, has to be studied in greater detail. But the main message of this review is that there is yet another, somewhat counterintuitive, dimension to the relationship between superconductivity and a magnetic field, exciting and largely unexplored. We hope we have been able to present the reader with the overall picture, however incomplete and biased, of this subject.

Finally we must add that these two authors, perhaps naively, believe in the boundless ingenuity of their experimental colleagues. If this new superconducting state in high magnetic fields is not forbidden by any fundamental reason, a dedicated experimentalist will find it and open yet another view of this truly fundamental relationship which exists between superconductivity and a magnetic field. It is the main intent of this review to give further encouragement to such a serious experimental effort.

ACKNOWLEDGMENTS

This work has been supported in part by the Division of Materials Sciences, U.S. Department of Energy under Contract No. DE-AC05-84OR21400 with Martin Marietta Energy Systems, Inc. The work at Los Alamos National Laboratory was performed under the auspices of the U.S. Department of Energy. Z.T. acknowledges support of the David and Lucile Packard Foundation.

REFERENCES

Abrikosov, A. A., 1957, Zh. Eksp. Teor. Fiz. **32**, 1442.
Abrikosov, A. A., 1969, Zh. Eksp. Teor. Fiz. **56**, 1391.
Akera, H., A. H. MacDonald, S. Girvin, and M. R. Norman, 1991, Phys. Rev. Lett. **67**, 2375.
Aslamasov, L. G., and A. I. Larkin, 1968, Phys. Lett. **26**, 238A.
Bardeen, J., L. N. Cooper, and J. R. Schrieffer, 1957, Phys. Rev. D **106**, 162; **108**, 1175.
Berghuis, P., A. L. F. van der Slot, and P. H. Kes, 1990, Phys. Rev. Lett. **65**, 2583.
Brandt, E. H., 1991, Int. J. Mod. Phys. B **5**, 751.
Brazovskii, S. A., 1971, Zh. Eksp. Teor. Fiz. **61**, 2401.
Brézin, E., A. Fujita, and S. Hikami, 1990, Phys. Rev. Lett. **65**, 1949.
Brézin, E., D. R. Nelson, and A. Thiaville, 1985, Phys. Rev. B **31**, 7124.
Brey, L., and B. I. Halperin, 1989, Phys. Rev. B **40**, 11634.
Celli, V., and N. D. Mermin, 1965, Phys. Rev. A **140**, 839.
Cohen, M. L., 1969, in *Superconductivity,* edited by R. D. Parks (Dekker, New York), Vol. I, p. 615.
de Gennes, P. G., 1966, *Superconductivity of Metals and Alloys* (Benjamin, New York/Amsterdam).
Dukan, S., A. V. Andreev, and Z. Tešanović, 1991, Physica **C183**, 355.
Eilenberger, G., 1967, Phys. Rev. **153**, 584.
Fröhlich, H., and C. Terreaux, 1965, Proc. Phys. Soc. **86**, 233.
Fukuyama, H., 1978, Solid State Commun. **26**, 783.
Fulde, P., and R. A. Ferrell, 1964, Phys. Rev. **135**, 550.
Gor'kov, L. P., 1958, Zh. Eksp. Teor. Fiz. **34**, 735.
Gossard, A. C., B. I. Halperin, and R. M. Westervelt, 1987, unpublished.
Gruenberg, L. W., and L. Gunther, 1968, Phys. Rev. **176**, 606.
Gunther, L., and L. W. Gruenberg, 1966, Solid State Commun. **4**, 329.
Gwinn, E. G., R. M. Westervelt, P. F. Hopkins, A. J. Rimberg, M. Sundaram, and A. C. Gossard, 1989, Phys. Rev. B **39**, 6260.
Halperin, B. I., 1987, Jpn. J. Appl. Phys. **26**, Suppl. 26-3, 1913.
Halperin, B. I., T. C. Lubensky, and S. K. Ma, 1974, Phys. Rev. Lett. **32**, 292.
Houghton, A., R. A. Pelcovits, and A. Sudbo, 1919, Phys. Rev. B **40**, 6763.
Kleener, W. H., L. M. Roth, and S. H. Autler, 1964, Phys. Rev., **133**, 1226A.
Kohn, W., and L. J. Sham, 1965, Phys. Rev. **140**, 1133A.
Laughlin, R. B., 1983a, Phys. Rev. Lett. **50**, 1395.
Laughlin, R. B., 1983b, Phys. Rev. B **27**, 3383.
Lee, P. A., and S. R. Shenoy, 1972, Phys. Rev. Lett. **28**, 1025.
MacDonald, A. H., H. Akera, and M. R. Norman, 1992, Phys. Rev. B **45**, 10 147.
Maniv, T., R. S. Markiewicz, I. D. Vagner, and P. Wyder, 1990, Physica B 165&166, 361.
Maniv, T., A. I. Rom, I. D. Vagner, and P. Wyder, 1992, Phys. Rev. B (in press).
Maniv, T., and Z. Tešanović, 1991, unpublished.
Markiewicz, R. S., I. D. Vagner, P. Wyder, and T. Maniv, 1988, Solid State Commun. **67**, 43.
Nelson, D. R., 1988, Phys. Rev. Lett. **60**, 1973.
Nelson, D. R., and H. S. Seung, 1989, Phys. Rev. B **39**, 9153.
Nicopoulos, V. N., and P. Kumar, 1991, Phys. Rev. B **44**,

12 080.
Norman, M. R., 1990, Phys. Rev. B **42**, 6762.
Norman, M. R., 1991, Phys. Rev. Lett. **66**, 842.
Norman, M. R., H. Akera, and A. H. MacDonald, 1992, in *Physical Phenomena at High Magnetic Fields,* edited by E. Manousakis *et al.* (Addision-Wesley, Reading, MA), p. 326.
Olivera, L. N., E. K. U. Gross, and W. Kohn, 1988, Phys. Rev. Lett. **60**, 2430.
Parks, R. D., 1969, Ed., *Superconductivity* (Dekker, New York).
Rajagopal, A. K., and J. C. Ryan, 1991, Phys. Rev. B **44**, 10 280.
Rajagopal, A. K., and R. Vasudevan, 1966a, Phys. Lett. **20**, 585.
Rajagopal, A. K., and R. Vasudevan, 1966b, Phys. Lett. **23**, 539.
Rasolt, M., 1987, Phys. Rev. Lett. **58**, 1482.
Rasolt, M., 1990, in *Solid State Physics,* Vol. 43, edited by H. Ehrenreich and D. Turnbull (Academic, New York), p. 93.
Rasolt, M., 1991, "Superconductivity induced by very high magnetic fields: Thermodynamics and transport properties," *Proceedings of Strongly Correlated Electron Systems,* Gordon Godfrey Workshop on Condensed Matter Physics, University of New South Wales, Australia, 1991 (Nova, New York, in press).
Rasolt, M., 1992, in Physical Phenomena at High Magnetic Fields, edited by E. Manousakis *et al.*, unpublished.
Rasolt, M., and Z. Tešanović, 1990, in *Field Theories in Condensed Matter Physics,* edited by Z. Tešanović (Addison-Wesley, Menlo Park, CA), p. 167.
Rasolt, M., and G. Vignale, 1990, Phys. Rev. Lett. **65**, 1498.
Rieck, C. T., K. Scharnberg, and R. A. Klemm, 1990, Physica C **170**, 195.
Ruggeri, G. J., and D. J. Thouless, 1976, J. Phys. F **6**, 2063.
Sajoto, T., J. Jo, L. Engel, M. Santos, and M. Shayegan, 1989, Phys. Rev. B **39**, 10464.
Scharnberg, K., and C. T. Rieck, 1991, Phys. Rev. Lett. **66**, 841.
Schrieffer, J. R., 1959, Phys. Rev. Lett. **3**, 323.
Sólyom, J., 1979, Adv. Phys. **28**, 201.
Stephen, M. J., 1991, Phys. Rev. B **43**, 1212.
Stephen, M. J., 1992, Phys. Rev. B **45**, 5481.
Tešanović, Z., 1991, Phys. Rev. B **44**, 12 635.
Tešanović, Z., and B. I. Halperin, 1987, Phys. Rev. B **36**, 4888.
Tešanović, Z., M. Rasolt, A. V. Andreev, and S. Dukan, 1991, unpublished.
Tešanović, Z., M. Rasolt, and L. Xing, 1989, Phys. Rev. Lett. **63**, 2425.
Tešanović, Z., M. Rasolt, and L. Xing, 1991a, Phys. Rev. Lett. **66**, 843.
Tešanović, Z., M. Rasolt, and L. Xing, 1991b, Phys. Rev. B **43**, 288.
Tešanović, Z., and L. Xing, 1991, Phys. Rev. Lett. **67**, 2723.
Vignale, G., and M. Rasolt, 1987, Phys. Rev. Lett. **59**, 2360.
Vignale, G., and M. Rasolt, 1988, Phys. Rev. B **37**, 10685.
Xing, L., and Z. Tešanović, 1990, Phys. Rev. Lett. **65**, 794.
Yakovenko, V. M., 1987, Zh. Eksp. Teor. Fiz. **93**, 627.
Zimanyi, G. T., S. A. Kivelson, and A. Luther, 1988, Phys. Rev. Lett. **60**, 2089.